Politecnico di Torino

Master of Science in Climate Change
Department of Environment, Land, and Infrastructure Engineering
20/03/2024

Performance Analysis of a Radar Rain Gauge in Alpine Environment and Small Glacier Shrinkage Projection

Supervisor:
Prof.ssa Stefania Tamea

Candidate:
Demartis Andrea

A.y 2023/2024

Contents

List of Tables

List of Equations

List of Figures

Abstract

The objective of the thesis is to explore new ways to monitor the evolution of glaciers and display that enhanced monitoring could allow a better prediction of glacial bodies reduction. The thesis is therefore divided in two parts.

The first part consists in the evaluation of the effectiveness of a radar rain gauge for precipitation measurements in high mountain environments. Radar rain gauges are instruments capable of recognizing and quantifying the type and amount of precipitation measuring the electromagnetic waves reflected by precipitation. The use of radar rain gauges would reduce the costs compared to the usual rain gauges installed in high mountain environments and enhance monitoring of precipitation to better assess the well-being of the monitored environments, in light also of predicting climate change consequences and glacier preservation. The data used in this analysis were gathered by difference bodies such as “ARPA Valle d’Aosta” (Agenzia Regionale della Protezione Ambientale) (Centro Funzionale Regione Autonoma Valle d'Aosta, 2023), on-site meteorological station installed by GlacierLab PoliTO and others. The results show consistency in the measurement’s precision of liquid precipitation, but high unpredictability in the measurements of solid precipitations, trending towards their overestimation. Through the indirect use of a weighted rain gauge also evaporation has been studied, assessing which are the parameters that can enhance evaporation and finding an order of magnitude of the evaporation in high mountain environments.

The second part of the thesis is a display of the capabilities of what enhanced monitoring could achieve: a projection of the evolution of “des Usellettes”, a small glacier in the “La Thuille” valley (AO) close to the Rutor Glacier. To analyze the evolution a pre-computed projection was used, carried out in “Open Glacier Global Model” (OGGM) which is an open-source glacier evolution model in python capable of producing per-glacier results using a large quantity of data and parameters (Digital Elevation Models, Gridded Climate Datasets, Geodetic Mass Balances and others). The results are then discussed after the comparison of the calibration data used by the model and an estimation of historical data based on the measurements gathered by different meteorological stations distributed in the area.

1. Introduction

1.1 Climate Change

Climate Change is underlined by the scientific community as one of the biggest challenges humanity has ever faced, mitigation and adaptation plans are according to the vast majority of experts an urgent priority.

The Intergovernmental Panel on Climate Change (IPCC), the globally acknowledged body that investigate causes and consequences on the matter, defines climate change as “a change in the state of the climate that can be identified by changes in the mean and/or the variability of its properties and that persists for an extended period, typically decades or longer. Climate change may be due to natural internal processes or external forcings, or to persistent anthropogenic changes in the composition of the atmosphere or in land use“ (C. Field, 2012). The last agreement on the subject is the Paris Agreement (UNFCCC, 2019), where Nations from all over the world promised to limit the global average temperature increase below 1,5°C, which is still 2°C higher compared with the pre-industrial phase. However, to reach this goal CO_2 emissions should be cut roughly of 50% before 2030 compared with 2015, a milestone that does not look achievable anymore. Adaptation is therefore fundamental to face the inevitable consequences that climate change will put the world through. In different extent, climate change affects every aspect of an environment, depending on the nature of the environment itself: ocean acidification, bio-diversity loss, wildfires floods are just some of the issues that humanity will be forced to face, and all aspects need deepened studies.

Part of the work carried out on the matter in the last years focus on the temperature variation measured across the globe. Many studies shows that temperature variations, and even how temperatures vary in the different environments, is not homogeneous on earth, with different consequences on the various environments.

Among the various discoveries of the studies on the matter in fact, there’s that average temperatures increase faster in cold environments compared with those in warmer environments and that minimum temperatures also increase faster than maximum temperature, narrowing the range of temperatures an environment can

experience. This means that, while climate change is influencing all environments, the cold ones like the poles or high-altitude areas are those being more impacted by the temperature variations. These two results foresee an Earth with more constant and homogeneous temperatures, which is greatly endangering for the vast diversity of environments on Earth.

1.2 Impact of climate change on alpine environments

Being amongst the most sensible environments to these changes, the mountain environments, and consequently the glaciers they host, are highly impacted by climate change. The impacts that climate change has on these environments go further than hotter mountains: higher temperatures across the year and lower minimum temperatures set in motion a series of positive feedbacks related to albedo which impact the snow covers and enhance glacial retreat already with little temperature increments. Higher temperatures reduce flora and fauna's biodiversity, further endangering these frail environments making them less resilient, beside causing the loss and migration of species.

Another impact that climate change has on high mountain is a shift in the tree line, which impact different aspect of the biodiversity in the environment. This phenomenon might favor some tree species and therefore damage the equilibrium with the other species, effect that might cascade on the fauna if animal species feeds on these plants, or if prey animal species can hide in them possibly endangering hunting animal species. (Christian Huggel, 2011)

Evidence also shows that climate change is increasing the amount of landslide events. In fact, by altering temperatures, favoring thawing and movement of ice, exposing once ice-covered areas and higher intensities rainfall are some of the possible aggravating causes of landslides. In particular, studies show how for example once a climatic driven mass movement is triggered, it evolves independently of climate change, or how the precipitation induced landslides are expected to increase due to intense rainfall events, despite the reduction in the precipitation amount (Xin Liu, 2024).

1.3 Impact of climate change on glacier and meltwater

Due to climate change, the water cycle in which snow accumulation and glaciers play a crucial role is also changing, having consequences on both natural and anthropogenic water requiring activities (Daniel Viviroli, 2007). This could impact population directly living on the mountains but also the directly downstream population that use water coming from water towers (W. W. Immerzeel, 2019) for their functioning like agriculture (H. Biemans, 2019) and hydro-power production. Less snow cover also impacts the touristic side of mountains related to skiing and winter sports, a form of tourism that while it could have harmful effects on the environment, is a big economical revenue for mountain communities (Siya Cholakova, 2023).

It is in this aspect of the problem that this master thesis finds its purpose: enhancing monitoring of the glaciers and estimating their melting rate can be considered an adaptation strategy, predicting the amount and the temporal distribution of the water availability, and allowing the human activities to prepare and adapt to the changes in water regimes.

In the field of monitoring glacial masses Polito has been working for years, especially in the last period with the “Glacier Lab” project, a multidisciplinary team of engineers that work together to monitor glaciers and help taking the appropriate adaptation strategies. They tackle various aspects of glacier monitoring such as surveying with aerial and geomatic techniques, snow-ice interactions, speed of the glacial front advancement and precipitations monitoring and analysis, while also perform studies concerning for example materials and technologies that can help minimize glacial melting; an example of work with a multidisciplinary approach taken on the Rutor Glacier, near the glacier object of this study, can be found in (Elisabetta Corte, 2023).

This work focuses on the evaluation of the performance of a Radar rain gauge in high mountain environments through comparison with a weighted rain gauge, and on the prediction of the evolution of “des Usellettes” glacier, a glacial body of modest dimensions located in Valle d’Aosta valley in the municipality of “La Thuile” close to the Rutor Glacier, whose meltwater feed a hydropower turbine owned by a nearby mountain refugee.

2.Data analysis and comparison of on-site station with ARPA station

The data gathered for the study is given by a station implanted by Glacier Lab PoliTO. The station is located at the base of the Rutor Glacier, at around 1.5 km from the Usellettes Glacier, and has been installed around August 2022 (Figure 1). In the station the data gathered can be divided in three main categories: precipitations from a weighted rain gauge, precipitations from a radar doppler sensor, ambient related parameters.

Figure 1 Distance between Glacier Lab station and Usellettes glacier (Google, 2024)

Since the data that this station could gather cover a not very long period, the data was compared with that of the closest ARPA station (Centro Funzionale Regione Autonoma Valle d'Aosta, 2023), La Thuile - La Grande Tête, to have a longer period of data for the modeling of the melting and to check if this longer data had to be corrected to be more accurate with the Usellettes area. The ARPA's station measures the same parameters that are measured by the Glacier Lab, the only difference being in the precipitation measurements, which is split in liquid precipitation and height of the snow from the ground. ARPA's station "La Grande Tête" is located in the

municipality of La Thuile in a valley which has the same name. It is situated at 2430 meters on the sea level and situated at around 7 km from the GlacierLab station (Figure 2).

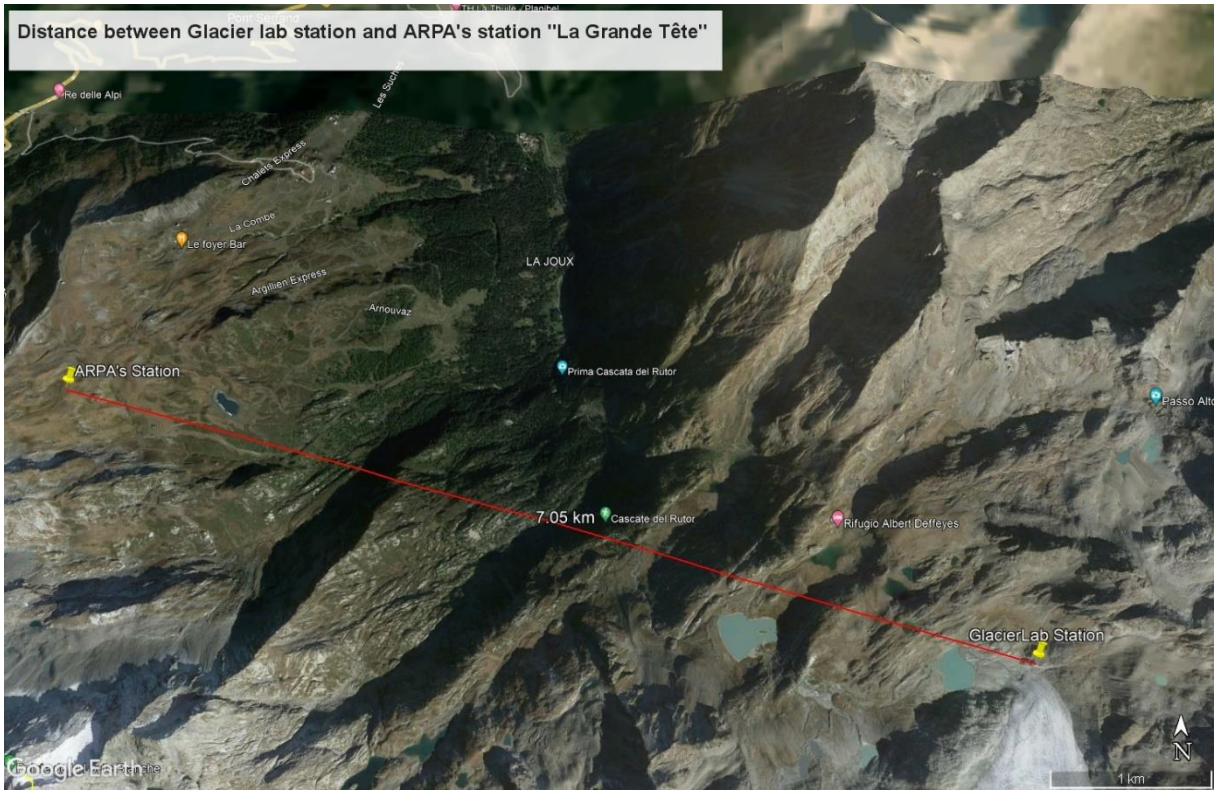

Figure 2 Distance between ARPA's station and Glacier Lab station (Google, 2024)

The ambient related parameters measured by both the station and glacier lab are temperature, relative humidity, pressure, radiation, wind velocity and wind direction.

It must be noted that the GlacierLab station, had some events of data loss. The data loss was due to a not optimal management of the server recording the data, that reached a full capacity and stopped storing data. The missing data, however, affected not all the machinery, but just the instrument measuring ambient parameters. The data recorded, compared with the ARPA's station, was enough to extrapolate a good approximation of the past data. The periods of missing data are the following:

1) From the 25/10/22 to the 17/11/22;

2) From the 24/12/22 to the 2/1/23;

3) From the 19/5/23 to the 17/7/23;

4) From the 14/11/23 to the 8/12/23.

2.1 Comparison of ambient parameters.

To validate the use of past data from the ARPA's station "La Grande Tête" all the parameters have been compared with the parameters measured by the Glacier Lab station. The comparison has been made, when it was possible and it was reasonable to do so, on both a daily and an hourly timescale, based on the nature of the parameter. In some of the parameters there might have been outliers clearly due to instrument or systematic errors which were correctly treated and/or removed.

Pressure

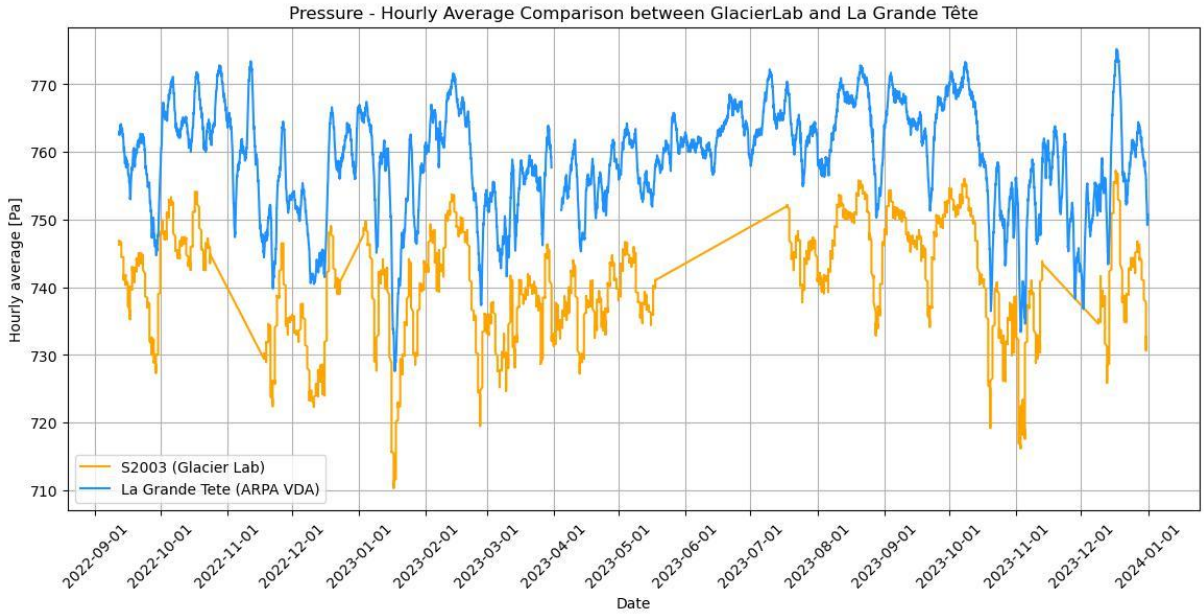

Figure 3 Pressure, hourly comparison between ARPA and GlacierLab

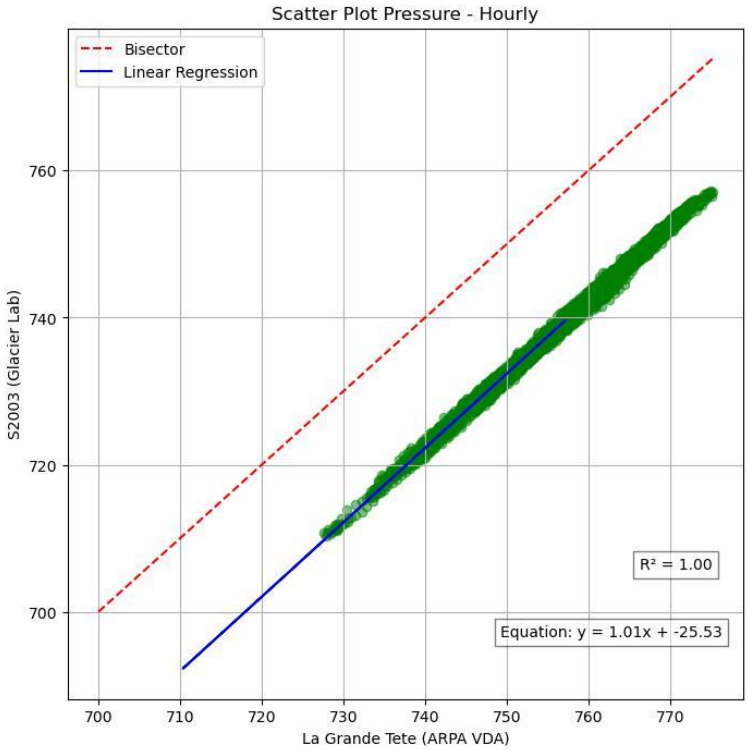

Figure 4 Pressure, hourly scatterplot between ARPA and GlacierLab

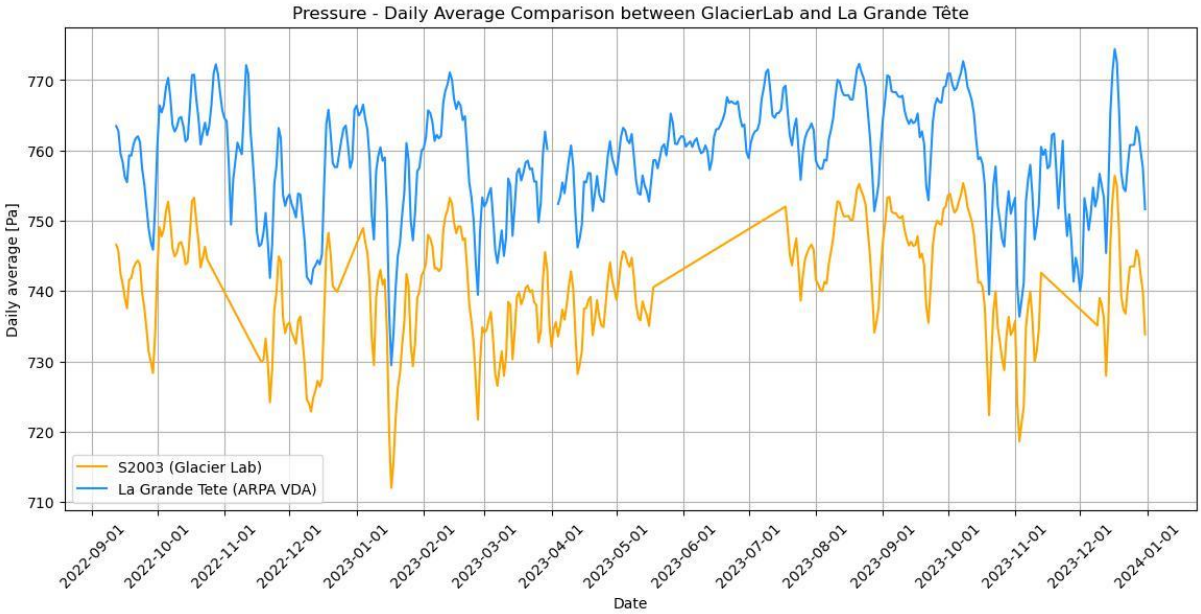

Figure 5 Pressure, daily comparison between ARPA and GlacierLab

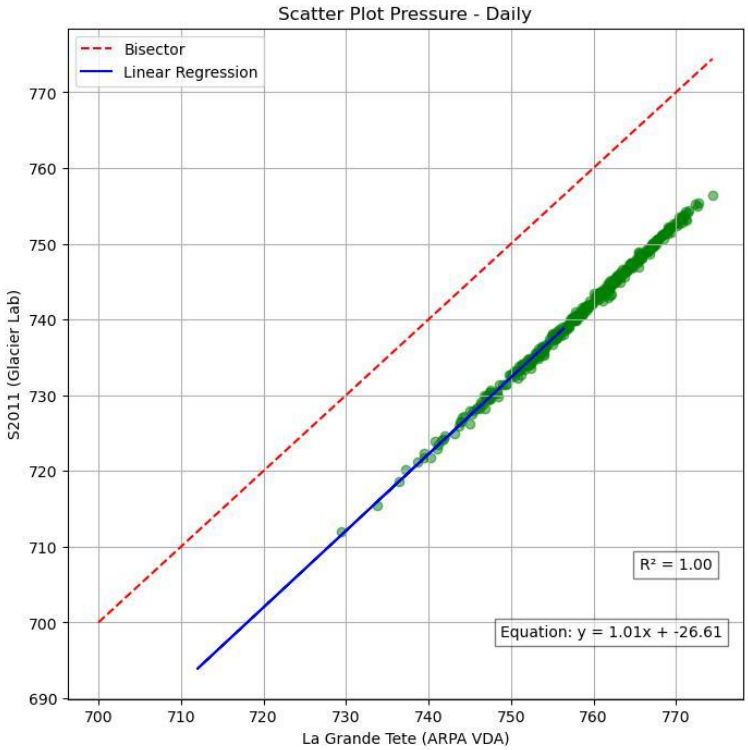

Figure 6 Pressure, daily scatterplot between ARPA and GlacierLab

Pressure comparisons are reported in figures 3, 4, 5, 6.

Pressure is one of the most direct methods to see if the instrument is working correctly. The obtained result is the expected one: the pressure is about the same in both places with a bias due to the altitude difference of the two stations.

The data is therefore very correlated, the data in the scatterplot is correctly aligned and shifted toward the ARPA's station side, since it's at lower altitude and at higher pressure.

Relative Humidity

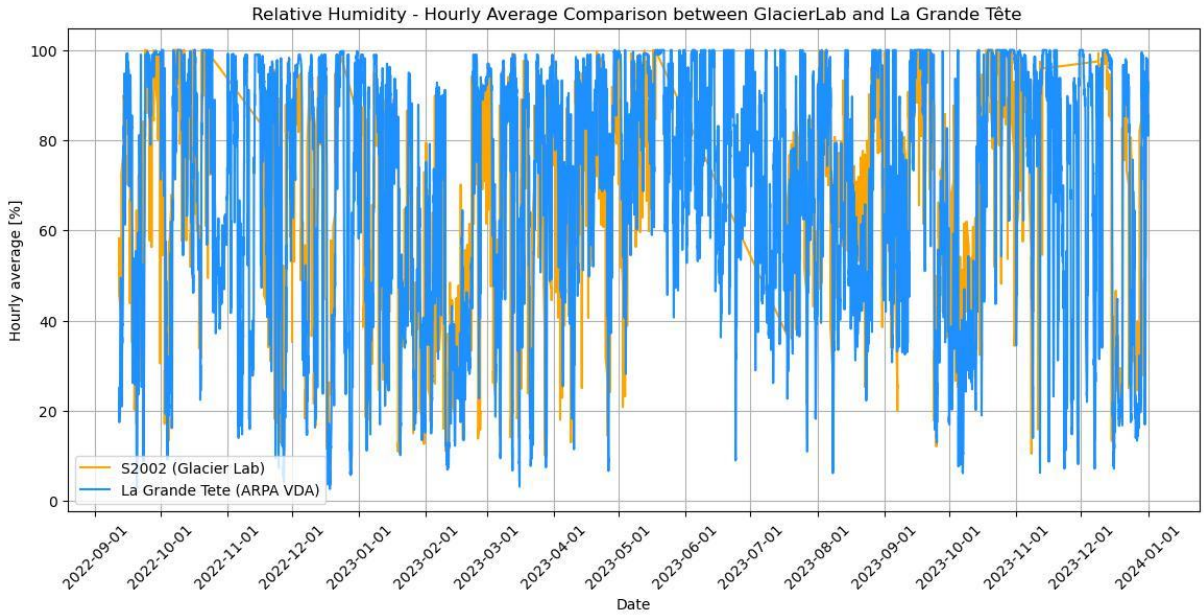

Figure 7 Relative Humidity, hourly comparison between ARPA and GlacierLab

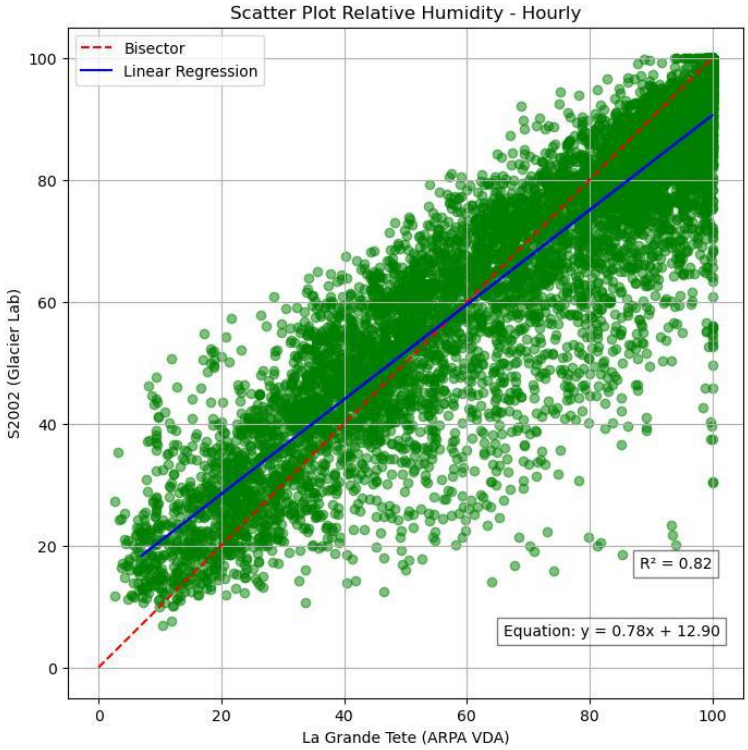

Figure 8 Relative Humidity, hourly scatterplot between ARPA and GlacierLab

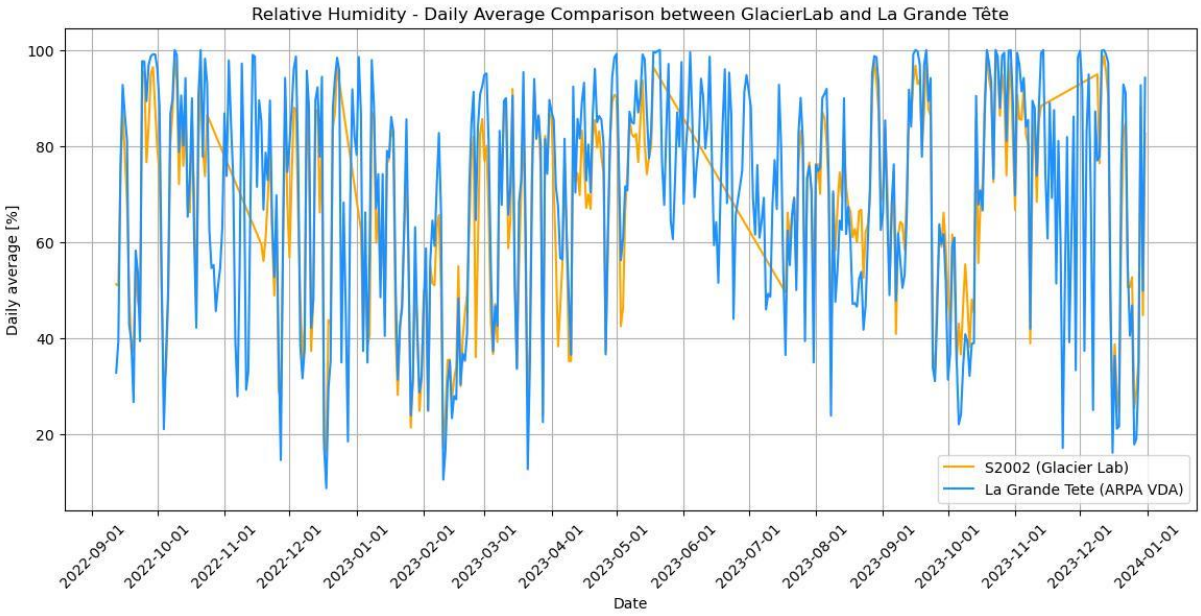

Figure 9 Relative Humidity, daily comparison between ARPA and GlacierLab

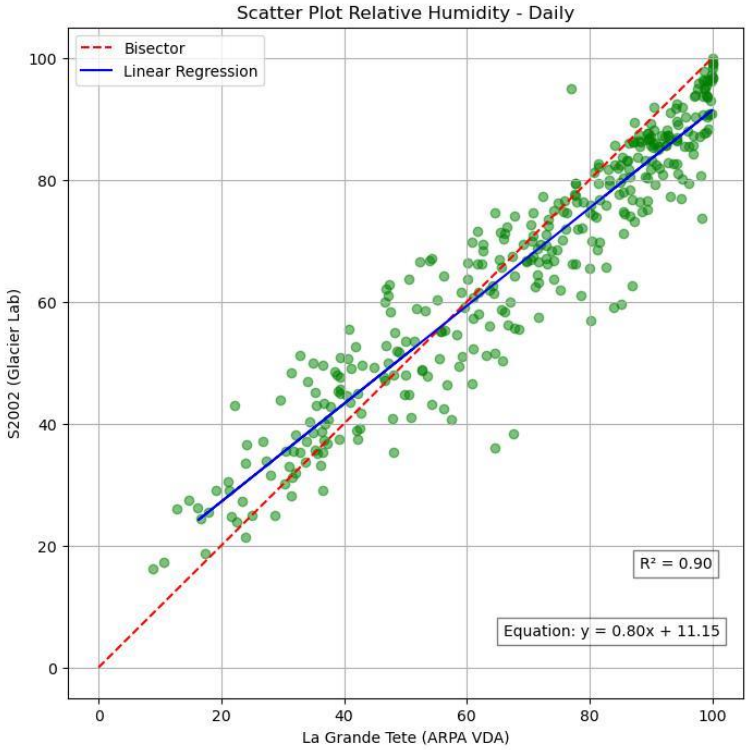

Figure 10 Relative Humidity, daily scatterplot between ARPA and GlacierLab

Relative humidity comparisons are reported in figures 7, 8, 9 and 10.

In Relative Humidity is harder to find a correlation since it is very dependent on the surrounding of the measurement. The data is however well correlated. It's noticeable in the hourly scale how the uncertainty of the regression is higher but the fit give still a good result. In the hourly timeseries are notable both day to night and seasonal variations. In the hourly scatterplot is also notable how relative humidity tends to be higher at lower altitudes when we are close to saturation. The measurements are reported in percentage.

Irradiance

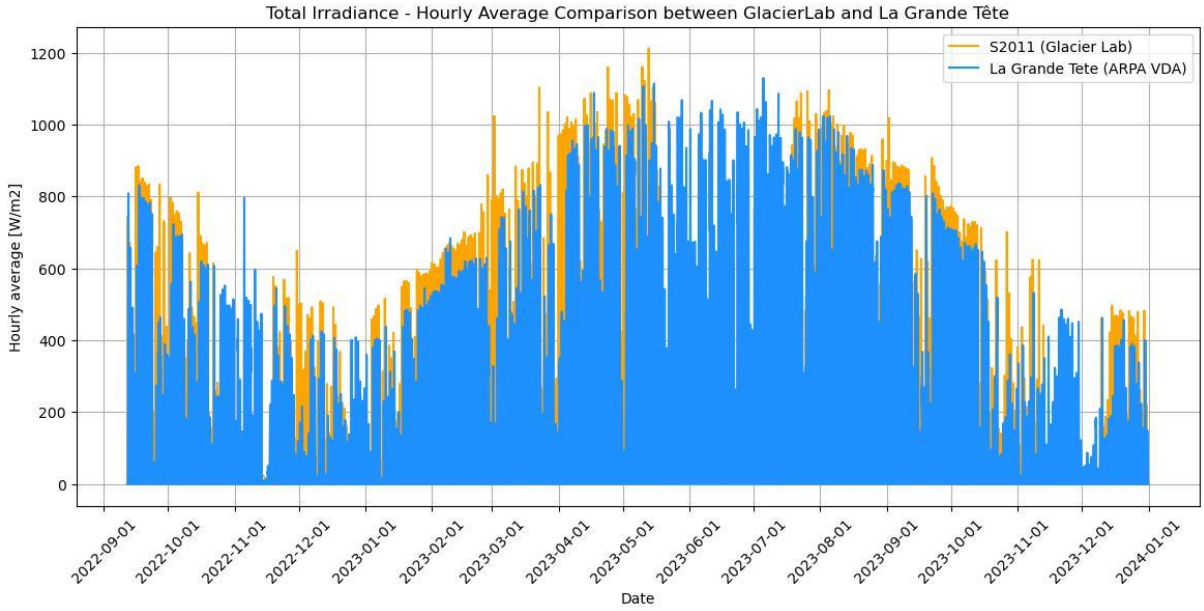

Figure 11 Irradiance, hourly comparison between ARPA and GlacierLab

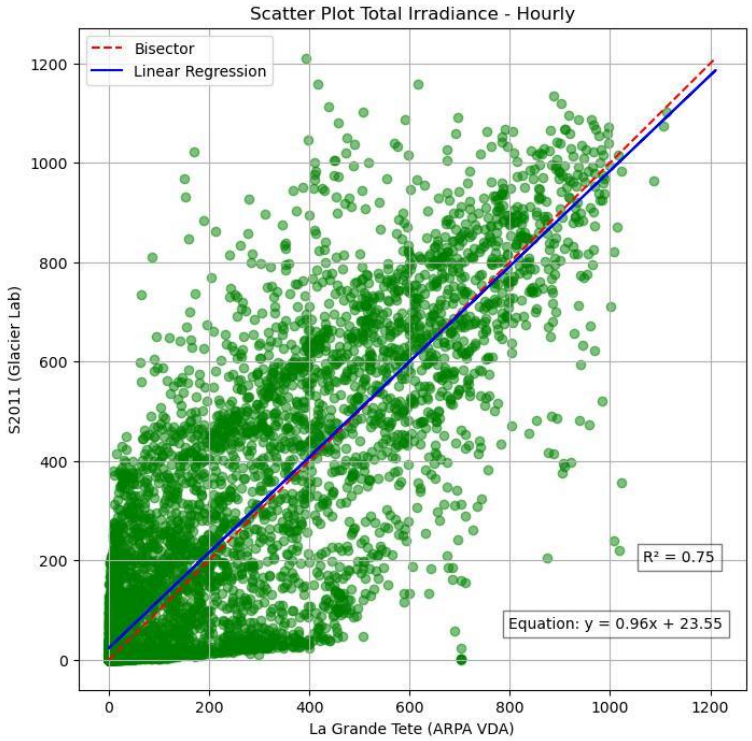

Figure 12 Irradiance, hourly scatterplot between ARPA and GlacierLab

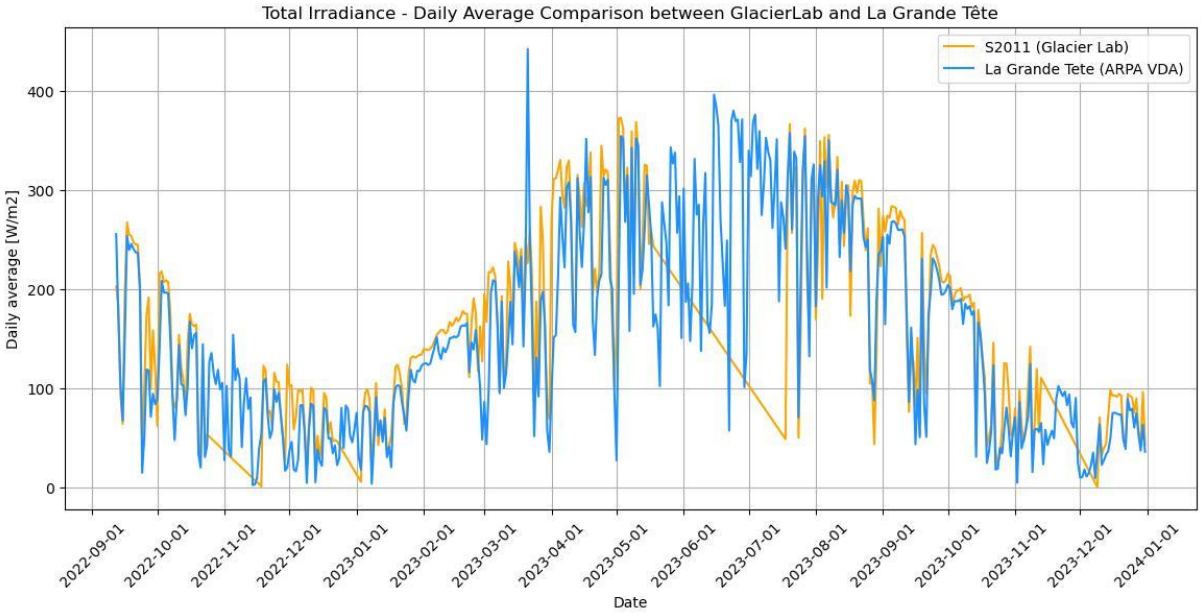

Figure 13 Irradiance, daily comparison between ARPA and GlacierLab

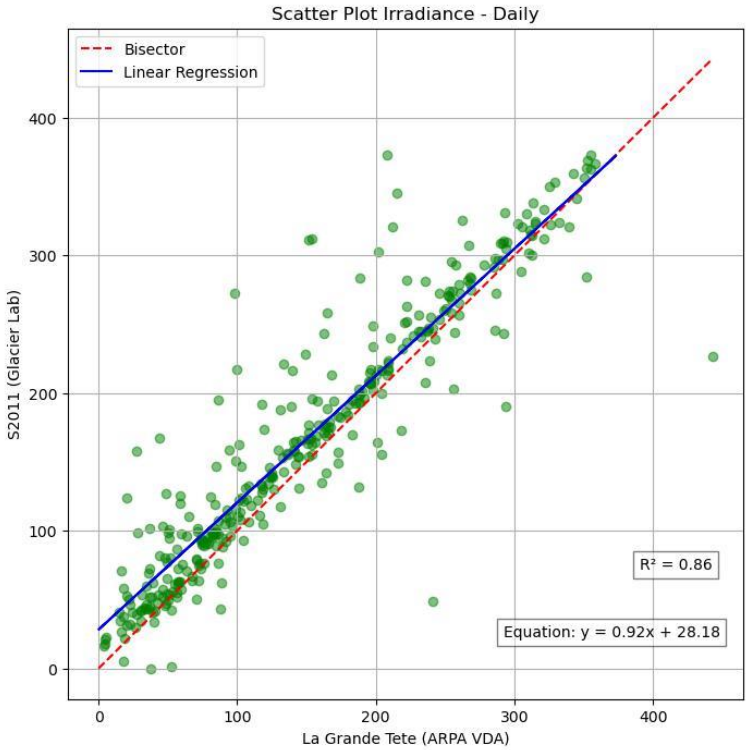

Figure 14 Irradiance, daily scatterplot between ARPA and GlacierLab

Reported in figures 11, 12, 13 and 14 are the Total Irradiance comparison measured by the stations. It's clear how at higher altitudes the Irradiance is always higher, since there's less air that can absorb the heat power emitted by the Sun. A peculiarity of this graph is the clear seasonality of the parameter, while in the hourly graph a lot of measurements report a zero value since they happen at night.

The scatterplots give the expected results also in this case. In the hourly scatterplot the many measurements in the night or in the first hours of the day deviate the regression on a lower ending. In the daily scatterplot is noticeable the observation made above: the irradiance at higher altitude is always a little higher, most of the points look aligned above the bisector. In both cases the regressions obtain a decent but not impressive R^2 score.

2.2 Temperature analysis

The temperature analysis has been deepened compared with the other parameters because of its importance in the melting model. Average, Maximum and minimum temperatures are provided by the PoliTO's station, while temperatures recorded by

ARPA are a single temperature value on an hourly timescale; therefore, temperatures have been compared on average, maximum and minimum terms but there's no difference in those represented by ARPA on an hourly scale.

Average Temperatures

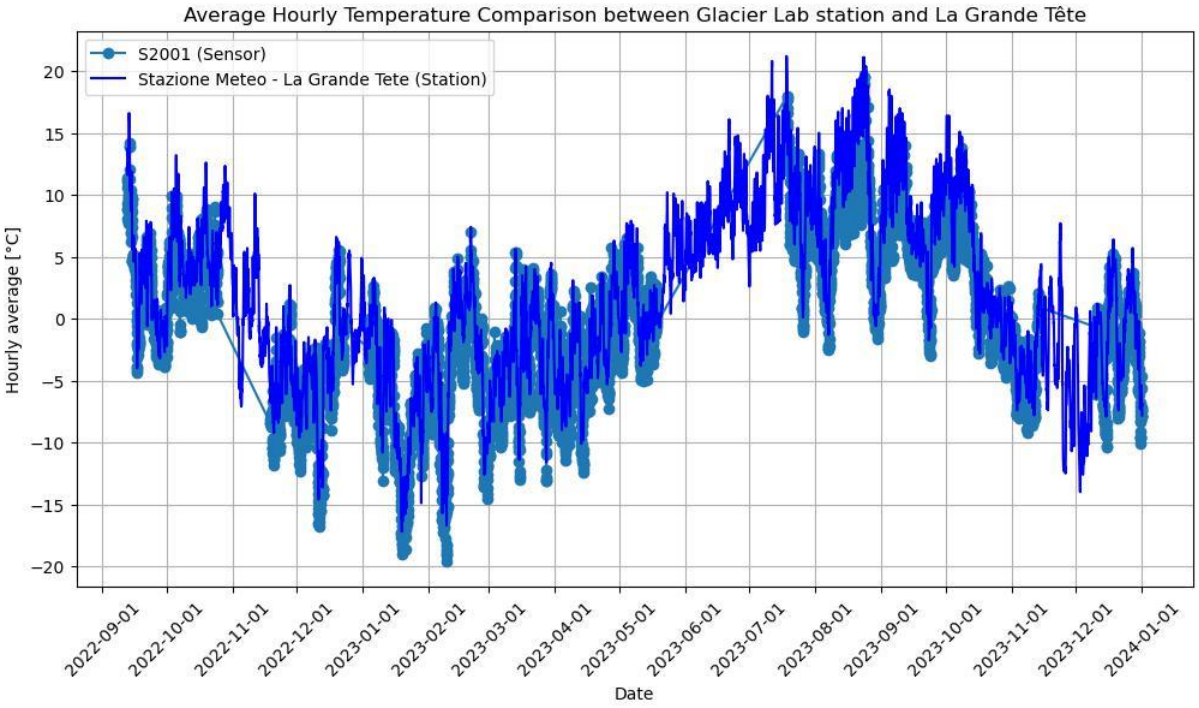

Figure 15 Average Temperature, hourly comparison between ARPA and GlacierLab

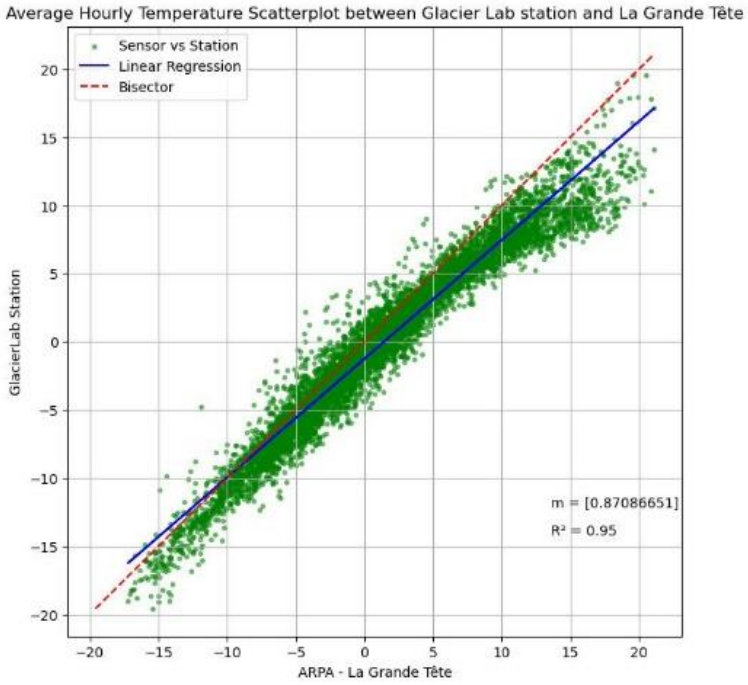

Figure 16 Average Temperature, hourly scatterplot between ARPA and GlacierLab

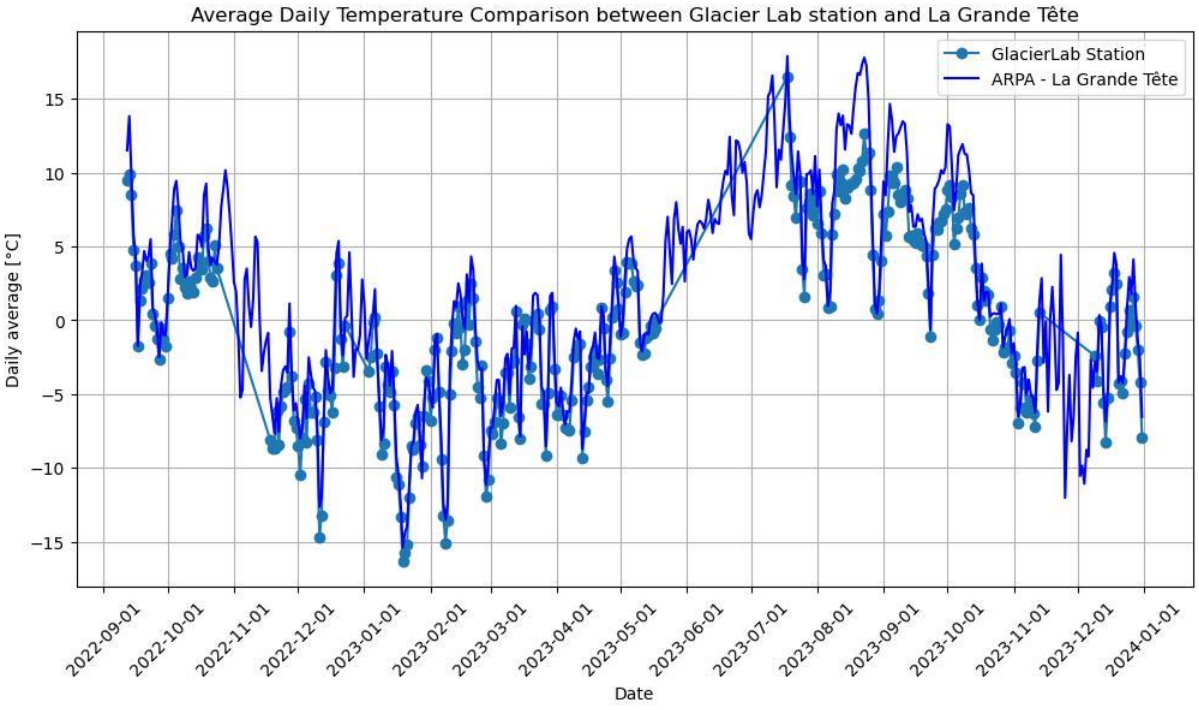

Figure 17 Average Temperature, daily comparison between ARPA and GlacierLab

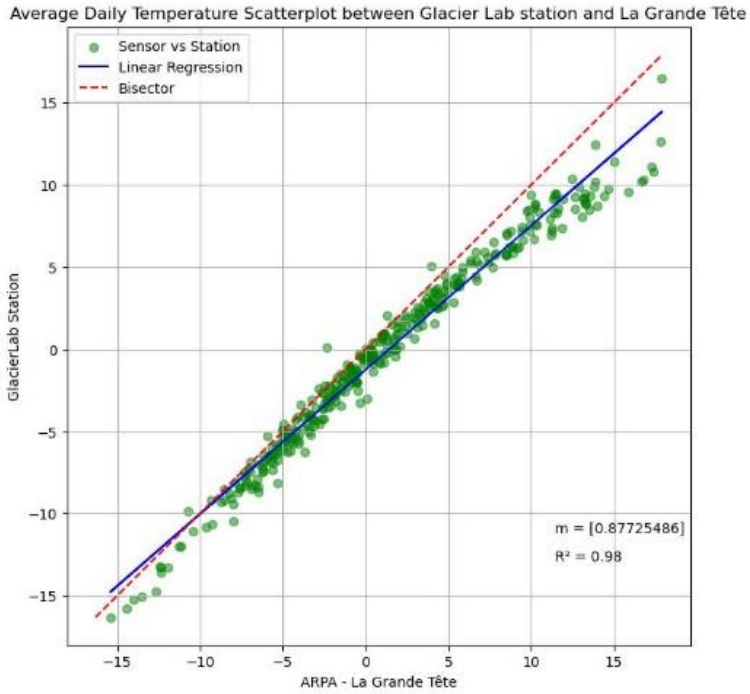

Figure 18 Average Temperature, daily scatterplot between ARPA and GlacierLab

Average Temperatures comparisons and scatterplots between the two stations are reported in figures 15, 16, 17 and 18.

The temperatures measured in the two stations are similar but with a bias due to altitude; temperatures at lower altitudes result higher than at higher ones. In the hourly scatterplot we can see how the points are well correlated and how to regression fits very well most of the points but not really the tails of the distribution, missed in the lower one and close but not enough in the upper one; this could be due to both a mathematical reason and a physical one. Being most of the points being in the center and top of the distribution the regression tends mostly toward ARPA in the upper part, but it could also be a symptom of the higher increase rate in the lower temperatures compared to higher temperatures. This effect is present also in the daily scatterplot even if it's less accentuated thanks to the lower number of measurements.

Maximum Temperatures

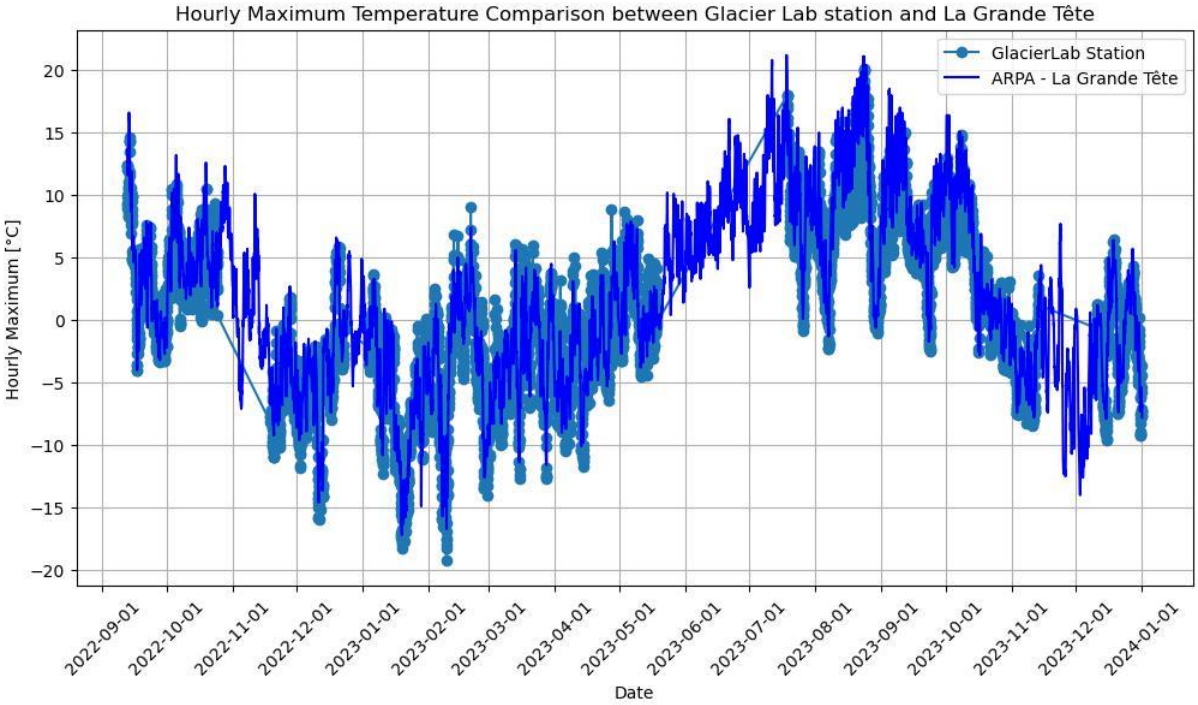

Figure 19 Maximum Temperature, hourly comparison between ARPA and GlacierLab

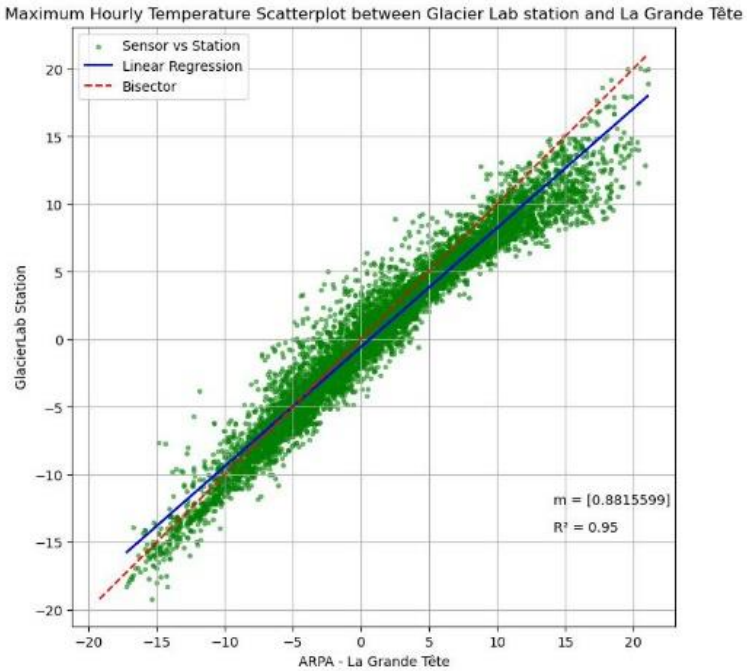

Figure 20 Maximum Temperature, hourly scatterplot between ARPA and GlacierLab

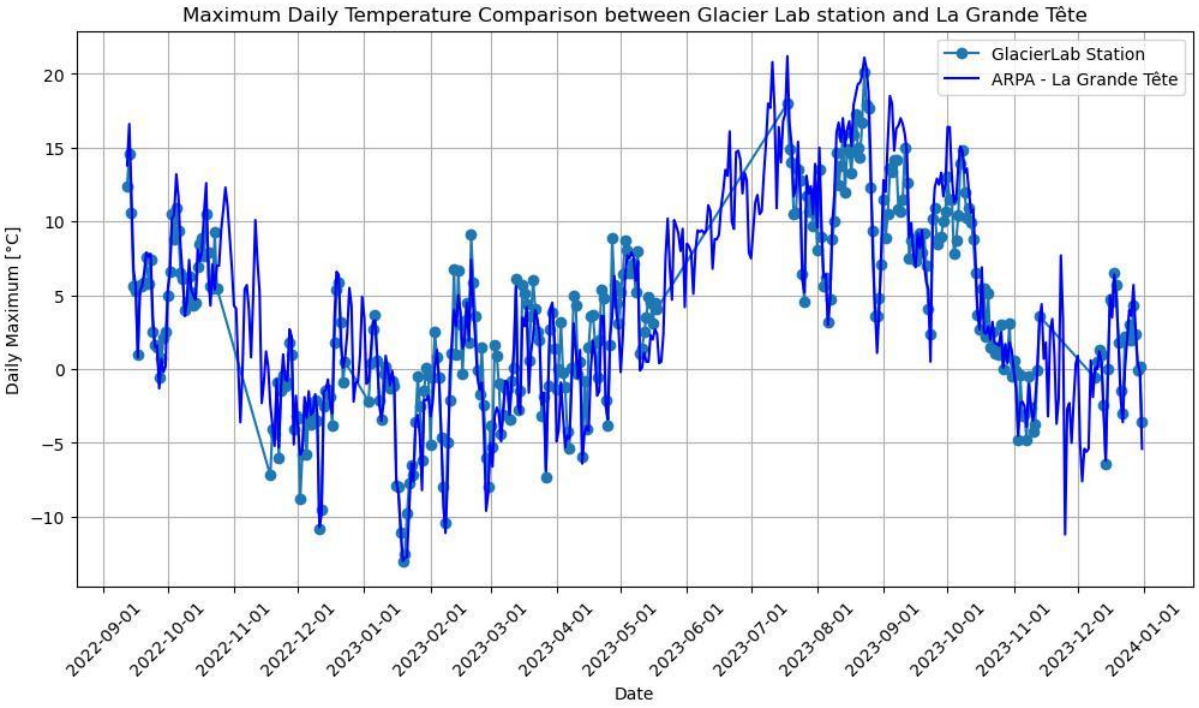

Figure 21 Maximum Temperature, daily comparison between ARPA and GlacierLab

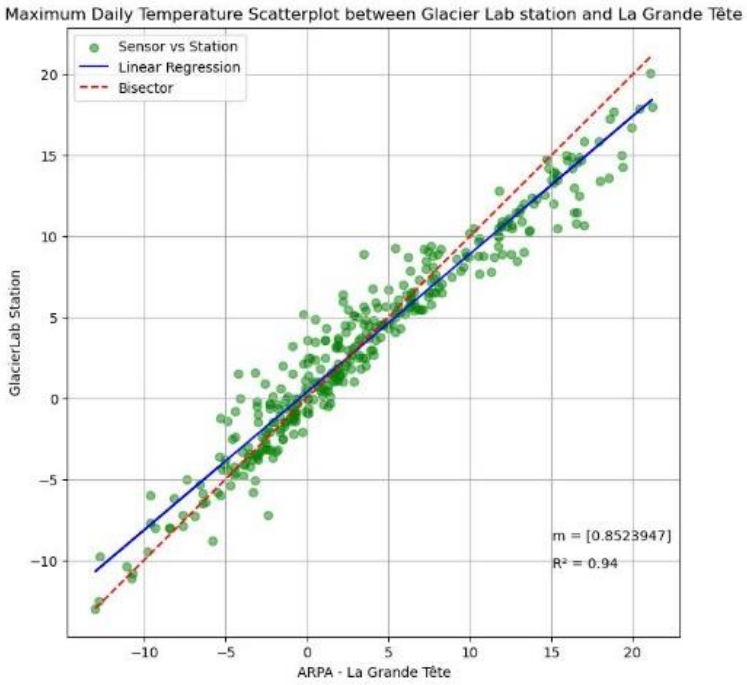

Figure 22 Maximum Temperature, daily scatterplot between ARPA and GlacierLab

The daily graphs in figures 21 and 22 show that there are many days where the maximum temperature is higher at the Rutor's foot than at La Thuile. The majority of points are however still oriented toward the ARPA's station, and the regression obtain a good R^2 score. In figure 19 and 20 are reported hourly time scale comparison and scatterplot.

Minimum Temperatures

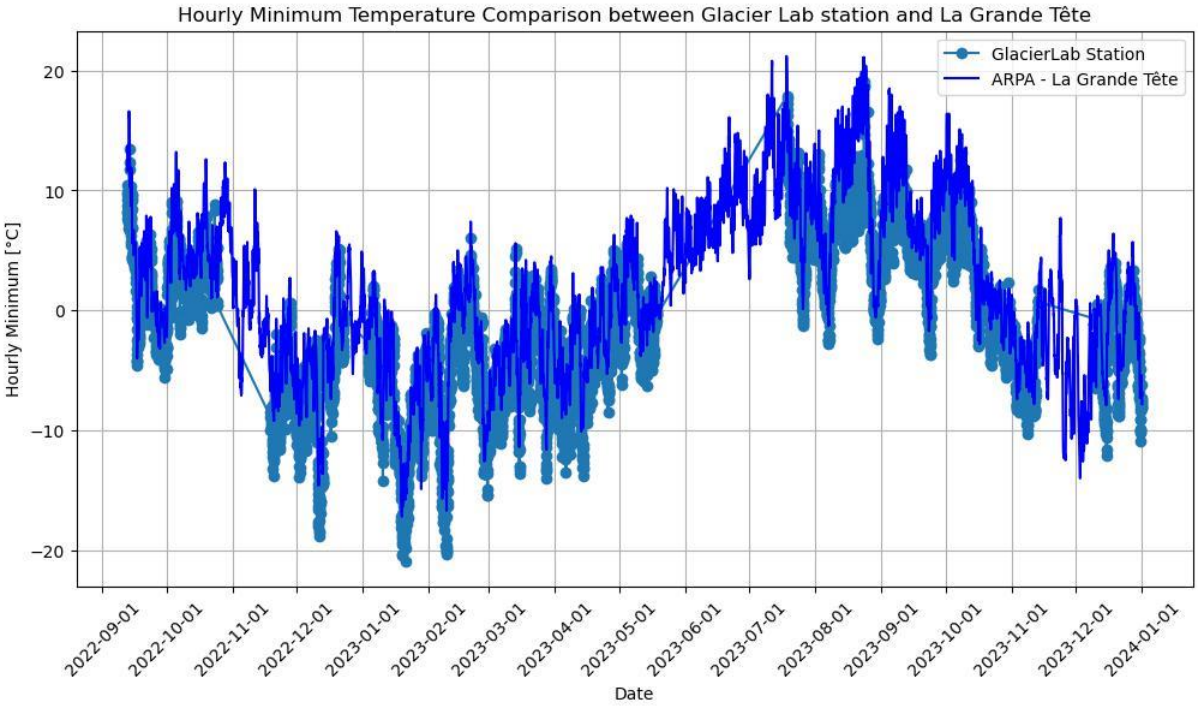

Figure 23 Minimum Temperature, hourly comparison between ARPA and GlacierLab

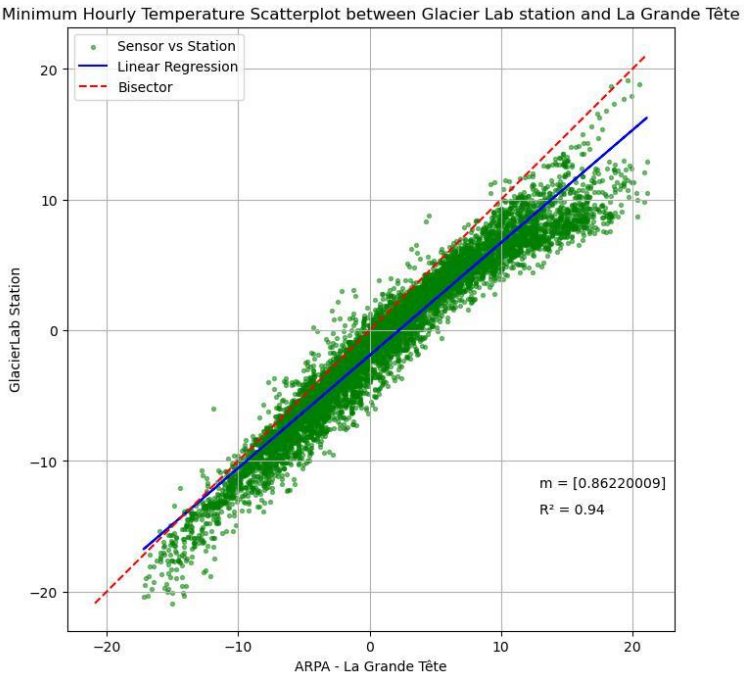

Figure 24 Minimum Temperature, hourly scatterplot between ARPA and GlacierLab

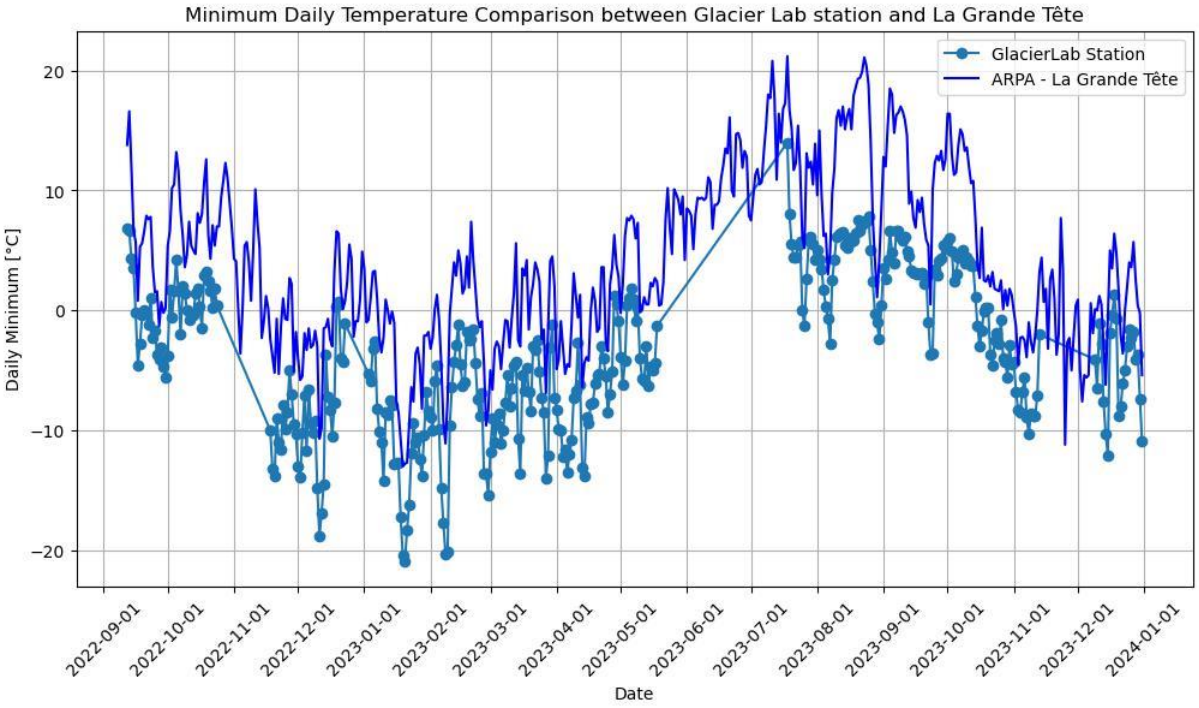

Figure 25 Minimum Temperature, daily comparison between ARPA and GlacierLab

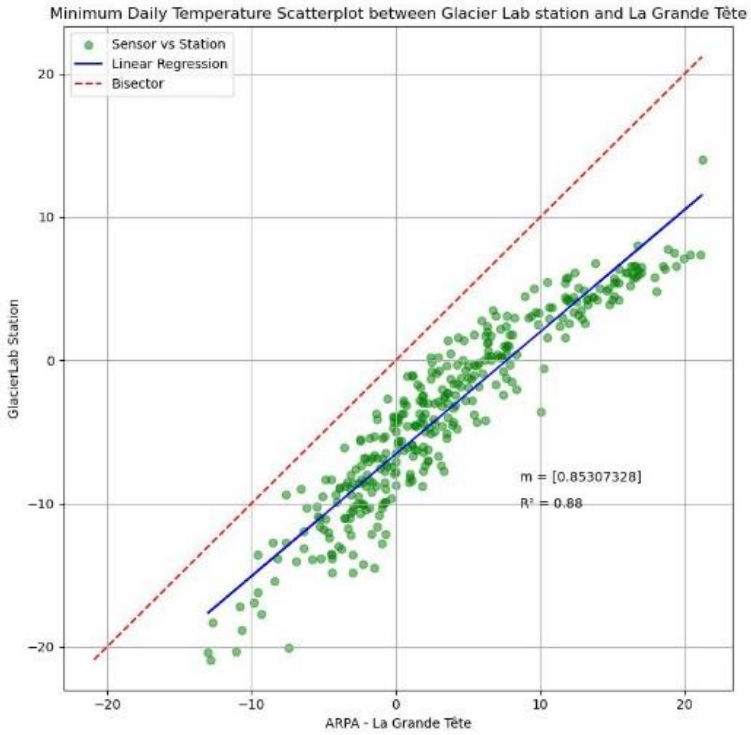

Figure 26 Minimum Temperature, daily scatterplot between ARPA and GlacierLab

Figures 23, 24, 25 and 26 reports comparisons and scatterplots about minimum temperatures. In the timeseries is clear how the minimum temperatures are always at the higher altitudes. While this is true at a daily scale, it can of course be false at an hourly timescale since a cloud is enough to change the single data. The regression in

the daily scatterplot is correctly shifted towards the ARPA's station since the temperatures are always higher than those recorded by the Glacier Lab's station. The hourly scatterplot tends correctly toward ARPA but doesn't show a shifted linear regression as in the daily scatterplot; this is due to same effect discussed above, the vast majority of points are in the middle and many on the top end but few in the bottom end.

2.3 Precipitation Analysis with weighed rain gauge comparison.

The precipitations assumed as a ground truth measured by the Glacier Lab station were those of a weighting, non-heated, recording rain gauge. Those data were compared with the precipitation measurements recorded by a weighting, non-heated rain gauge located in La Thuile owned by ARPA; this comparison allows to evaluate the difference in precipitation due to height and basin's side. The weighted rain gauge owned by ARPA is installed in the same station where the instrument that measured ambient parameters is also located, a picture of it is reported in figure 27.

Figure 27 OTT Pluvio2, weighted rain gauge.

ARPA publishes for all their instruments an hourly timescale, the precipitation measured is the sum of the amount of rain fallen within the hour. ARPA does not include snow in the precipitation timeseries but measures the snow height from the ground, with the use of the Snow Water Equivalent (Equation 1) these two series has been merged into the correct precipitation series. A density of 350 kg/m^3 has been assumed for snow.

Equation 1 Snow Water Equivalent equation

$$SWE = H_{snow} * \rho_{snow}$$

In figure 28 is shown the total precipitation measured by ARPA with snow converted into water equivalent included and corresponding to the same period of data available in the PoliTO station, while in figure 29 is reported the precipitation regime at La Grande Tête.

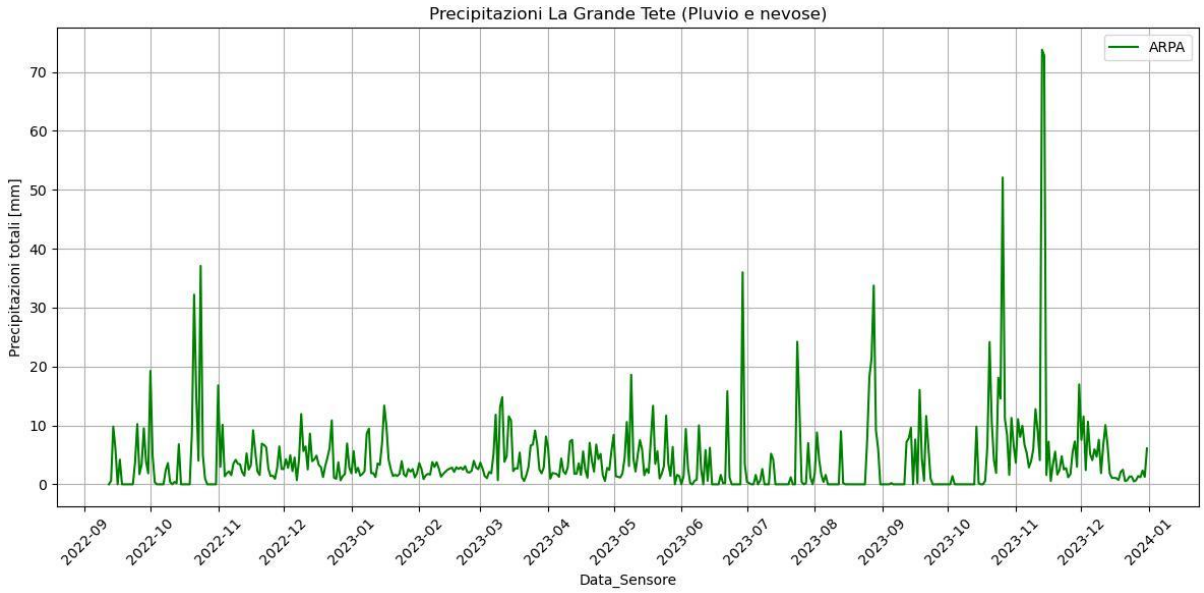

Figure 28 Total Precipitation ARPA – Daily timescale.

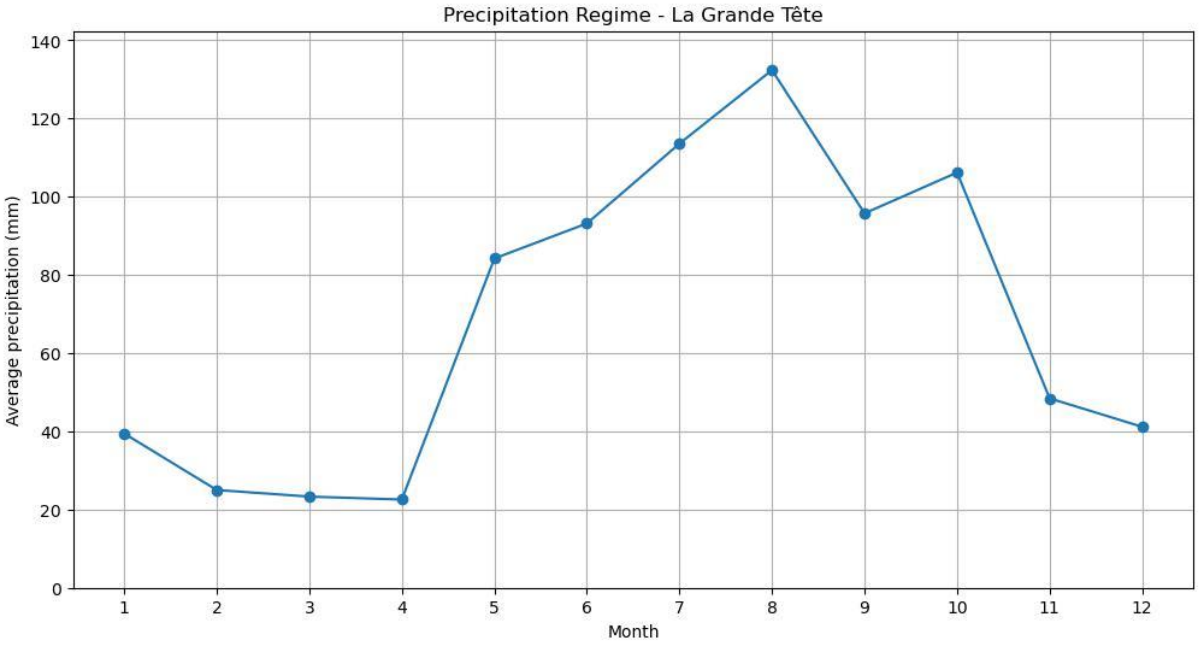

Figure 29 Precipitation regime, ARPA – "La Grande Tête"

The GlacierLab instruments measures at a fine timescale, recording measurements every 5 minutes, that while it can be useful to compare them between them and to have a higher understanding of the dynamics in the area, is not useful to compare it with ARPA's instrument since it has a bigger time scale. ARPA's finest timescale is the hourly one, but considering the distance between the stations a more useful time scale is the daily one, since a finer timescale might cause lag in the recording due to traveling precipitation event. In figure 30 are reported the daily measurements of both the instruments, while in figure 31 the cumulative sum of the precipitations in the two station is reported. The shape of the two curves is very similar and a couple of phenomena can be identified here; there are periods (for example the one around the February 2023) where the Glacier Lab curve reports a flattening that can be accused to a lack of precipitation at high altitude, but there are other events (for example end of May 2023) where a flattening period is followed by a quick growth which is due to melting of the snow cap that can form on the rain gauge. After the whole period of the analysis, ARPA reaches a value around 1950 mm, while the weighting rain gauge reaches a value around 1450 mm, resulting in a difference in the cumulative precipitation around 500 mm.

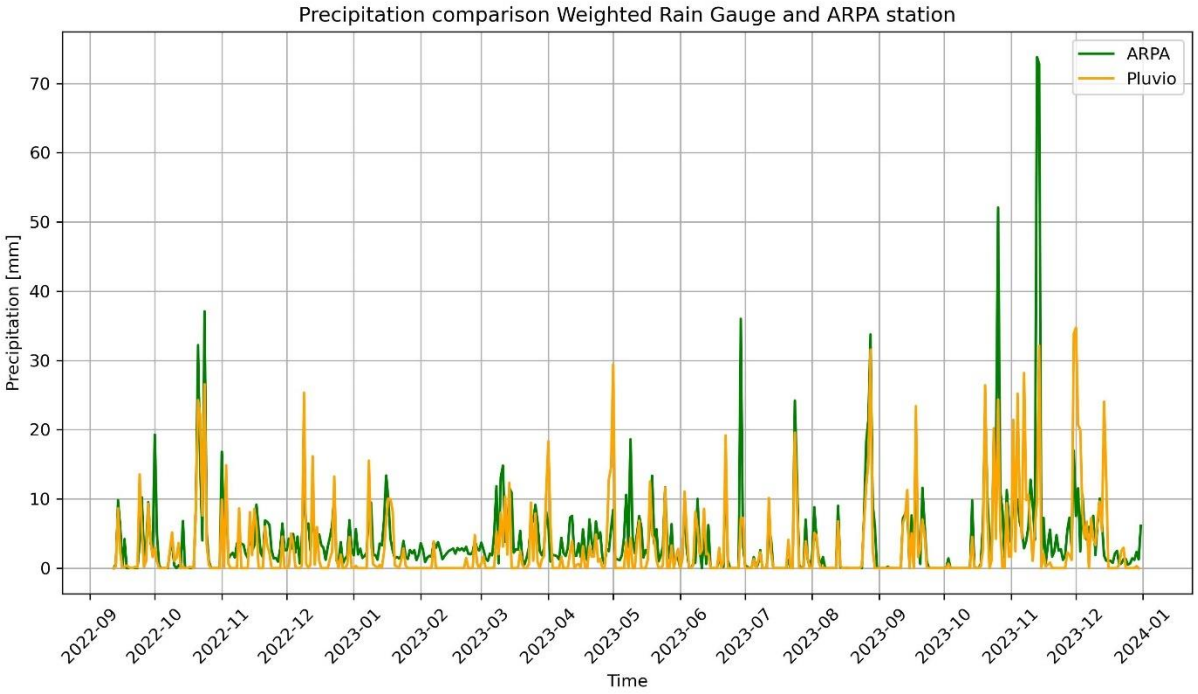

Figure 30 Precipitation, daily comparison ARPA and weighted rain gauge.

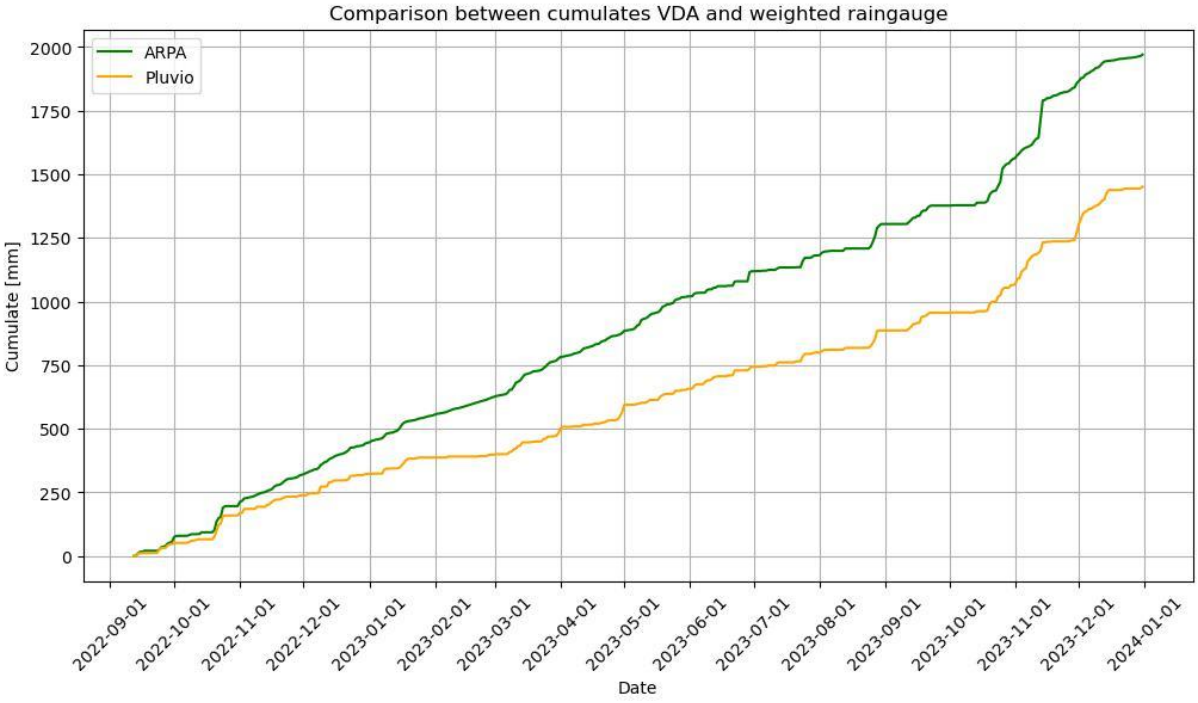

Figure 31 Precipitation, comparison of cumulates according to ARPA and weighted rain gauge.

3.Radar Rain Gauge and Evaporation Analysis

As explained by (S. Ochoa-Rodriguez, 2019), “Rain gauge is a broad term, which can be used to refer to any instrument employed to measure the amount of liquid precipitation over a set period.” Rain gauges are widely used instrument that provide low-cost direct and relatively accurate point rainfall estimates. They can be categorized according to various characteristics; a rain gauge can be catching or non-catching if it retains (or not) the water it is measuring. Among the non-catching rain gauges category falls the optical or acoustic rain gauges, while in the catching rain gauges category falls the weighted rain gauges and tipping bucket rain gauges. Another categorization can be made if a rain gauge is recording or nonrecording; recording rain gauge measures precipitation automatically by means of mechanical and/or electronic mechanisms and can provide measurements at finer timescale, while nonrecording rain gauges collect volumes of water over a set period of time that must be measured manually. The rain gauges object of this study are both recording rain gauges, but differ in the catching category.

Rain gauge measurements are subject to two main sources of error:
- instrumental errors, which include systematic, local random, and malfunction errors
- spatial sampling errors (SSEs), related to the spatial representativeness of point rain gauge measurements. In order of general importance, systematic errors common to all rain gauges include errors due to wind effects (including wind deformation due to poor siting and localized field deformation above the gauge orifice), wetting loss in the internal walls of the collector, evaporation from the container, and errors due to in and out-splashing of water.

Further details on the rain gauges categorization and functioning can be found in (S. Ochoa-Rodriguez, 2019)

3.1 Radar rain gauge performances analysis and evaluation

A picture of the radar rain gauge installed in the Glacier Lab station is reported in figure 32. WS-100 is an optical rain gauge, meaning that it works through the reflection of electromagnetic waves. The rain gauge emits waves constantly at a frequency of 24-GHz and with a radar sensor it measures those returning to the instruments, that coupled with a time difference allows to measure precipitation. This kind of instruments have some perks compared to weighted rain gauges since they can not only measure the quantity but also the type of precipitation, while also keeping a lower cost of the instrument and lower maintenance. However these benefits come with a trade-off, and the precision of the instrument is usually lower; the manufacturers guarantee a precision of ±0.16mm or ±10% of the measured value for liquid precipitation (HydroMet, 2023). Since the instrument is also able to identify different types of precipitations, in this study is assessed the performance of this instrument also with precipitation different from liquid, especially snow.

Figure 32 Lufft WS-100 Radar rain gauge. (HydroMet, 2023)

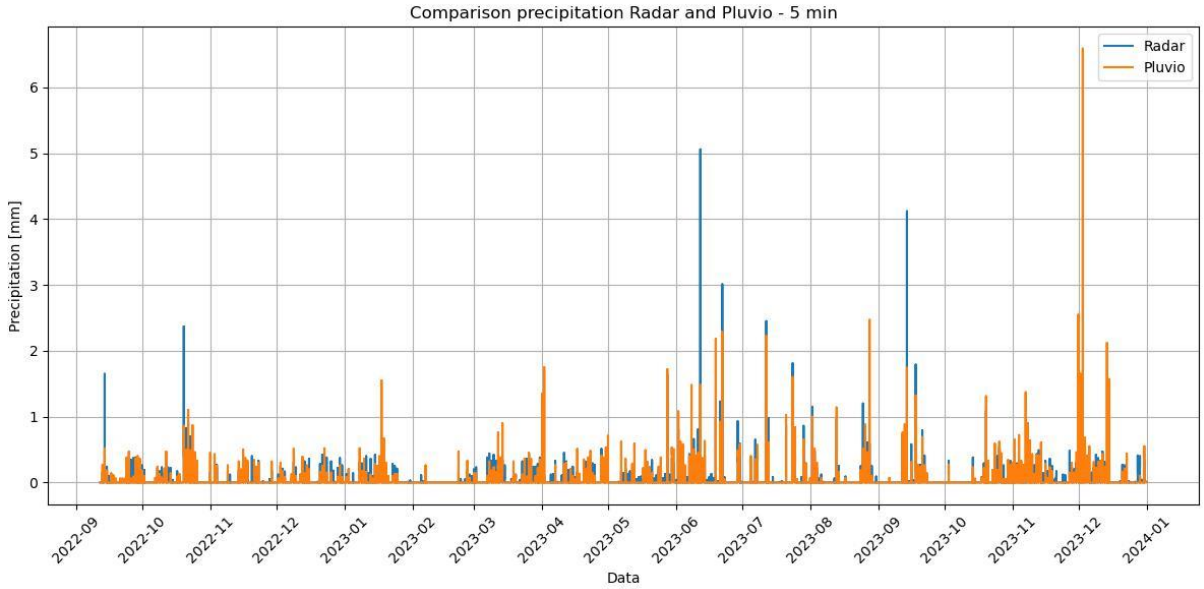

Figure 33 Precipitation, 5min comparison Radar and Weighted rain gauge.

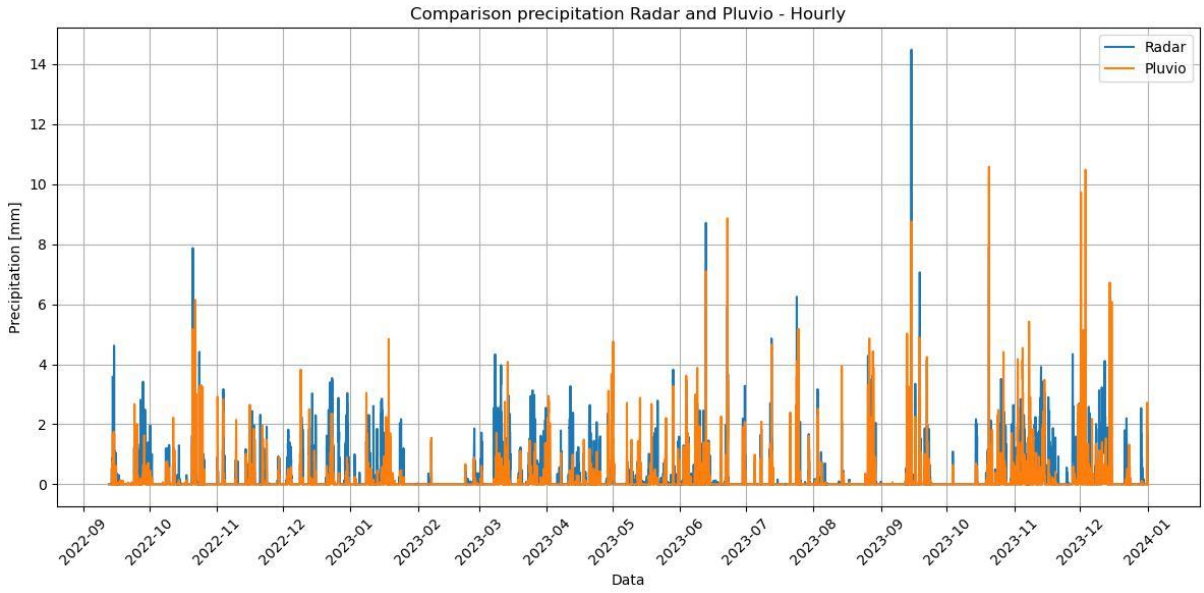

Figure 34 Precipitation, hourly comparison Radar and Weighted rain gauge.

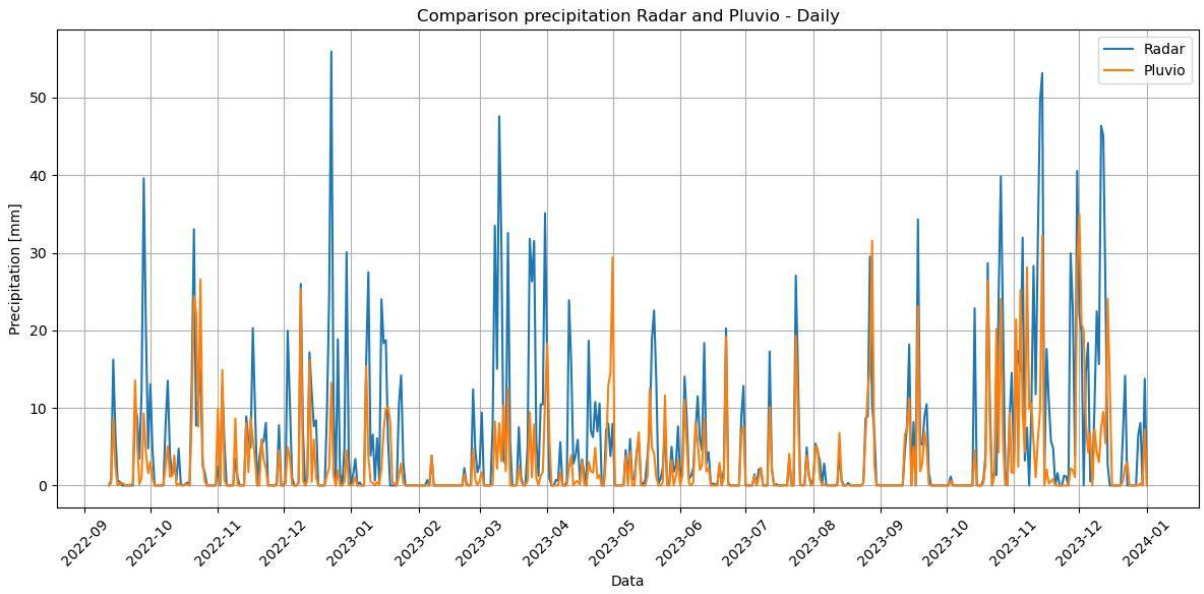

Figure 35 Precipitation, daily comparison Radar and Weighted rain gauge.

In figures 33, 34 and 35 are reported the measurements of the two instruments at 5 minutes, hourly and daily timescale respectively; it is evident and is even clearer with the representation of the differences, that the radar rain gauge overestimates the precipitations in almost all the measurements, but the error is not systematic, and fairly distributed. In the differences reported in figures 36, 37 and 38 if the value is positive the measurement is an overestimation of that amount, if it is negative, it is an underestimation.

A first comment can be made about the distribution and entity of the errors: in the winter periods where precipitation is most likely snow the radar overestimates (first winter) the measurements or the error is very distributed (second winter), but in the summer periods the precipitation is surely liquid and the error is much smaller. Also, an argument can be made about the events where error in a direction is quickly compensated with an error in the opposite direction, since it could be again due to accumulation of snow on top of the weighted rain gauge which is recorded only after it melts or falls in the bucket. A scatterplot of the daily precipitation is reported in figure 39, the points lean toward the radar rain gauge axis confirming the global overestimation, but are scattered without showing any correlation.

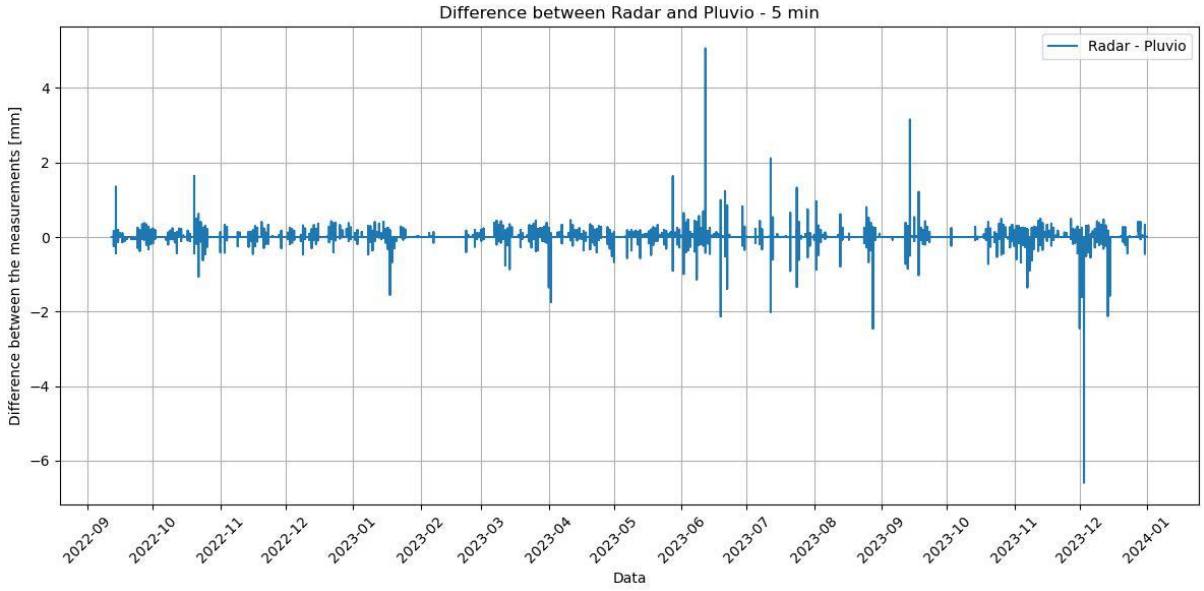

Figure 36 Precipitation, 5min difference of Radar and Weighted rain gauge measurements (Radar – Pluvio)

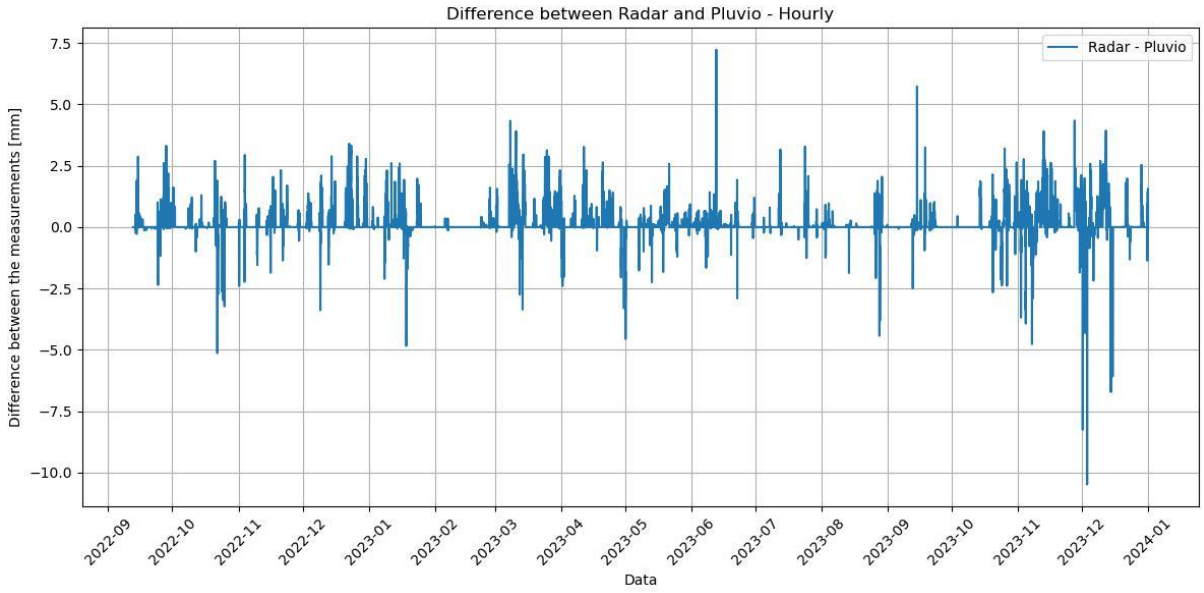

Figure 37 Precipitation, hourly difference of Radar and Weighted rain gauge measurements (Radar – Pluvio)

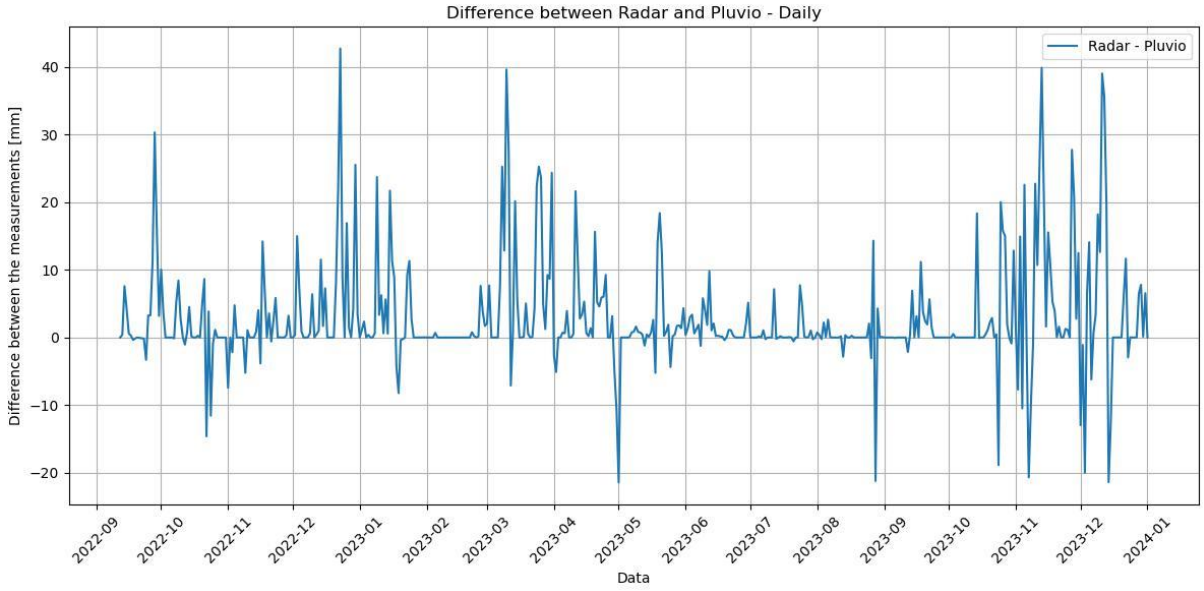

Figure 38 Precipitation, daily difference of Radar and Weighted rain gauge measurements (Radar – Pluvio)

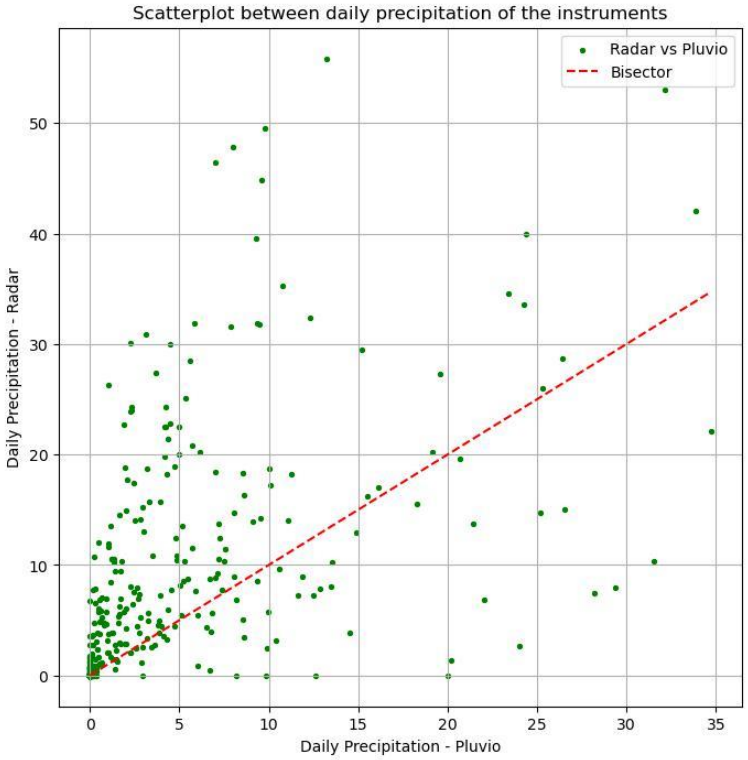

Figure 39 Precipitation, daily scatterplot Radar and Weighted rain gauge.

In figure 40 are reported the cumulates of the two instruments. The shape of the curves is similar meaning that the radar correctly detects the precipitation events, but the entity of the measurements is different. Considering the whole season of data, the difference is corresponding to almost 200%: Radar rain gauge records 2760 mm

and the weighted rain gauge records 1450 mm, corresponding to a difference of more than a 1300 mm on a year.

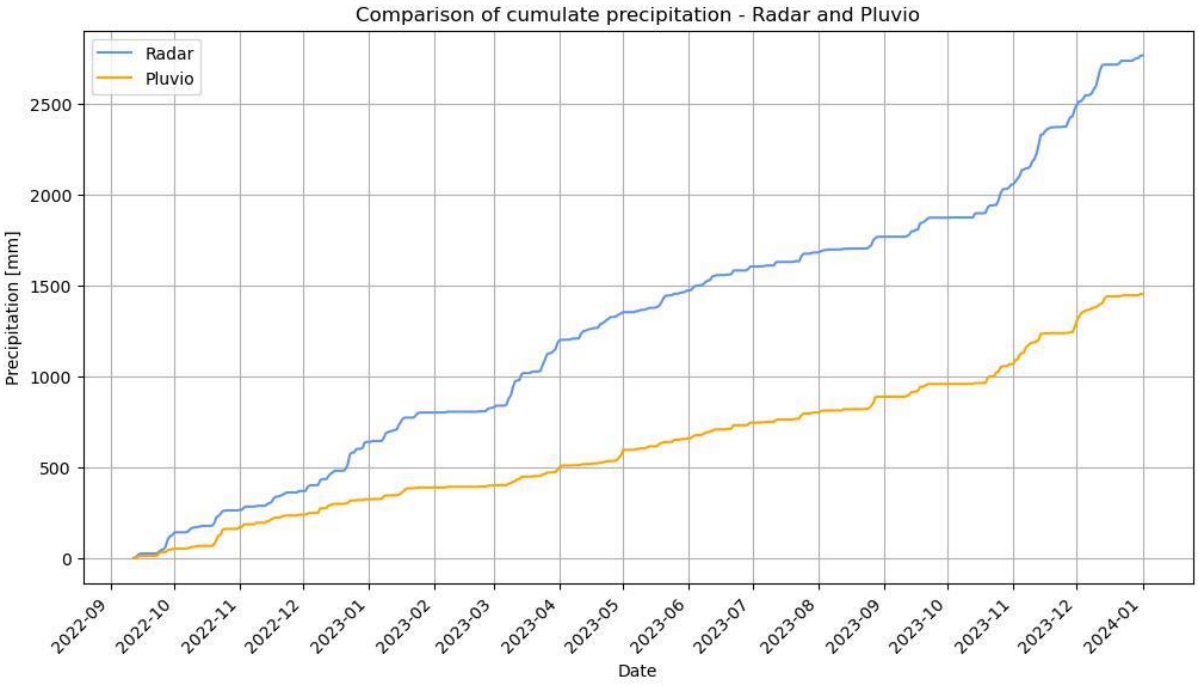

Figure 40 Precipitation, comparison of cumulates according to radar and weighted rain gauge.

Thanks to the ambient parameters measurement and the radar rain gauge ability to recognize the precipitation type, it was possible to determine which are the conditions that worsen the performances of the radar sensor.

Here follows a series of comparisons between the measurements difference of the two instruments and different ambient parameters in order to find a correlation between them; the comparisons have been carried out at different timescales based on which were the parameters analyzed.

Precipitation type

The first and most important factor that affect the radar rain gauge performance is the precipitation type. The radar rain gauge returns a value identifying the precipitation type that is recording and corresponds to the values reported in the left-hand side of the graphs (Figures 41, 42, 43). It is hard to notice any correlation on fine timescales due to variation in the precipitation type identification but consulting the daily timescale graph (figure 43) and the related boxplot (figure 46) it is evident that the periods with greater errors are related to snowy precipitations. The daily precipitation type was obtained selecting the mode of the measurements of that day (excluding the no precipitation).

In the boxplots (figure 44, 45, 46) are observable the ranges of measurements related to precipitation type. In a 5-minute timescale, the range reported in the liquid precipitation is wider than the one in the solid precipitation but the points in the solid precipitation are more numerous and the points reporting an error greater than ±2 mm are few. The trend is in fact inverted in the daily scatterplot with a wider error distribution in the solid precipitation category with a median value higher than zero, and a small and mostly overestimating error in the liquid precipitation category.

Due to their little presence the other forms of precipitations were not considered but being them a mix of the two main conditions (snow and rain) they show values between the two main category results.

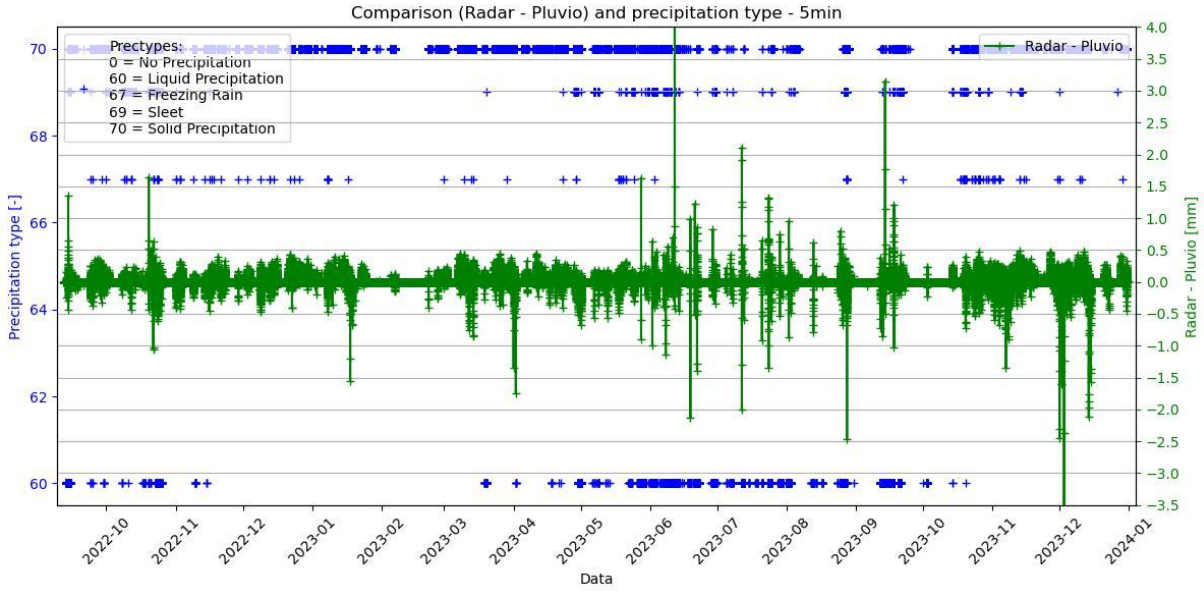

Figure 41 Error evaluation, 5min comparison of measurement error with precipitation type.

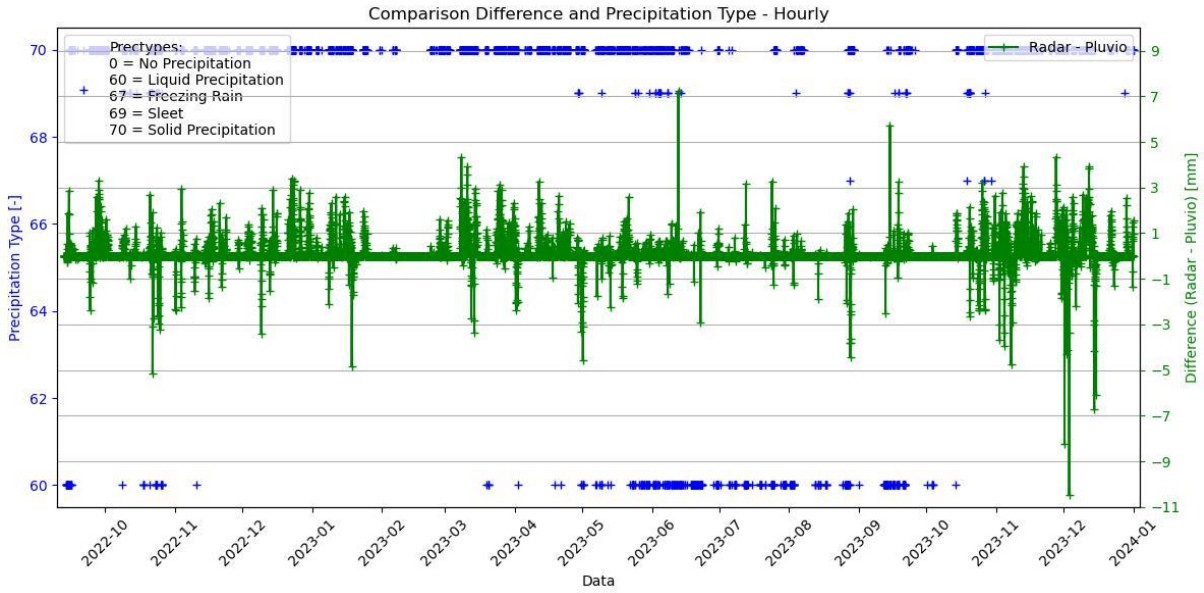

Figure 42 Error evaluation, hourly comparison of measurement error with precipitation type

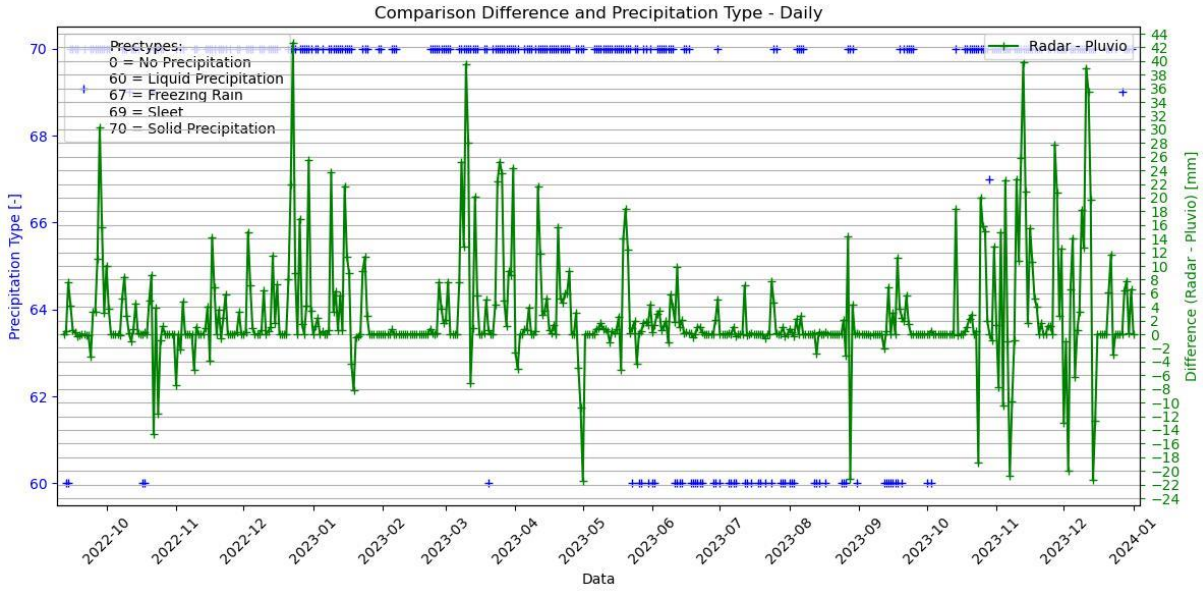

Figure 43 Error evaluation, daily comparison of measurement error with precipitation type

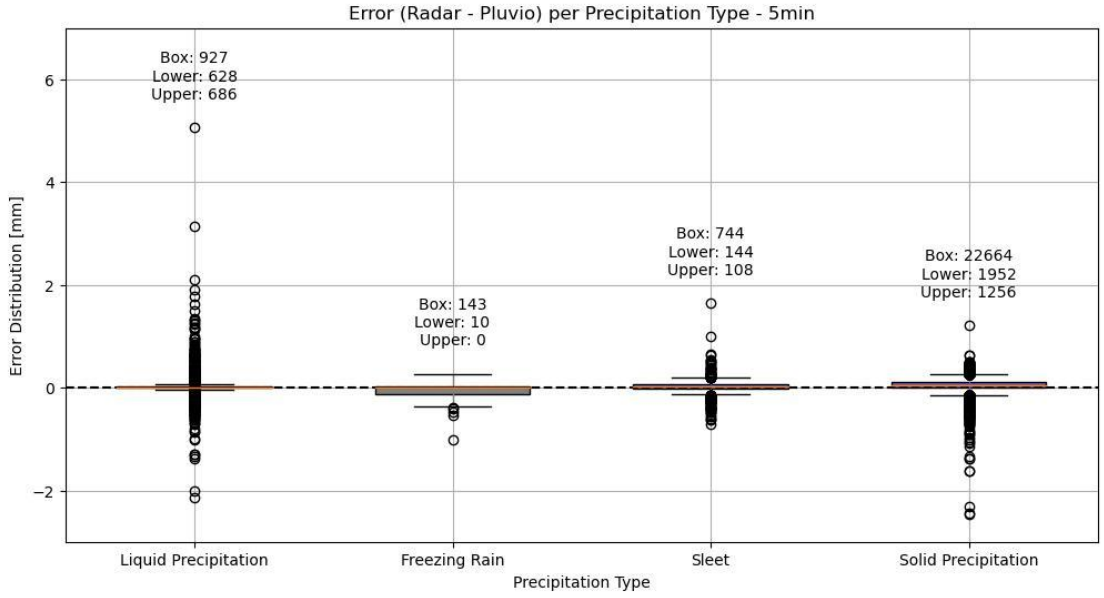

Figure 44 Error evaluation, 5min boxplot of measurement error with precipitation type.

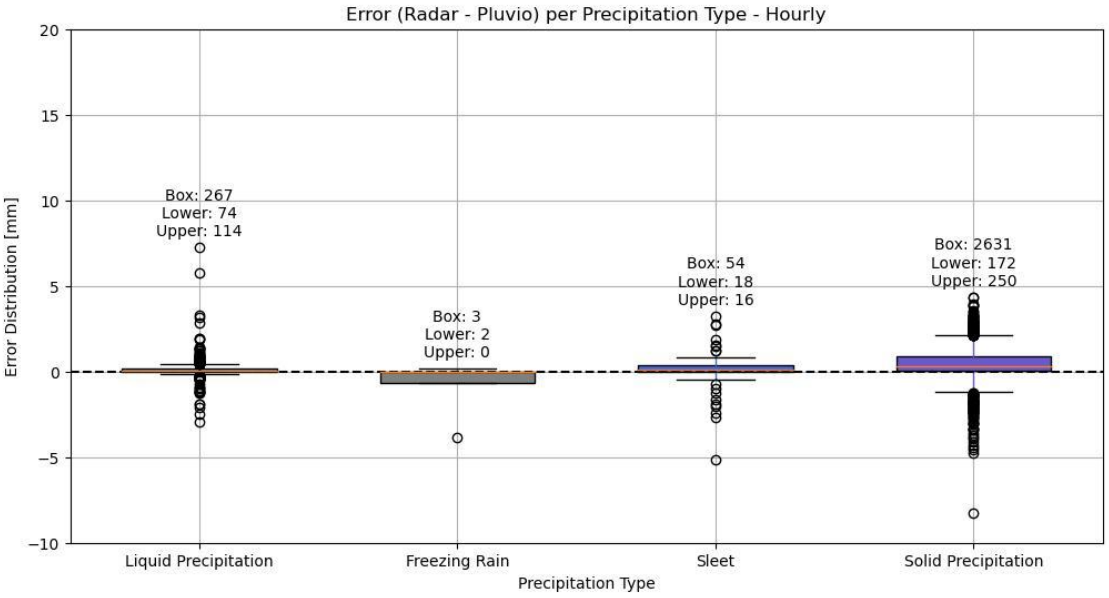

Figure 45 Error evaluation, hourly boxplot of measurement error with precipitation type.

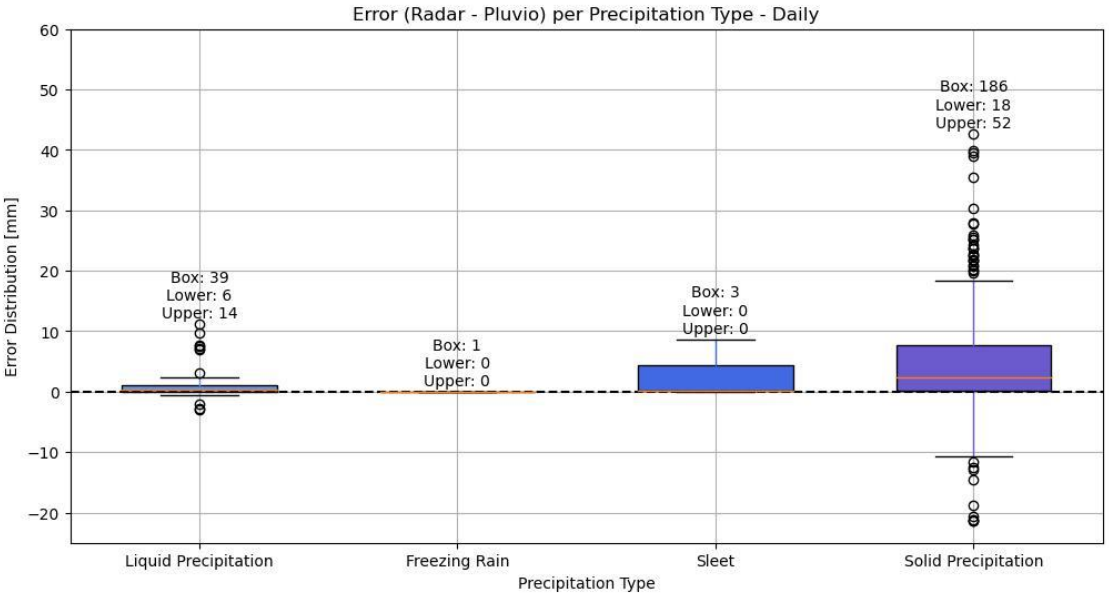

Figure 46 Error evaluation, daily boxplot of measurement error with precipitation type.

Maximum Wind Speed

The next important parameter that can affect the accuracy of the radar rain gauge is the wind, here the error measurements are related to the max wind speed recorded by the Glacier Lab station. Unfortunately the wind measurements are subjected to the missing values described in chapter 2 and the portion of the series with most distributed errors are missing in the wind series. This would have been useful to understand if winds could have an impact on the liquid precipitation measurements and justify the errors found in the previous comparison with precipitation type. In the 5 minutes timescale scatterplot (figure 50) there seem to be no correlation with max wind speed, but in the daily time-scale (figure 52) it looks clearer that a bigger error is weakly related to maximum wind speeds, meaning that is a contributing but not determining factor.

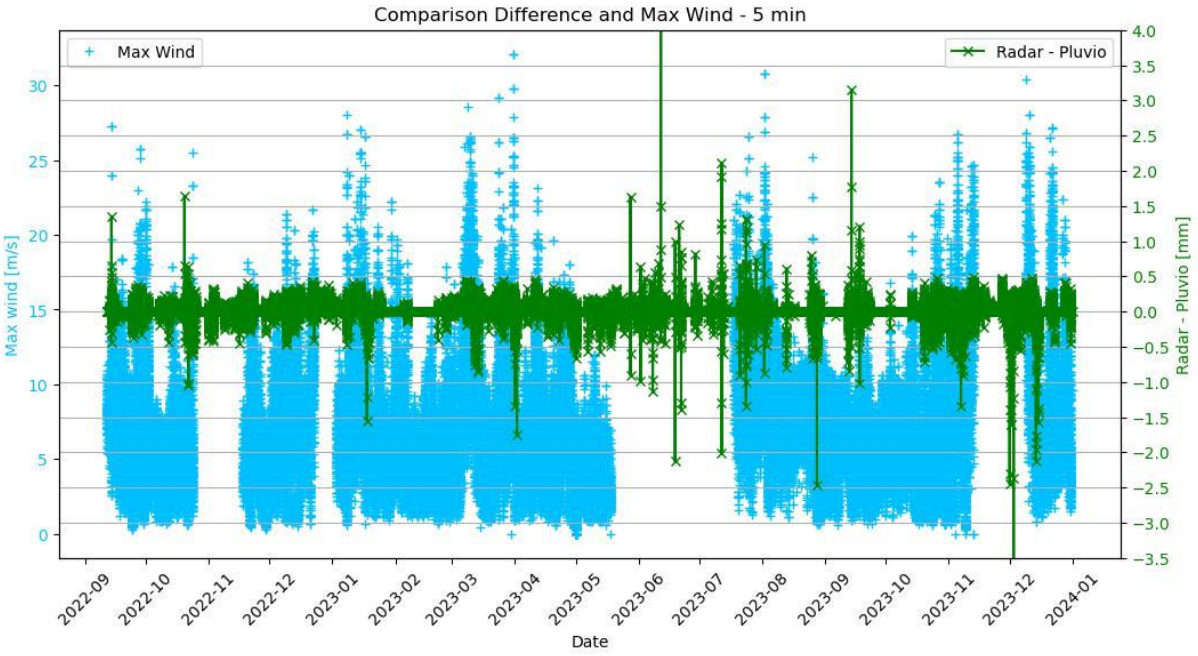

Figure 47 Error evaluation, 5min comparison of measurement error with maximum wind speed.

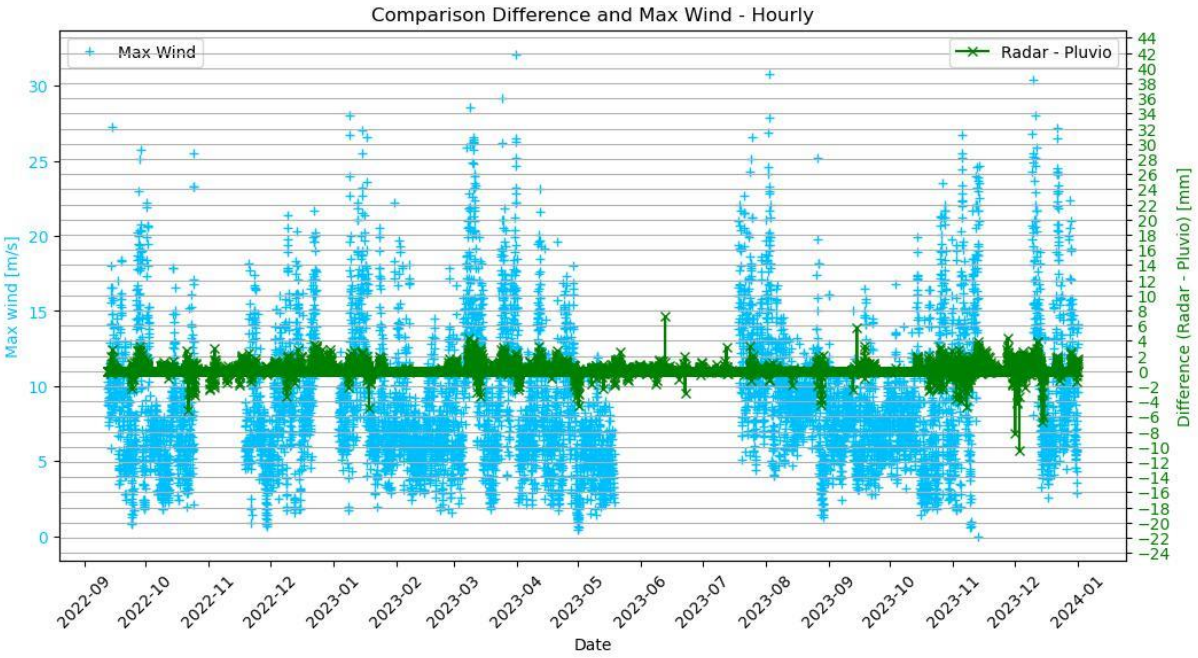

Figure 48 Error evaluation, hourly comparison of measurement error with maximum wind speed.

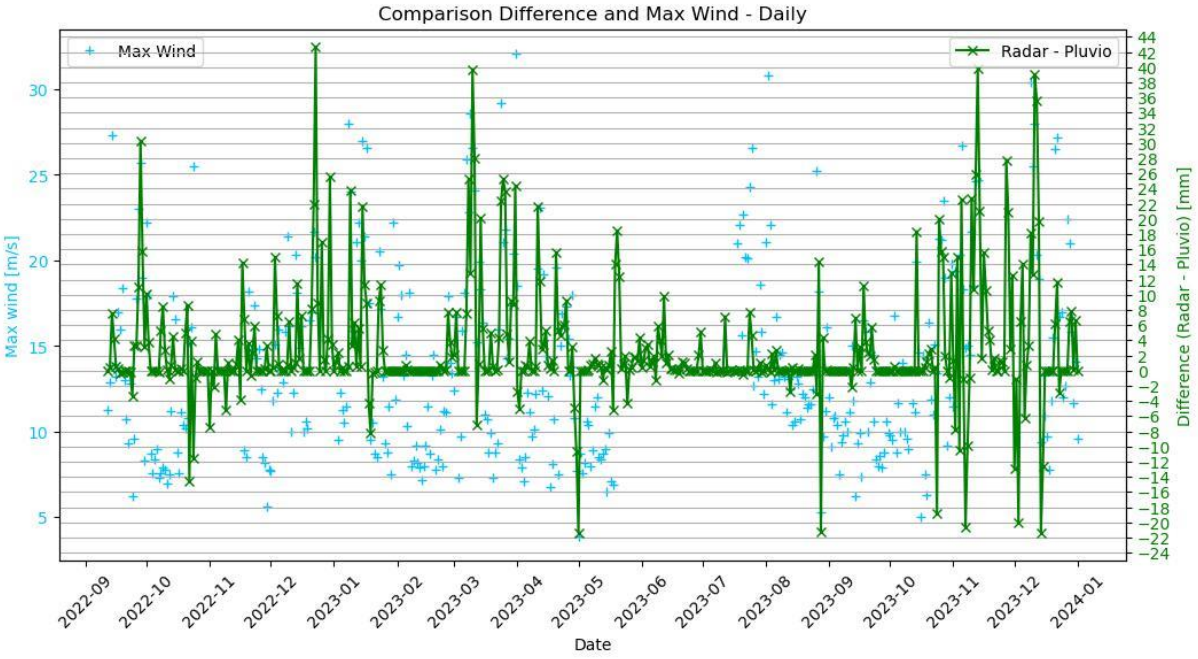

Figure 49 Error evaluation, daily comparison of measurement error with maximum wind speed.

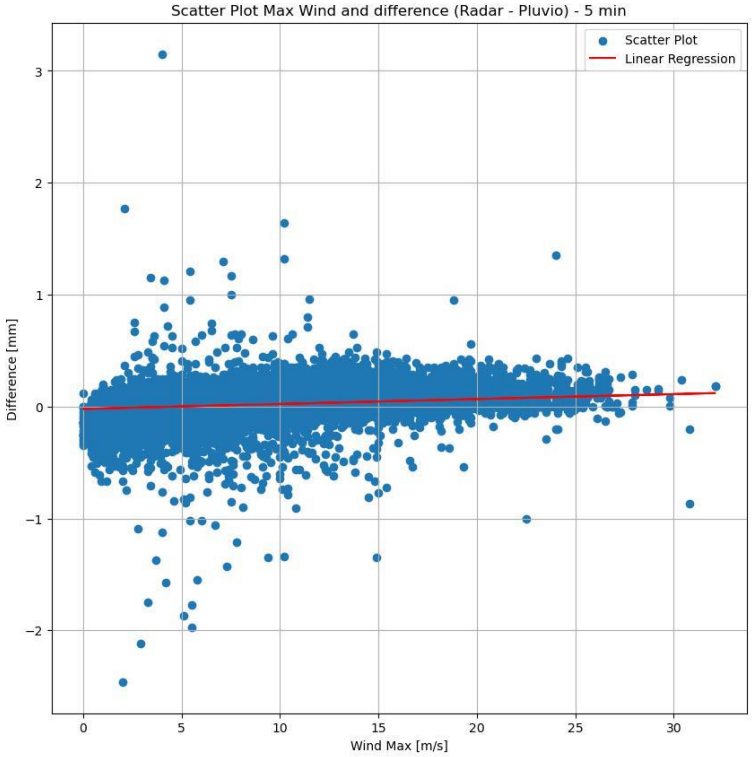

Figure 50 Error evaluation, 5min scatterplot of measurement error with maximum wind speed.

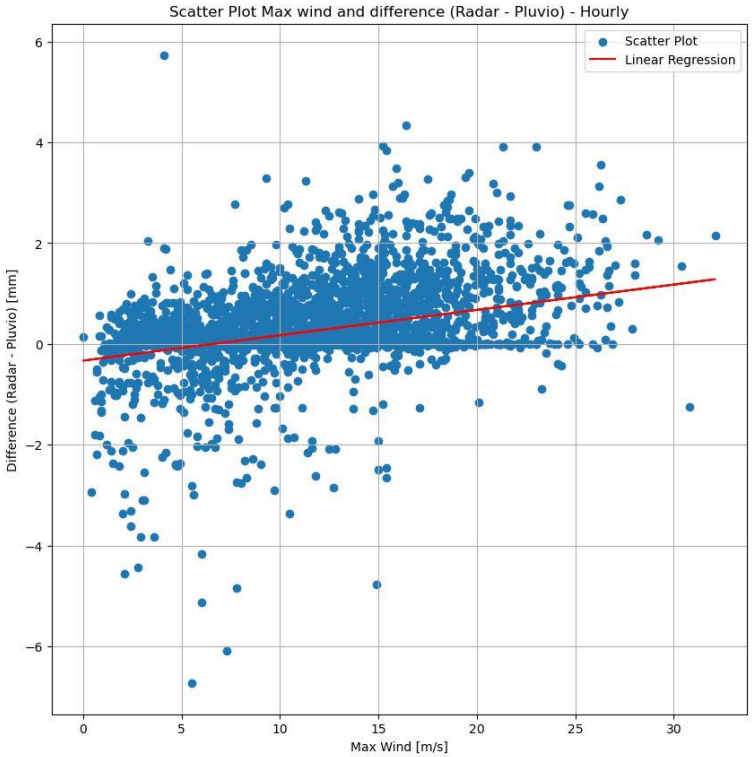

Figure 51 Error evaluation, hourly scatterplot of measurement error with maximum wind speed.

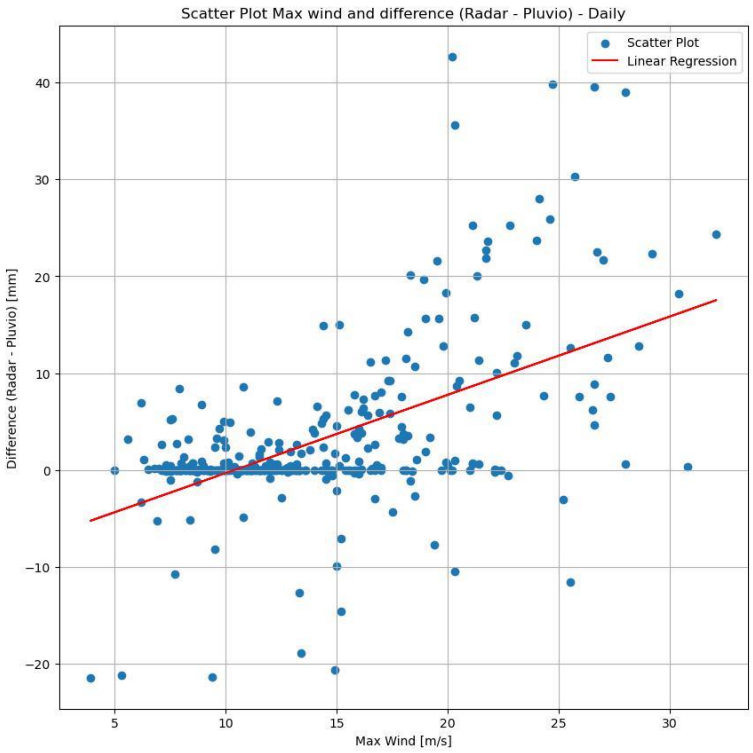

Figure 52 Error evaluation, daily scatterplot of measurement error with maximum wind speed.

Total Irradiance

Another parameter that has been analyzed is total irradiance; the comparison has been made to investigate the hypothesis that visible light could interfere with the reflection of electromagnetic waves from precipitation, despite the fact that the wavelengths of visible light are significantly bigger than those used by radar rain gauges. The scatterplot (figure 54) shows that with higher irradiances the error is smaller, but these results must be furtherly commented: these data are also subjected to the missing values and therefore points with high error are missing a coupling point; if those data were available they would sensibly influence the analysis. Another argument can be made considering that high irradiance can be associated with a low cloud coverage, also meaning a reduced precipitation amount and consequently smaller relative errors. The analysis therefore must be deepened with more data.

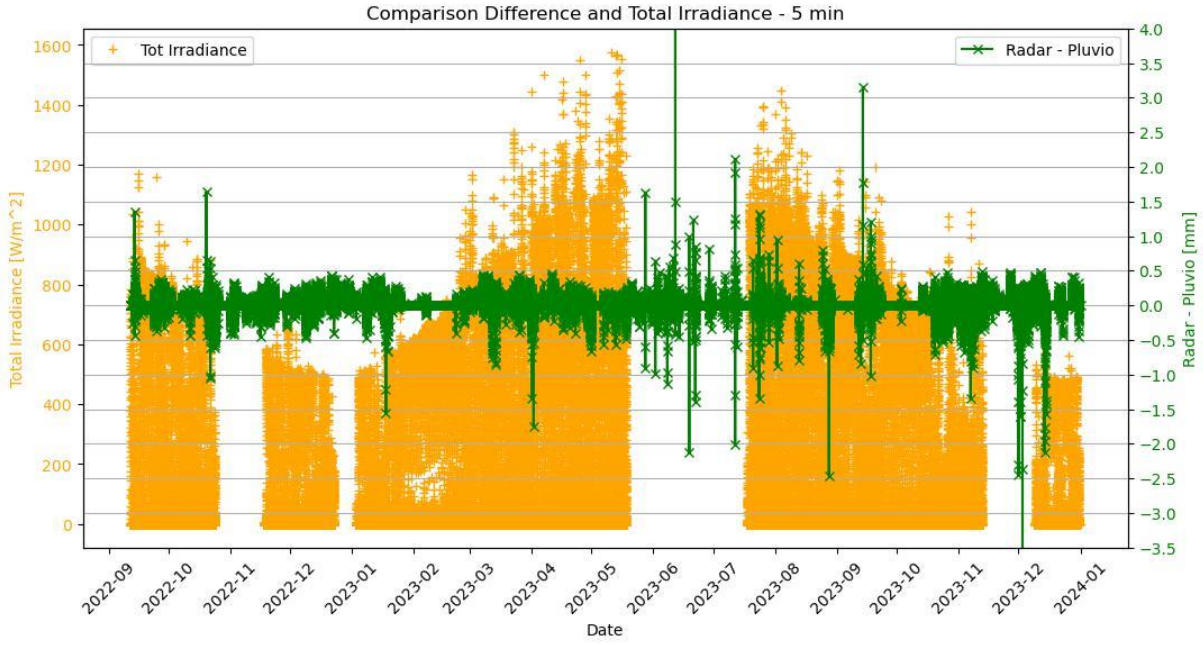

Figure 53 Error evaluation, 5min comparison of measurement error with total irradiance.

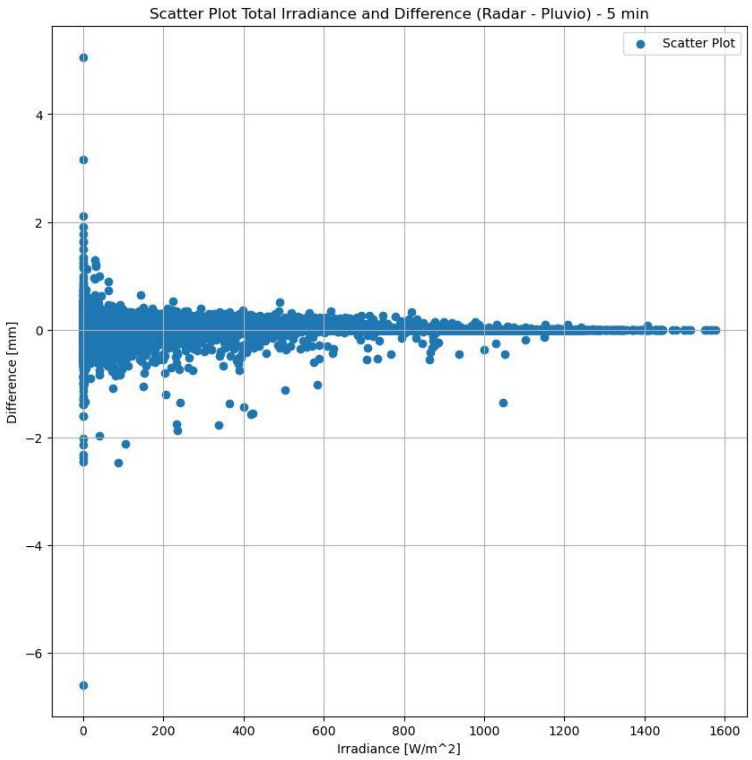

Figure 54 Error evaluation, 5min scatterplot of measurement error with total irradiance.

Relative Humidity

The next parameter that has been analyzed is relative humidity, with the theory that when relative humidity is high condensation is favored. The radar rain gauge might have issues in correctly measuring precipitations due to water drops deposited on the surface of the sensor. This resulted to be true, and it is notable in the plots but more clearly in the scatterplots; the error from the radar doppler instrument seems to be fairly distributed with a tendance towards overestimation.

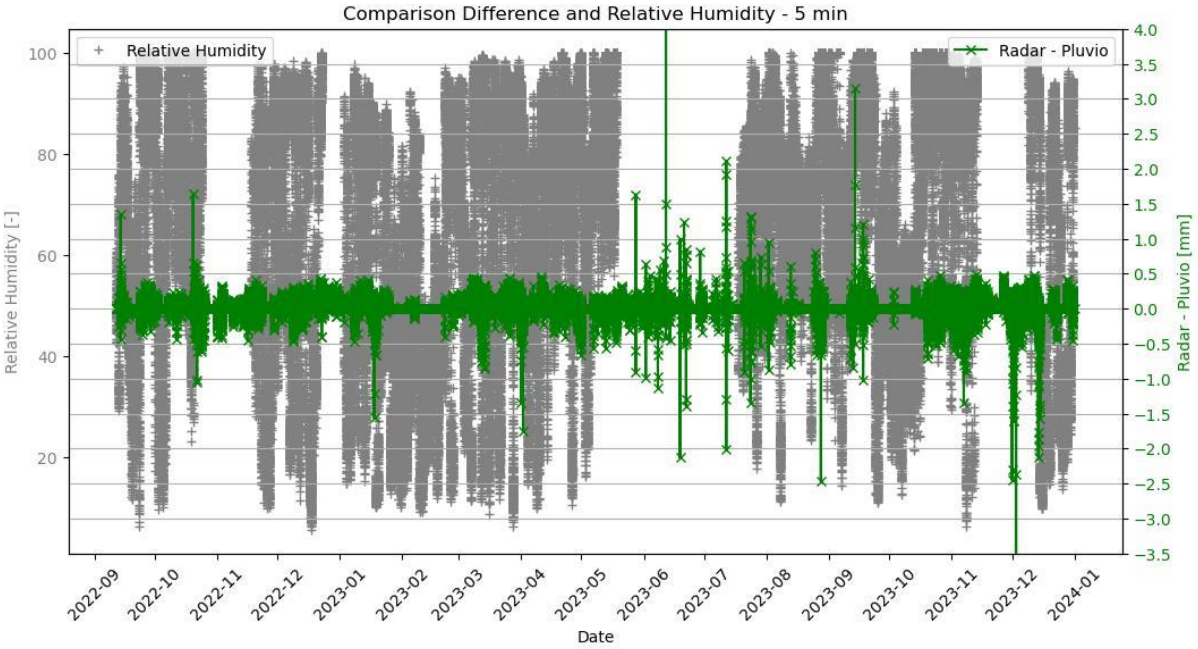

Figure 55 Error evaluation, 5min comparison of measurement error with relative humidity.

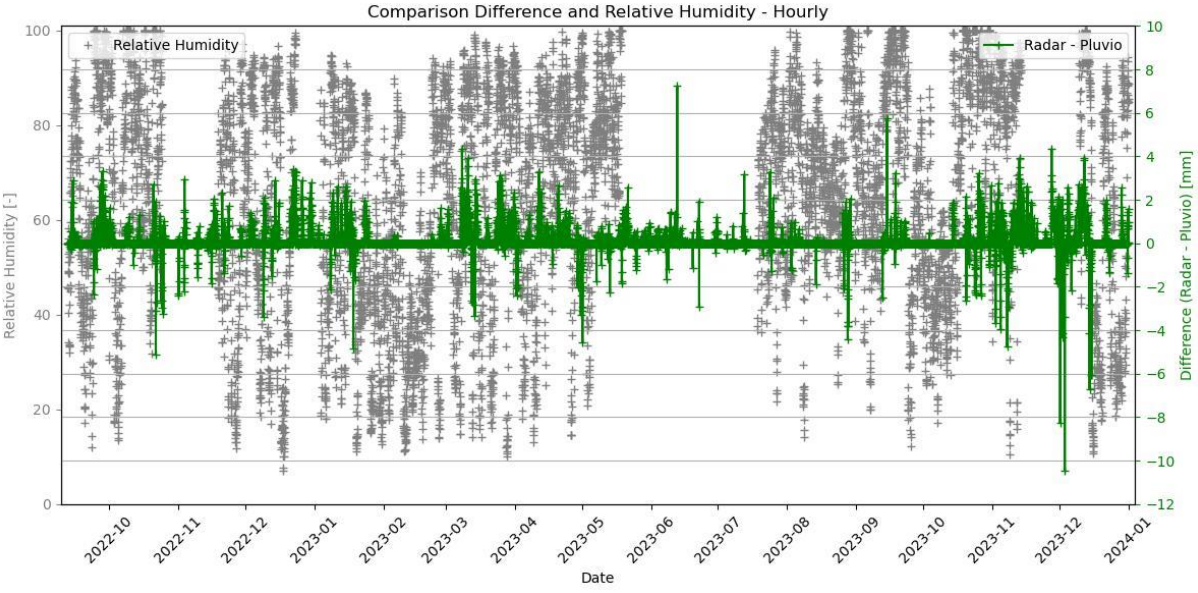

Figure 56 Error evaluation, hourly comparison of measurement error with relative humidity.

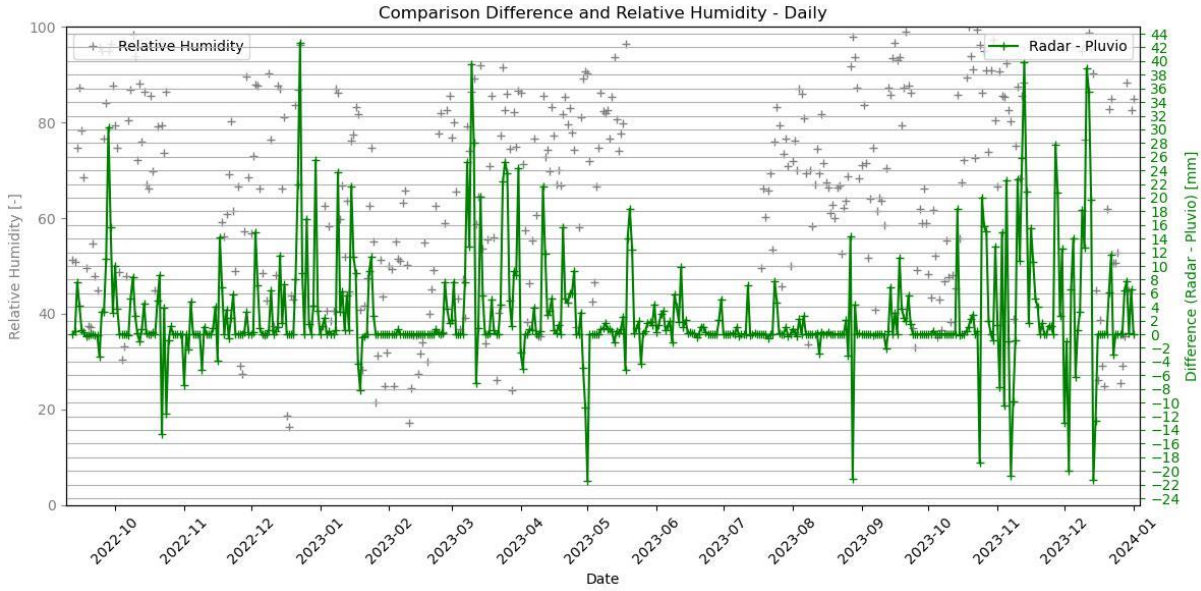

Figure 57 Error evaluation, daily comparison of measurement error with relative humidity.

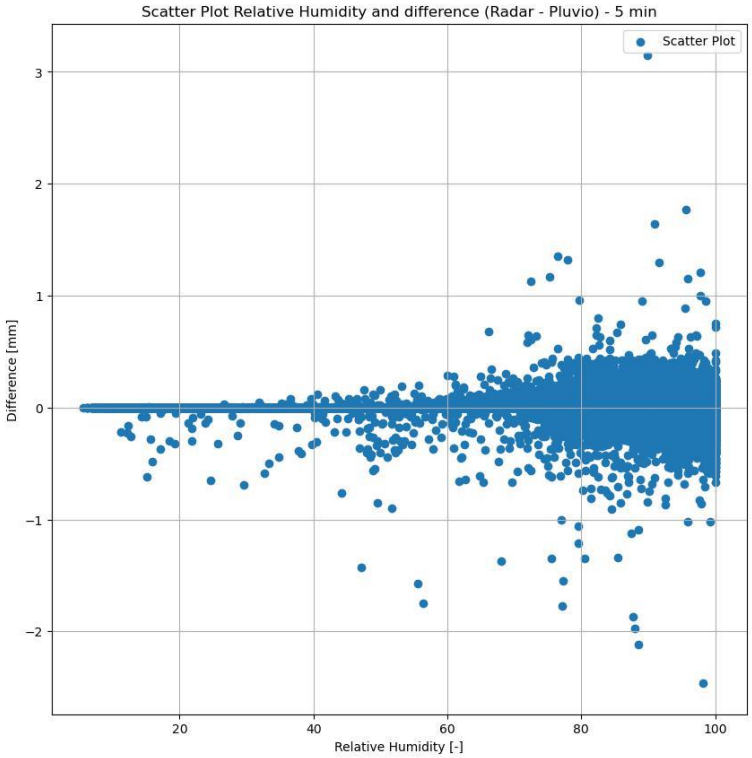

Figure 58 Error evaluation, 5min scatterplot of measurement error with relative humidity.

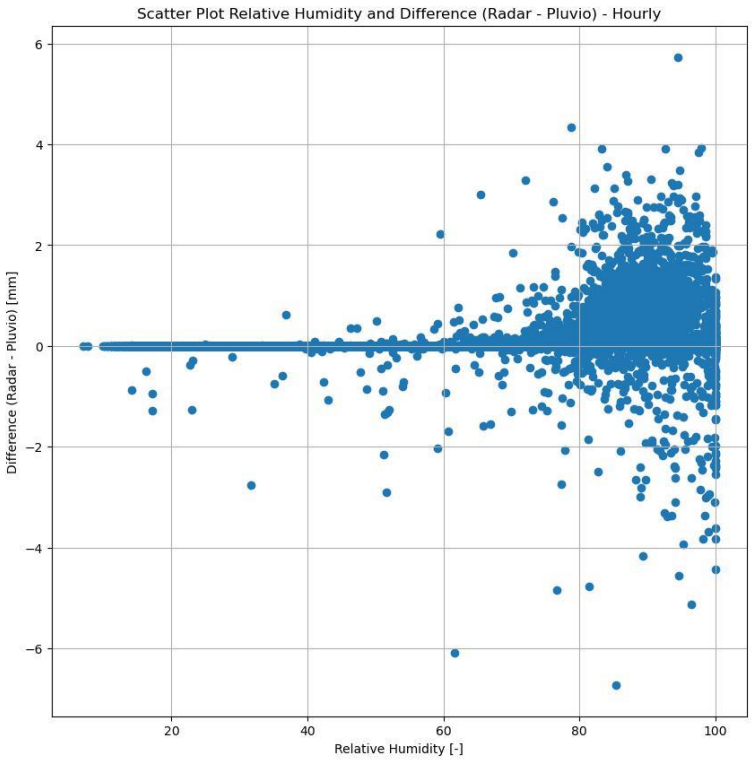

Figure 59 Error evaluation, hourly scatterplot of measurement error with relative humidity.

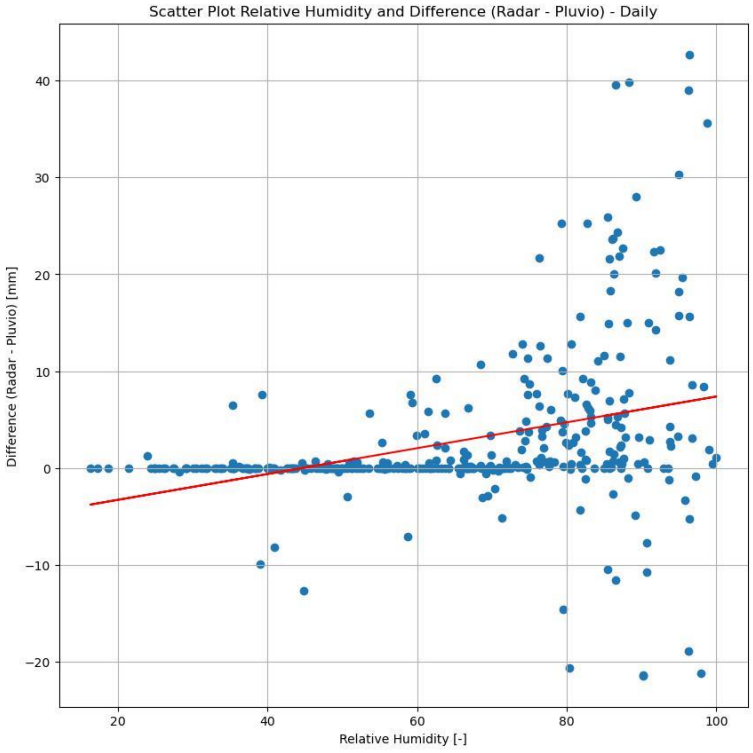

Figure 60 Error evaluation, daily scatterplot of measurement error with relative humidity.

Average Wind Speed

The last parameter that has been analyzed was average wind speed. Contrary to the results obtained with the max wind speed comparison, here the correlation is noticeable already on small time scales where even if the linear regression doesn't show a clear slope, many points are trending towards the radar rain gauge with average wind speed growth. This result is more accentuated in the higher timescales, where also the linear regression trend is more defined.

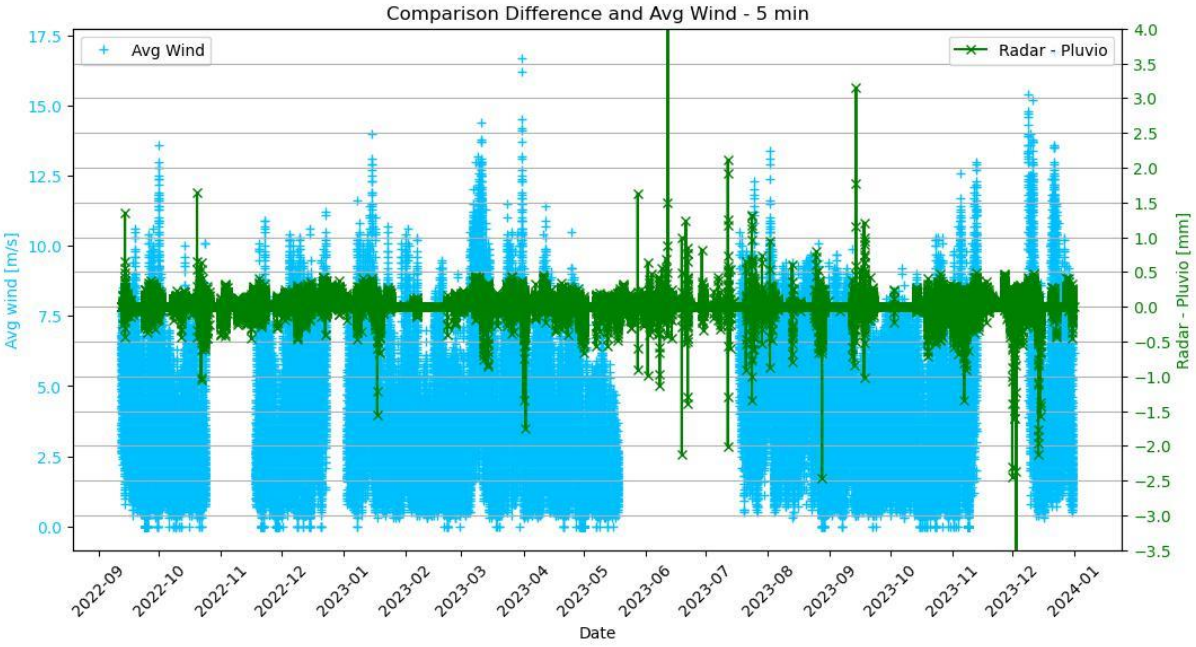

Figure 61 Error evaluation, 5min comparison of measurement error with average wind speed.

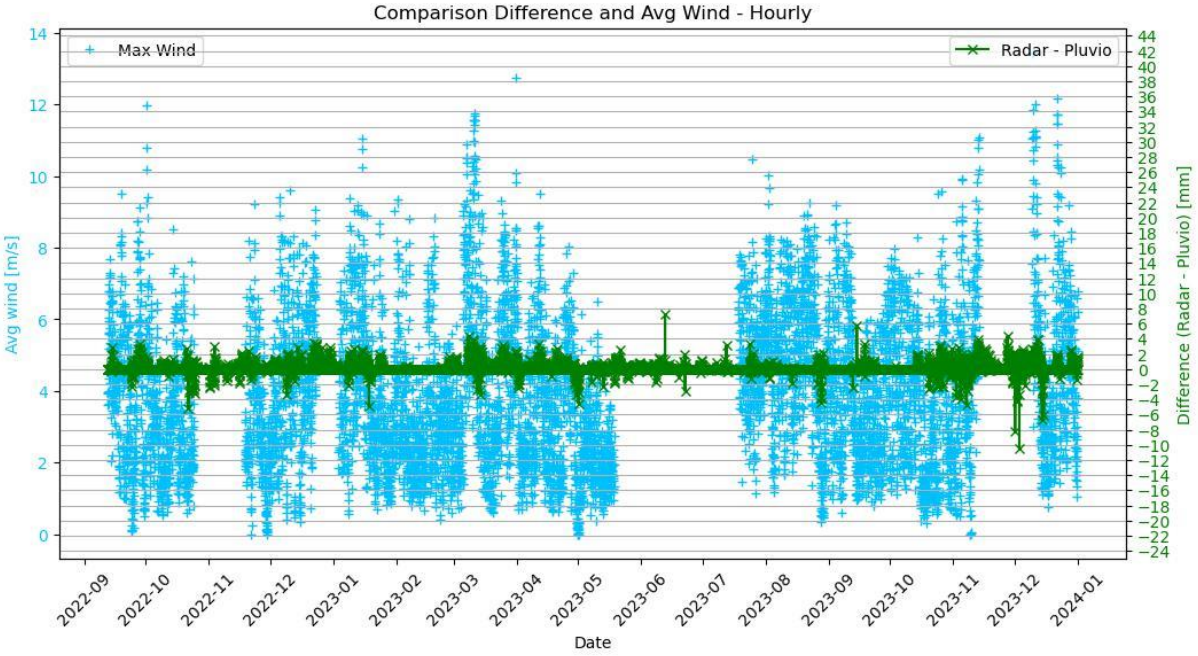

Figure 62 Error evaluation, hourly comparison of measurement error with average wind speed.

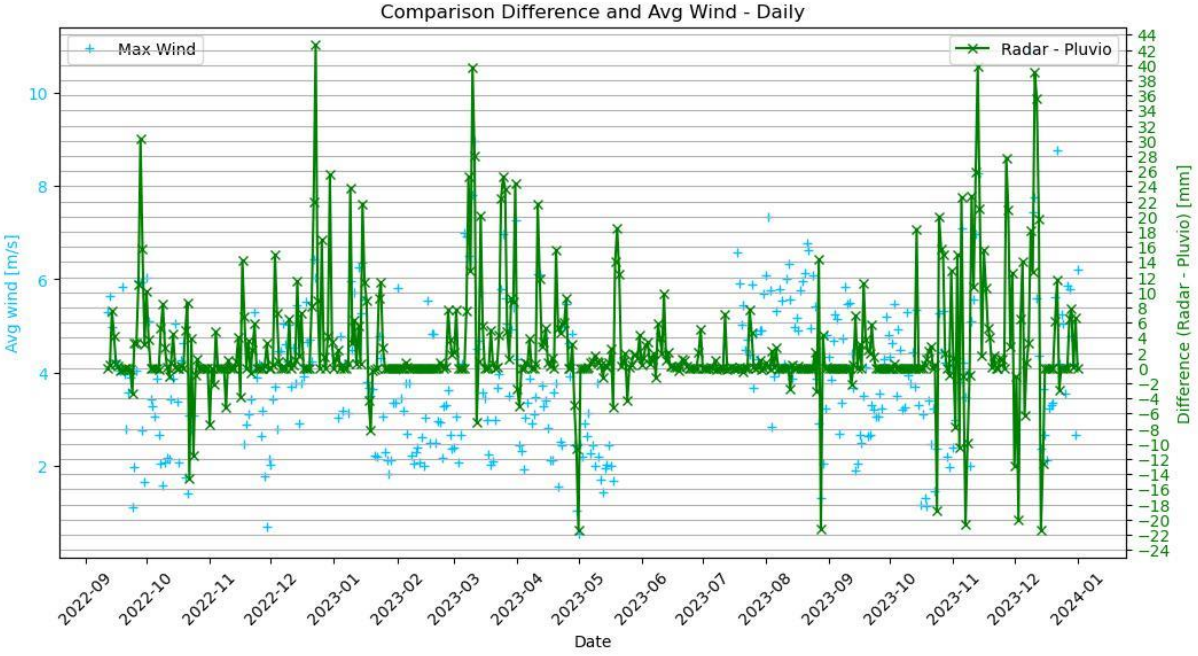

Figure 63 Error evaluation, daily comparison of measurement error with average wind speed.

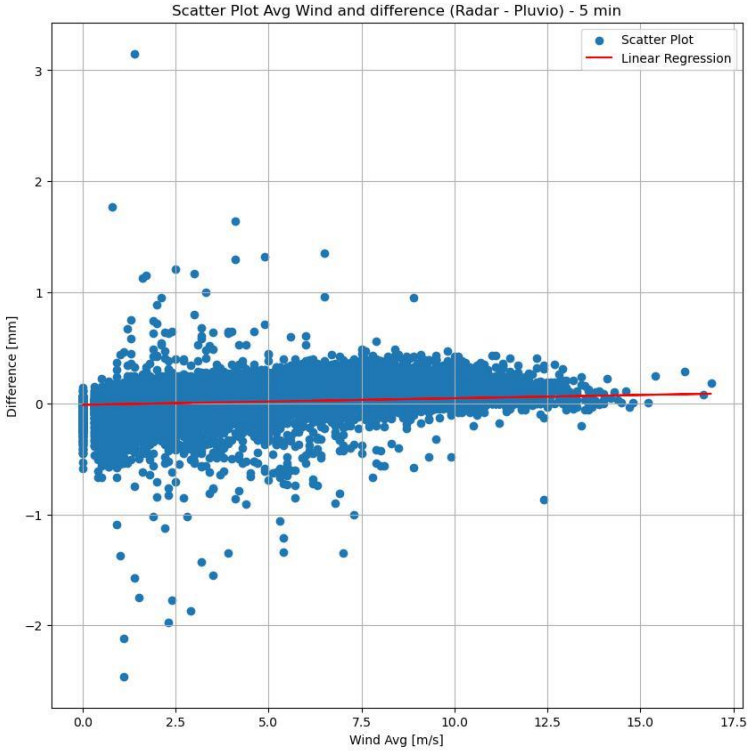

Figure 64 Error evaluation, 5min scatterplot of measurement error with average wind speed

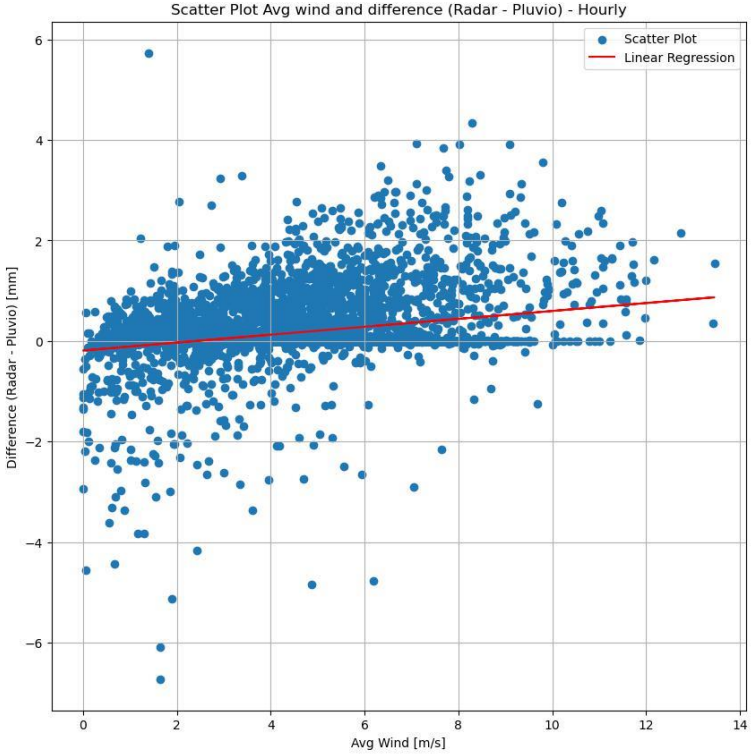

Figure 65 Error evaluation, hourly scatterplot of measurement error with average wind speed.

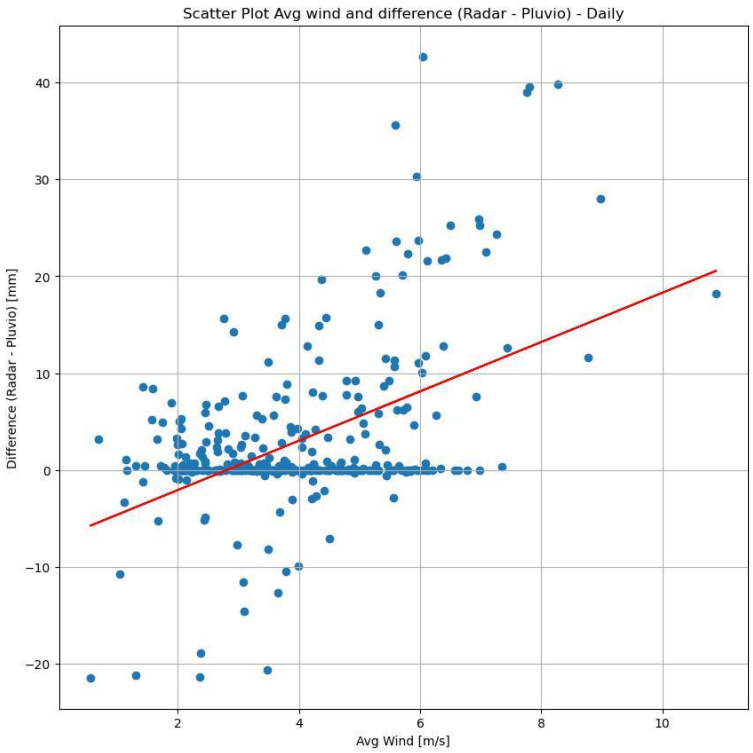

Figure 66 Error evaluation, daily scatterplot of measurement error with average wind speed.

Monthly Precipitation comparison

To conclude the error estimation precipitation were compared on a monthly time scale. As expect the summer months in which precipitation is mostly liquid are those in which the error is smaller, while it is not safe to entrust the radar rain gauge in the winter months. Exception is made for February 2023 due to the low amount of precipitation.

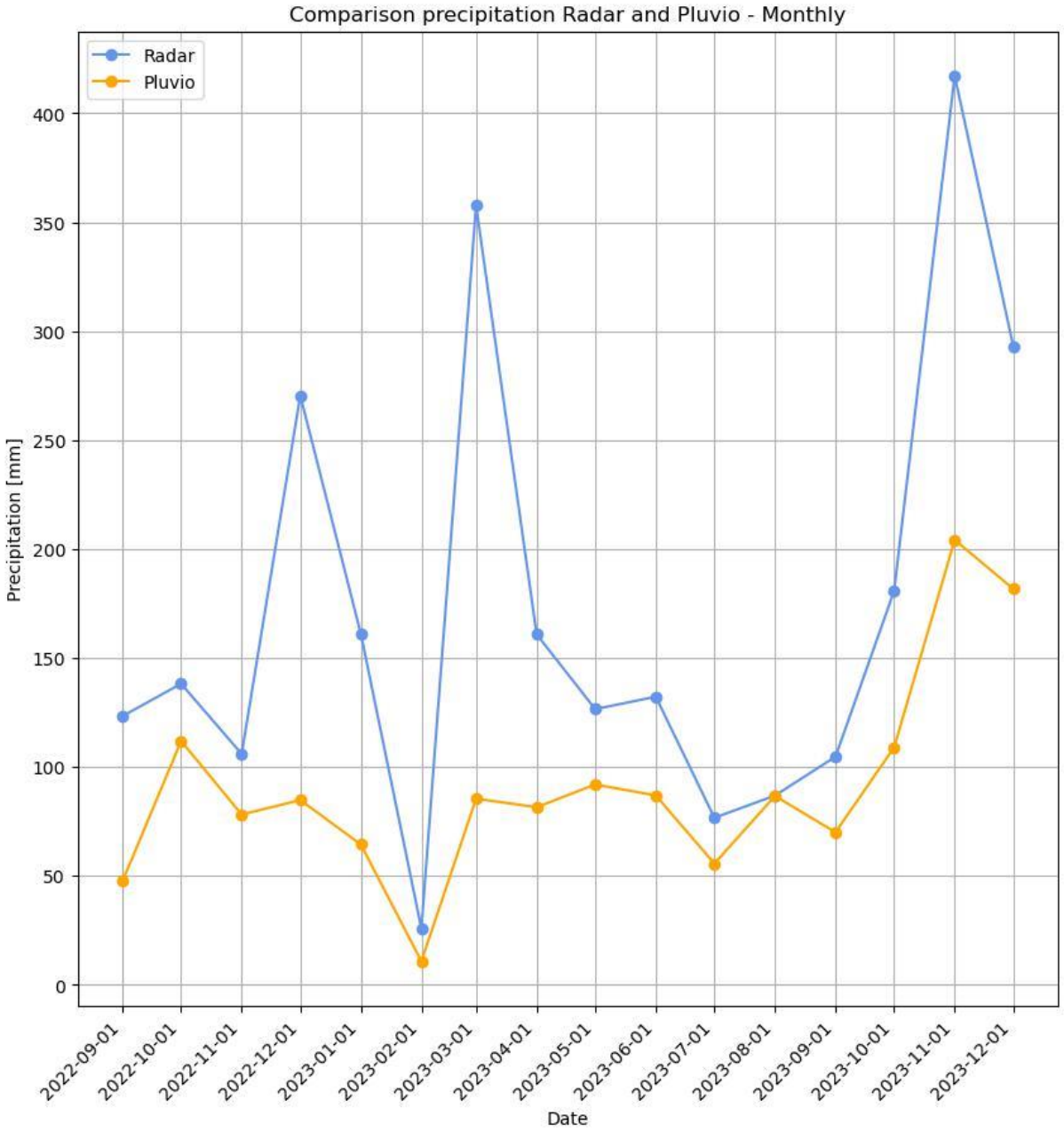

Figure 67 Precipitation, monthly comparison of Radar and Weighted rain gauge.

3.2 Evaporation Analysis

A catching weighting rain gauge functions measuring the weight of precipitation accumulated into its bucket. Along with the precipitation series, the weighted rain gauge installed by the Glacier Lab team also provides the raw data of the weight inside the instrument. With indirect use of the instrument, it is possible to measure evaporation isolating the weight loss and highlighting evaporation. Evaporation has been analyzed only on a daily timescale, since the 5-minute and hourly timescale resulted too fine to give significant results due to instrument sensitivity.

The raw data of the instrument is an unfiltered data in which systematic and instrumental errors are present; beside the emptying of the weighting rain gauge, significant variation in the content of the bucket due to unknown causes were registered. To evaluate evaporation these data were pre-processed, discarding all data that crossed certain thresholds. A considered acceptable threshold for an hourly time scale is 1 mm/h, while for a daily time scale the threshold taken is 7 mm/day, given the hypothesis that the conditions in which the phenomenon could happen exhibit only in the hottest hours' time window.

Relative Humidity

The strongest correlation has been found with Relative humidity; looking at the daily graph and scatterplot (figure 69 and 70, respectively) is notable that when relative humidity decreases evaporation is favored and increases, while the contrary is also true. This correlation is the result of the phenomenon of humidity equilibrium between air and free surface water/soil.

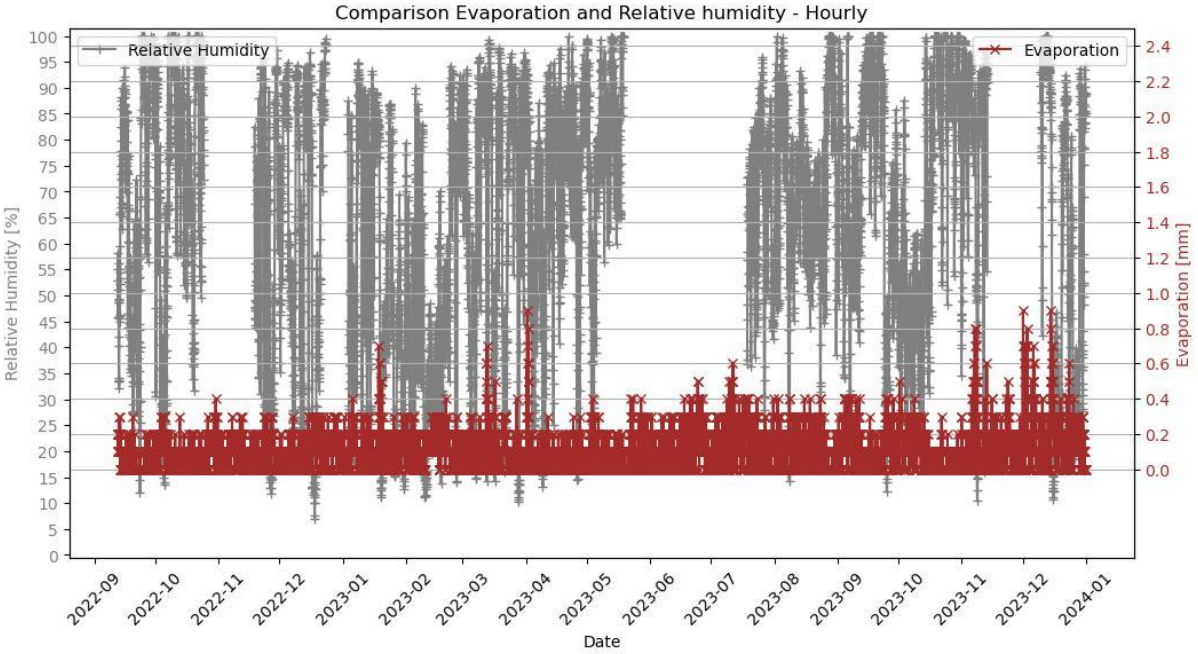

Figure 68 Evaporation, hourly comparison of evaporation and relative humidity.

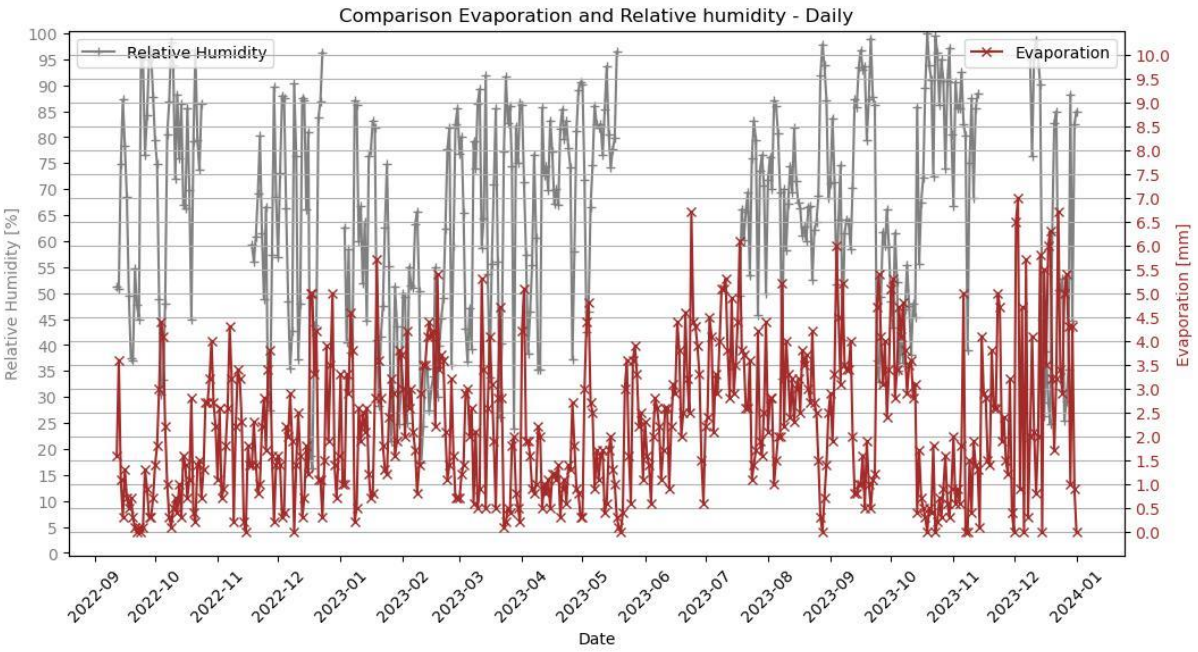

Figure 69 Evaporation, daily comparison of evaporation and relative humidity

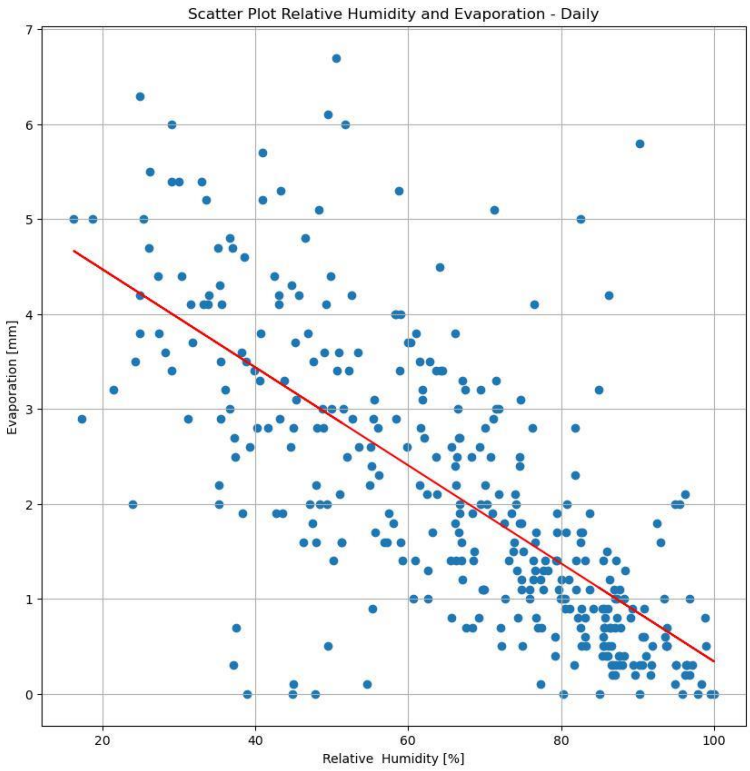

Figure 70 Evaporation, daily scatterplot of evaporation and relative humidity.

Evaporation was then analyzed in relation with temperature. 30 non-rainy days of a winter and summer period were taken and for both periods the daily evaporation, from midnight to midnight, has been plotted in a scatterplot with the average temperature recorded between 11:00 and 15:00, which are supposed to be the hottest hours.

In figure 71 all the points considered are shown and no correlation is found, but in figures 72 and 73 it's possible to find a correlation between the maximum hours' temperatures and evaporation.

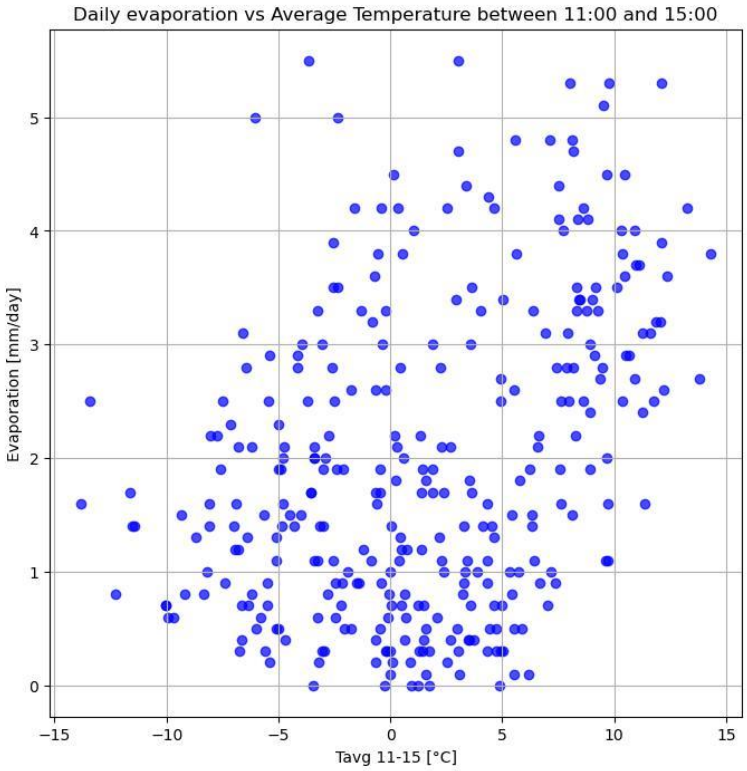

Figure 71 Evaporation, scatterplot of evaporation in sample months and temperature of hottest hours

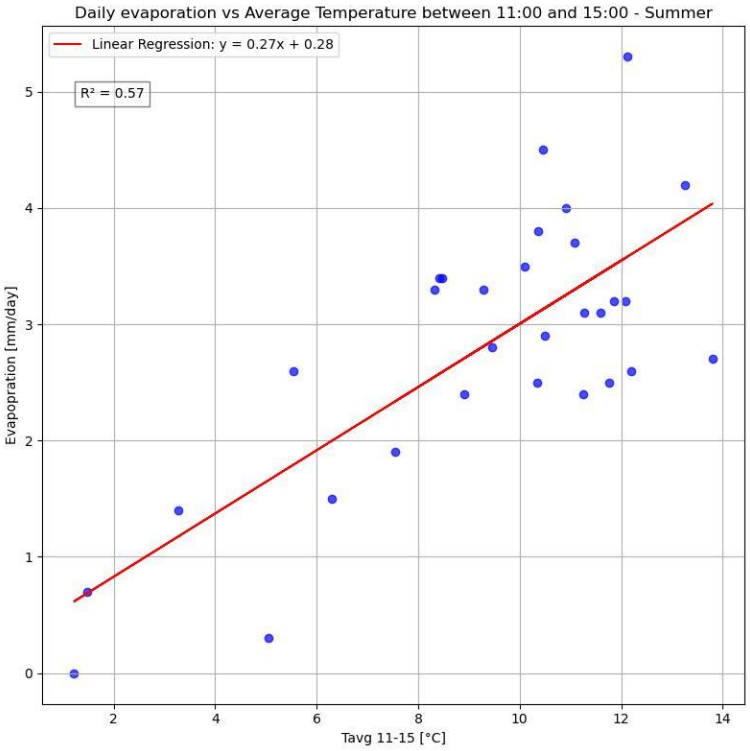

Figure 72 Evaporation, scatterplot of evaporation in 30 summer non rainy days and temperature of hottest hours.

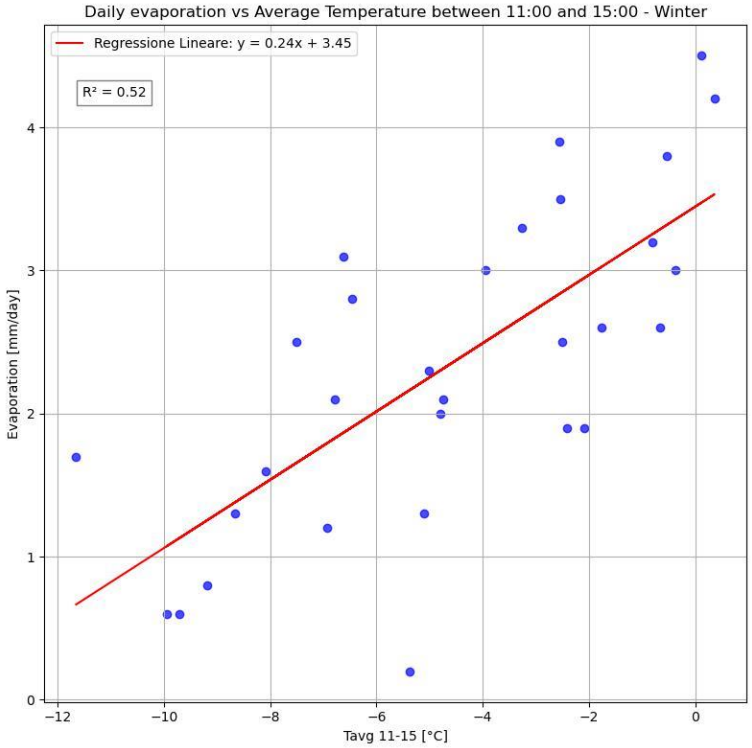

Figure 73 Evaporation, scatterplot of evaporation in 30 winter non rainy days and temperature of hottest hours.

Evaporation was also analyzed in relation with almost all the parameters available, but no meaningful results were found. It's also important to note that at lower time scales the sensibility of the instrument strongly influenced the results, making them too discrete.

4. ‘Glacier des Usellettes’ and topography description

4.1 Introduction, history and area estimation.

The “Usellettes” glacier (“Glacier des Usellettes”) is a circus glacier located in the Graie Alps, close to the summit of the Paramont mountain and not far from the Rutor Glacier at a peak altitude around 3150 m (recorded in 09/2022). Differently from Rutor, Usellettes is a small glacier, it has a N-O exposure and its origin is due to snow accumulation from precipitation and wind, both the ablator and the collector basins are not exposed.

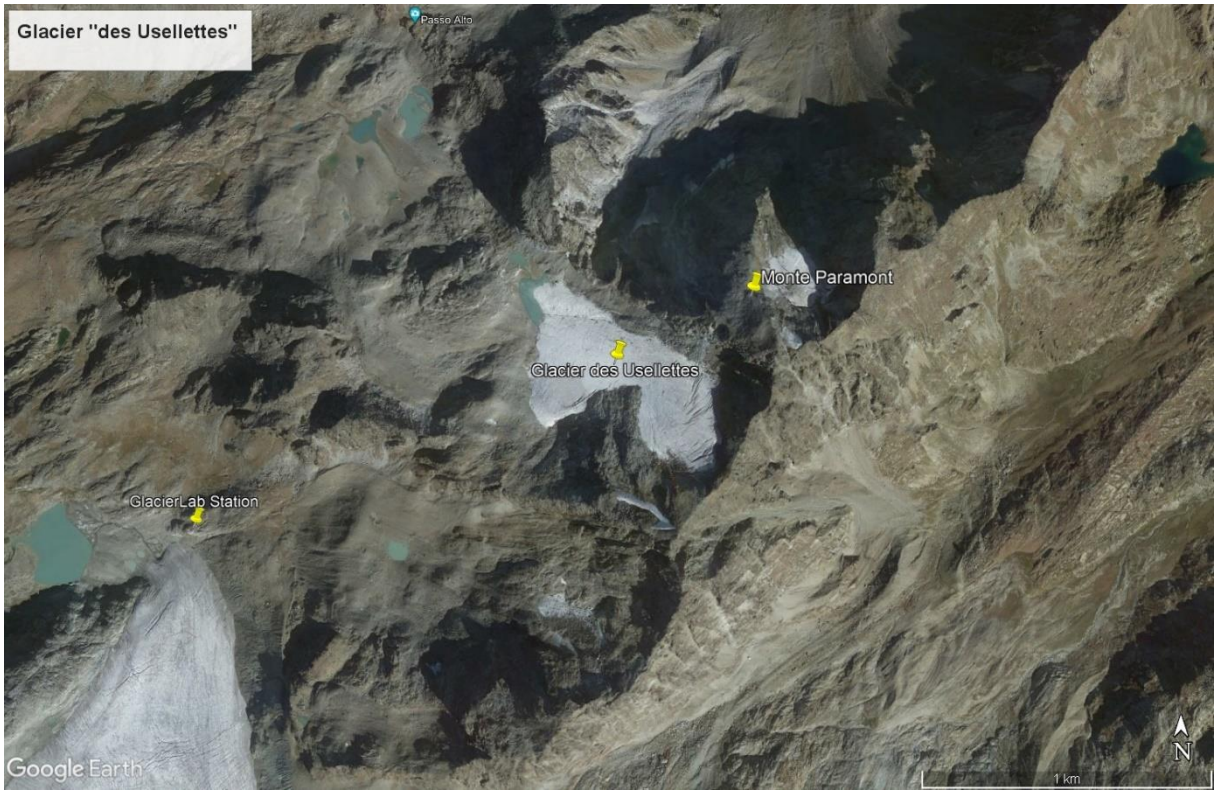

Figure 74 Glacier des Usellettes as it shows on Google Earth, 9/2022. (Google, 2024)

The glacier has been studied across the years with a non-regular temporal distribution by private and public bodies. Around year 2000 the glacier had an appendix on the left-hand side, which due to erosion and melting first disconnected from the main glacier and afterwards disappeared entirely. The same happened for a portion of glacier which was at a higher altitude, around 3200 m; both the appendixes are still visible in figure 74, respectively in the south-west and south with respect to

the glacier. At the base of the glacier are visible the glacial and periglacial lakes that originate from the melting of the glacier that, more towards the valley, feed a hydropower turbine owned by a mountain refugee.

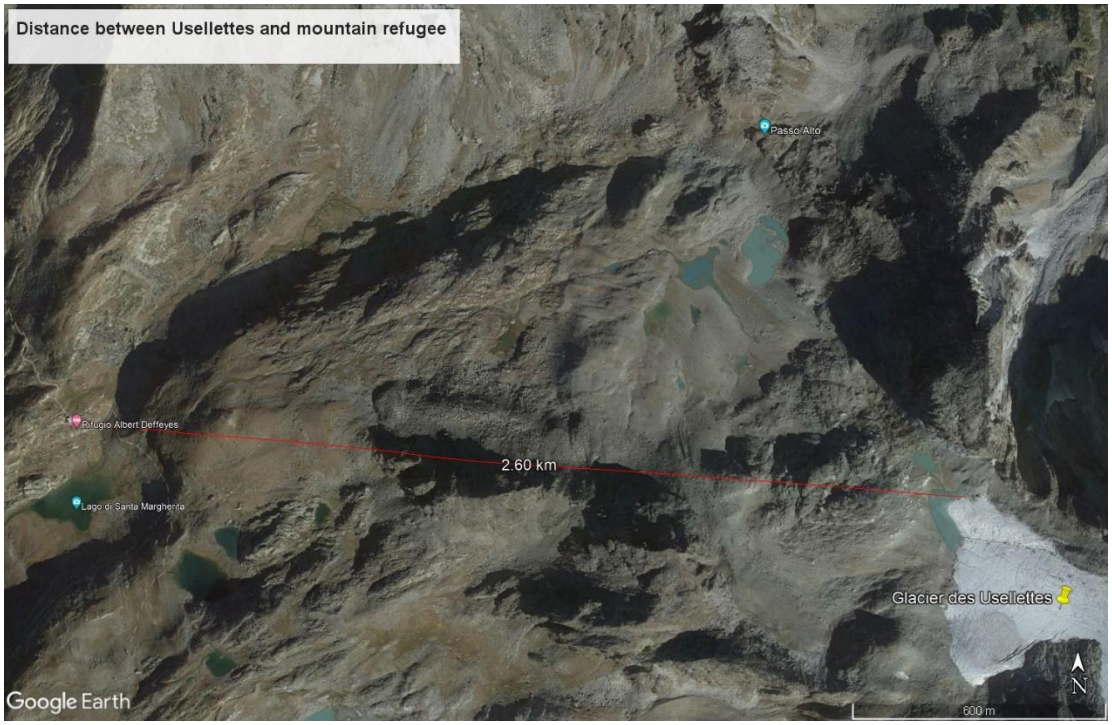

Figure 75 Approximate distance between meltwater source and the hydropower turbine. (Google, 2024)

In figure 75 is reported the distance from the base of the glacier up to the whereabouts of the turbine, which means the glacier's meltwater feed the turbine that gives electricity to a refugee at around 2.6 km from the glacier itself. The meltwater follows its natural path and is channeled into a pipe closer to the refugee, where it then meets the turbine.

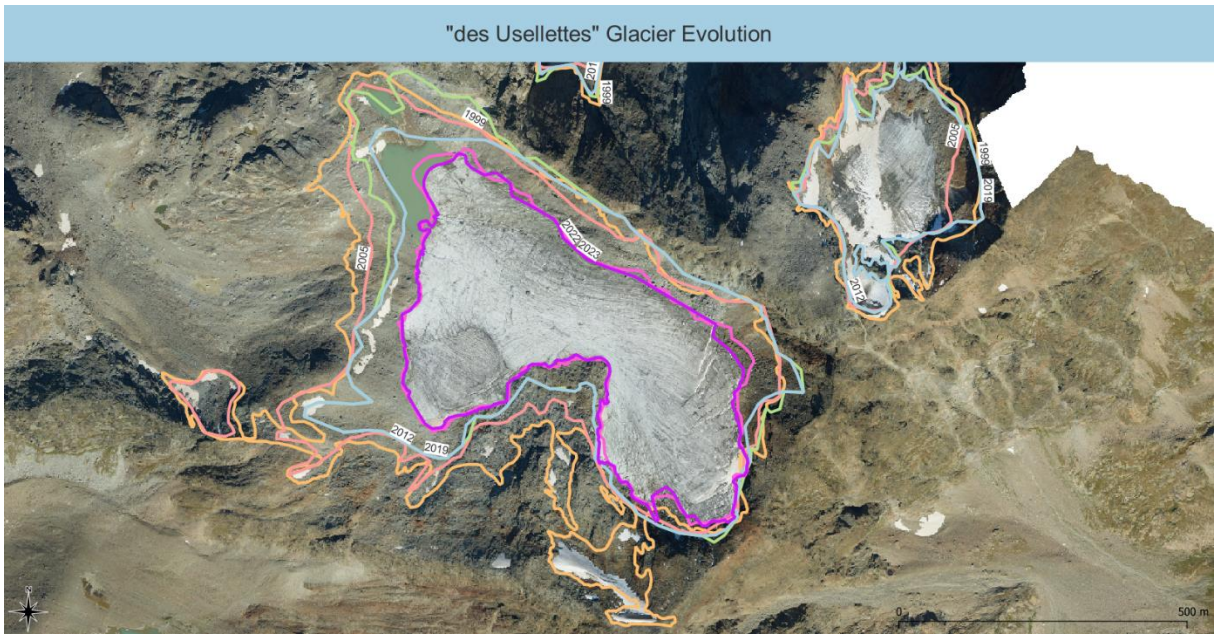

Figure 76 Border variation across the years. Made with QGIS.

In figure 76 is reported an area analysis of the glacier from 1999 to 2023. Shown under the reported glacier's borders there's the result of the last survey taken from the Glacier Lab in their last expedition in summer 2023, an ortophoto with a 20cm resolution from which the border for the same year area estimation has been taken. The 2022 border is extracted from Google Maps Ortophoto (Google, 2024), while the other borders can be found on "Catasto Ghiacciai" (SCT, 2023) from Valle d'Aosta. From the historical representation reported in figure 76 are notable both the appendixes mentioned above; those appendixes stopped being considered part of the glacier during the years, the south one was considered only in the 1999 survey, while the west one even if it was already detached in 2005 stopped being considered part of the glacier only in 2012. All perimeters have been imported into QGIS and the areas have been estimated with the software obtaining the following result:

Table 1 History of Area recordings of Usellettes

Year	Area [km^2]	Source
1999	0.41	Catasto Ghiacciai
2005	0.35	Catasto Ghiacciai
2012	0.33	Catasto Ghiacciai
2019	0.30	Catasto Ghiacciai
2022	0.20	Ortophoto Google
2023	0.19	Ortophoto Glacier Lab

4.2 Drainage Basins and on-site hydrology characterization

To assess if the hydro-pump is exclusively fed by the meltwater of Usellettes, it's important to assess if there are other water bodies that feed the pump. In figure 77 are shown the drainage basins that characterize the area around the Usellettes Glacier, looking at the borders there are visible other glacial bodies which however does not contribute with the hydrology of the studied glacier:

- The top two glaciers are "Tete de Paramont" (the northerly) and "Paramont" (the southerly). They are close to Usellettes but belong to the Miravidi-Lechaud mountain group and belong to another basin.
- The southern is the Invergnures glacier, it belongs to the same basin and mountain group of Usellettes, but as it is notable in figure 77, they produce two different hydrology which are separated by a ridge. The Invergnures glacier's torrent rapidly joins the Rutor glacier's one, while the Usellettes takes a longer path and joins the Rutor's hydrology only after passing close to the hut and through the hydro-turbine.

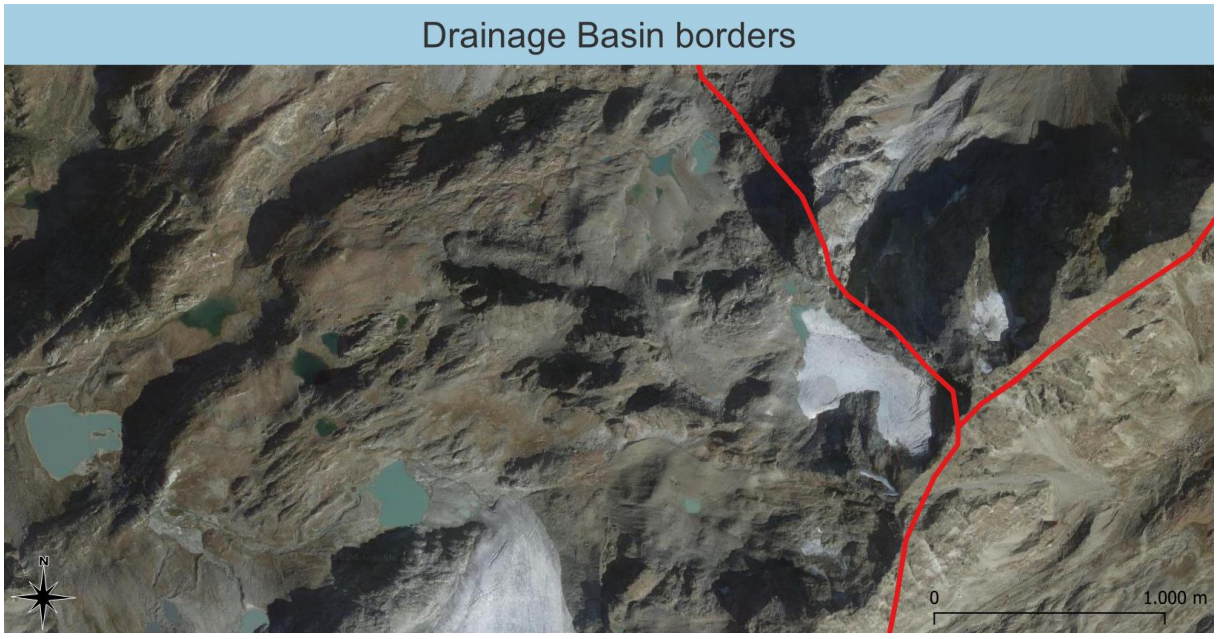

Figure 77 Drainage Basin borders around the Usellettes area. Made with QGIS.

4.3 Meteorological Observatory “Bivacco Edoardo Camardella”

In this section is introduced the Meteorological Observatory “Bivacco Edoardo Camardella” (MeteoProject, s.d.). This hut is located at an altitude of 3364 m a.s.l. and at around 3 km from the GlacierLab station. In this hut was installed, around the same time of the installment of the PoliTO one, a station able to record the same ambient parameters recorded by the GlacierLab station. This station was therefore used to compute a Lapse Rate used to estimate more accurate temperatures for the Usellettes glacier, accounting for the difference in altitude between the station at the feet of the Rutor Glacier and the glacier of interest. The difference in altitude considered was 485 m (Usellettes glacier altitude in the centroid = 3035 m a.s.l., GlacierLab station altitude = 2550 m a.s.l.).

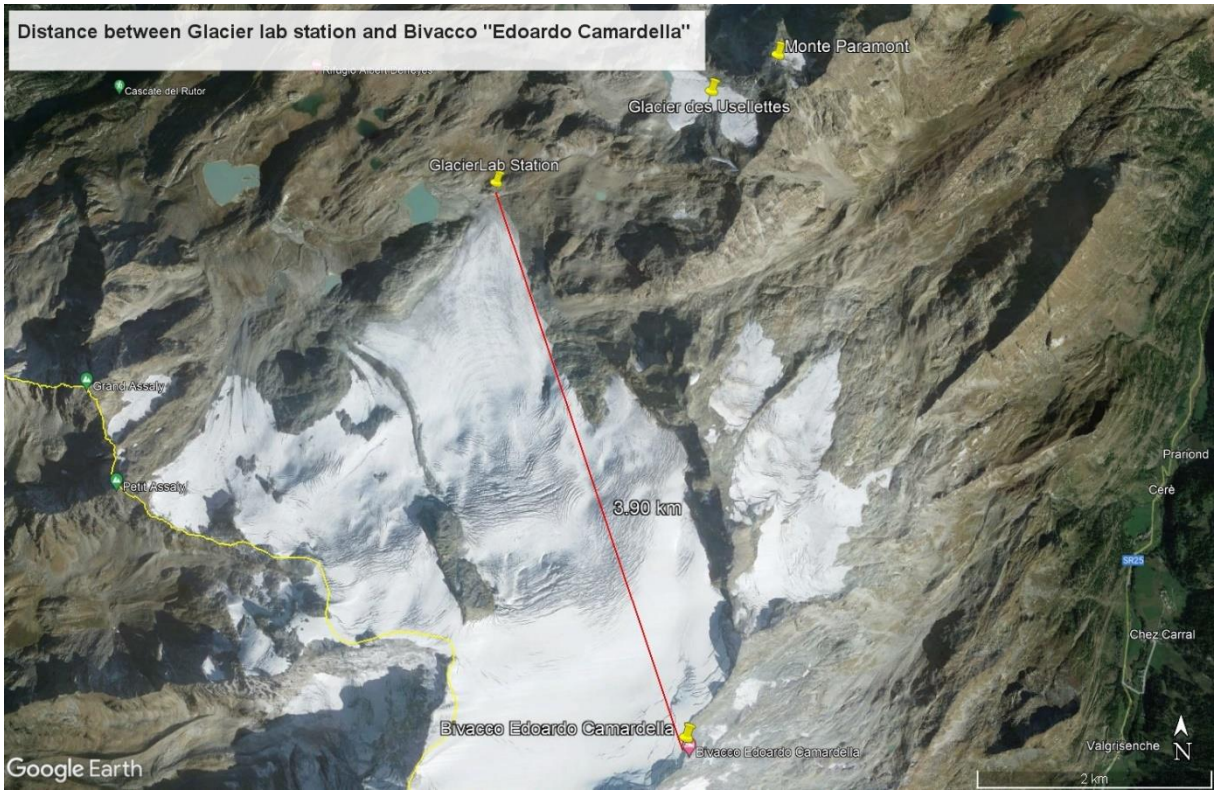

Figure 78 Bivacco “Edoardo Camardella” location and distance respect to the GlacierLab station. (Google, 2024)

5. Pre-processed projection of the glacier's evolution with "OGGM", Open Global Glacier Model

5.1 Model, pre-processed projection and input data description.

To model the evolution of the glacier a python model called "Open Global Glacier Model" (OGGM) has been used (Fabien Maussion, 2019). OGGM is an open-source glacier evolution model coded in Python that is designed to model the transient evolution of glaciers on regional and global scales. The model allows the implementation of own data in the model, but in this particular case to predict the evolution of the glacier a pre-computed projections available in the model has been used. Pre-computed projections are projections computed by the OGGM team, they are available for both a regional and a per-glacier glacial mass balance and are available for all the main future projections scenarios. Pre-computed projections use public datasets (e.g. W5M5 Climate Dataset (Stefan Lange, 2021), Randolph Glacier Inventory (Consortium, 2017)) to calibrate the model from the climatic point of view and pair them with a starting thickness estimation and mass balance data obtained from World Glacier Monitoring Service (WGMS, 2024), in Figure 79 is reported the ice thickness estimation of the model. OGGM can be run with different pathways scenario and can be run with all the different scenarios contained in CMIP 6 for future projections. Model compatibility with data can differ based on the version of the model which is in use, the version of OGGM that has been used in this thesis is OGGM v1.6.1 and for the future projection the chosen scenario was "SSP126", a remake of the optimistic scenario "RCP2.6": in this scenario the increase in radiative force is 2.6 W/m^2 by year 2100 and is designed simulating a development which is coherent with the 2°C target with climate protection measures taken. (DKRZ, s.d.).

The result of a precomputed projection is contained in a NetCDF file containing the evolution of the parameters of the glacier (or region if the aggregated data isused

instead) under investigation. A collection of all the parameters projected by the model is reported in table 2. All the variables that are given at a yearly time scale are also given on a monthly time scale.

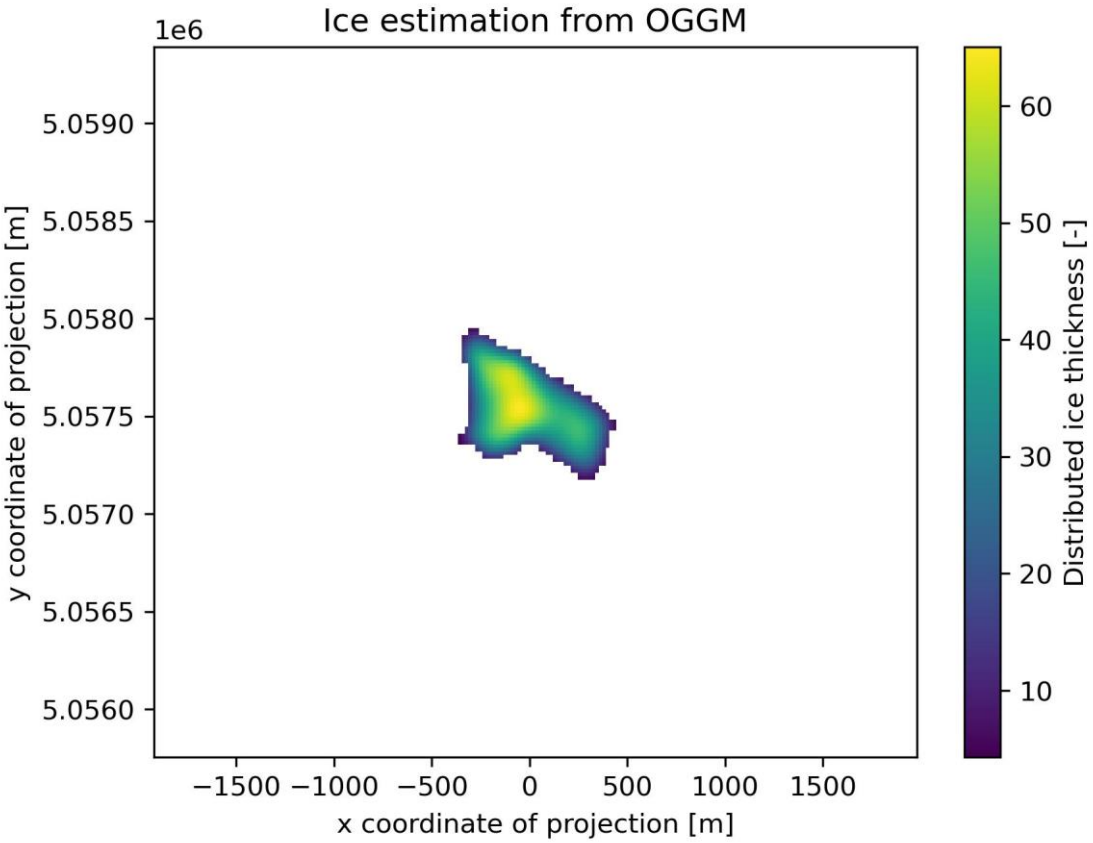

Figure 79 Pre-computed projection, ice thickness estimation used by the model. (Fabien Maussion, 2019)

Table 2 Parameters projected by OGGM pre-computed projections.

Variable	Description	Unit
volume	Total glacier volume	m^3
volume_bsl	Glacier volume below sea-level	m^3
volume_bwl	Glacier volume below water-level	m^3
area	Total glacier area	m^2
length	Glacier length	m
calving	Total accumulated calving flux	m^3
calving_rate	Calving rate	m/year
off_area	Off-glacier area	m^2
on_area	On-glacier area	m^2
melt_off_glacier	Off-glacier melt	kg/year
melt_on_glacier	On-glacier melt	kg/year
liq_prcp_off_glacier	Off-glacier liquid precipitation	kg/year
liq_prcp_on_glacier	On-glacier liquid precipitation	kg/year
snowfall_off_glacier	Off-glacier solid precipitation	kg/year
snowfall_on_glacier	On-glacier solid precipitation	kg/year
snow_bucket	Off-glacier snow reservoir (state variable)	kg
model_mb	Annual mass balance from dynamical model	kg/year
residual_mb	Difference (before correction) between mb model and dyn model melt	kg/year

5.2 Output results.

Some of the results of the precomputed projections are reported in figure 80 and 81.

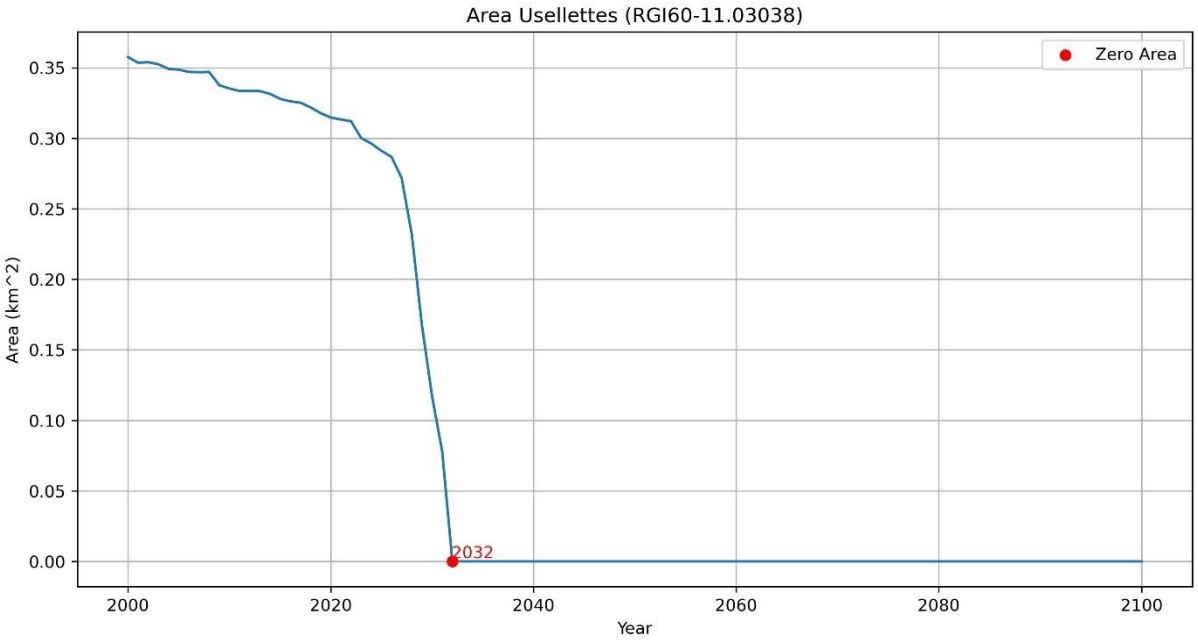

Figure 80 Pre-computed projection, evolution of Usellettes' Area 2000-2100. (Fabien Maussion, 2019)

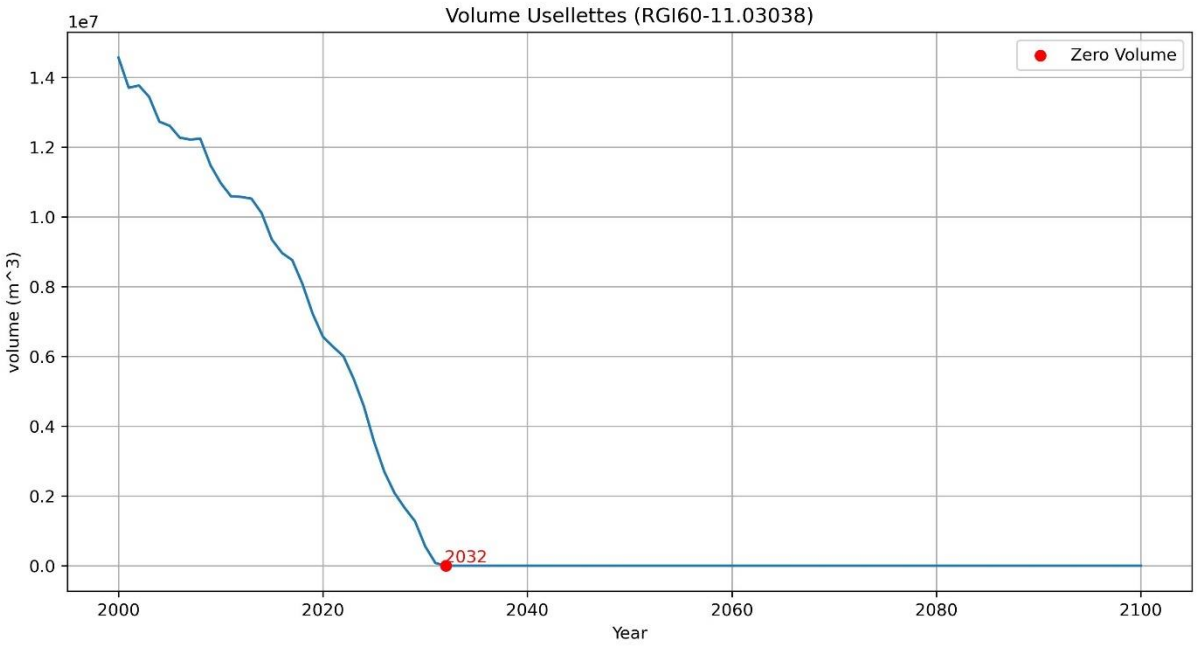

Figure 81 Pre-computed projection, evolution of Usellettes' Volume 2000-2100. (Fabien Maussion, 2019)

The model with the given input parameters predicts 2032 as the extinction year for the glacier. Given the trend of the glacier borders showed in 4.1, this result was expected and compliant with other studies performed on the matter of glacier

evolution, where is showed that any glacier whose area is smaller than 1 km^2 is expected to disappear before year 2100 (David R. Rounce, 2023).

5.3 Data preprocessing for evaluation.

The results showed in 5.2 are obtained using as input calibration data for temperatures and precipitation the global dataset W5M5 (Stefan Lange, 2021). The W5E5 dataset covers the entire globe at 0.5° horizontal and daily temporal resolution from 1979 to 2019, which correspond to a spatial resolution of 3078.75 km^2, several orders of magnitude higher than the glacier's area; this low spatial resolution risks to compromise the results of the model. To better evaluate the results of the model, the temperatures and precipitations data measured by the Glacier Lab on-site station has been combined with the longer data available at "ARPA - La Grande Tête" to obtain a longer series, corrected with the use of a bias accounting for the distance and altitude's difference. In the case of temperatures, they were corrected through the use of a Lapse Rate obtained thanks to the data available at "Bivacco Edoardo Camardella" (MeteoProject, s.d.).

The following data processing has been performed to evaluate the results of the pre-computed projection used in the study, but it allows also to run the model with the resulting data to obtain an evolution projection of the glacier in the future. Preprocessing carried out on temperatures and precipitation is hereby described.

Temperatures pre-processing

To obtain temperatures at the Usellettes' glacier the first step was to download from ARPA the history of temperatures and to compute a Lapse Rate for each season; the Lapse Rate is measured between two stations and express the rate at which temperatures change in relation with altitude, it is expressed in °C/km and can be obtained with the following equation:

Equation 2 Lapse Rate Equation

$$LR = -{}^{\Delta T}/_{\Delta z}$$

Where ΔT is the temperature difference between the two stations and Δz the relative altitude difference. To calculate the Lapse Rate the designed stations were ARPA "La Thuile - La Grande Tête" and "Bivacco Edoardo Camardella".

Being this last station at an altitude of 3360 m a.s.l it gives a better approximation of the temperature variation, since thanks to the higher altitude the difference of the measurements can be discretized with the height difference instead of computing a Lapse Rate with the lower stations (La Grande Tête 2430 m a.s.l. and the GlacierLab 2640 m a.s.l) and then extrapolate temperatures at higher altitudes. Lapse Rates however work better when the morphology of the mountain is homogeneous, which isn't the case with these two stations: Bivacco Camardella is situated on top of the "Rutor Glacier", which affects the temperature distribution and consequently the Lapse Rates. To reduce this BIAS error temperatures were computed through Lapse Rate at the Glacier Lab station's altitude and compared with the measured temperatures. The mean monthly difference between these two has been considered as a BIAS and used to correct the history of temperatures. A set of equation explaining the procedure is reported in equations 3 and 4, where "X" is the BIAS

Equation 3 Calculation of the Bias between LapseRate computed and measured temperatures

$$T_{GlacierLab_{LapseRate}} - T_{GlacierLab} = X$$

Equation 4 Calculation of temperatures at Usellettes glacier altitude

$$T_{Usellettes_{LapseRate}} + X = T_{Usellettes}$$

This procedure was applied to average, maximum and minimum temperatures and in Table 3 are reported both the seasonal Lapse Rates and the BIAS correction obtained from this procedure. While for the average value the correction seems reasonable, for maximum and minimum temperatures the correction was in a wide range and inconsistent; in light of this observation only average temperatures were considered. It's important to note that due to the missing of the whole month of June in terms of data, to obtain the correction relative to that month an average of May and July was considered.

This methodology has the limitations of calibrating the BIASes on only a year of data, which does not take into account the possibility the rate of growth of temperatures which has been recorded in the last period and the possibility of year 2023, used as calibration, being an outlier year. The result of the procedure is reported in figure 82, compared with ARPA's temperatures.

Table 3 Lapserates and BIASes obtained in respect to temperature type and month.

Month	LapseRate Avg	LapseRate Max	LapseRate Min	Bias Average Temperature [°C]	Bias Max Temperature [°C]	Bias Min Temperature [°C]
Jan	0.0075	0.0074	0.0076	0.43	3.16	-3.89
Feb	0.0075	0.0074	0.0076	0.35	6.36	-5.19
Mar	0.0075	0.0074	0.0077	0.9	5.84	-3.89
Apr	0.0075	0.0074	0.0077	0.86	6.14	-3.49
May	0.0075	0.0074	0.0077	-0.48	2.24	-2.59
Jun	0.0069	0.0071	0.0066	-0.62	1.92	-2.65
Jul	0.0069	0.0071	0.0066	-0.76	1.59	-2.71
Aug	0.0069	0.0071	0.0066	-1.5	3.79	-1.91
Sep	0.0054	0.0055	0.0053	-1.44	1.45	-1.89
Oct	0.0054	0.0055	0.0053	-0.53	2.65	-2.29
Nov	0.0054	0.0055	0.0053	-0.19	0.35	2.81
Dec	0.0075	0.0074	0.0076	2.26	3.46	0.61

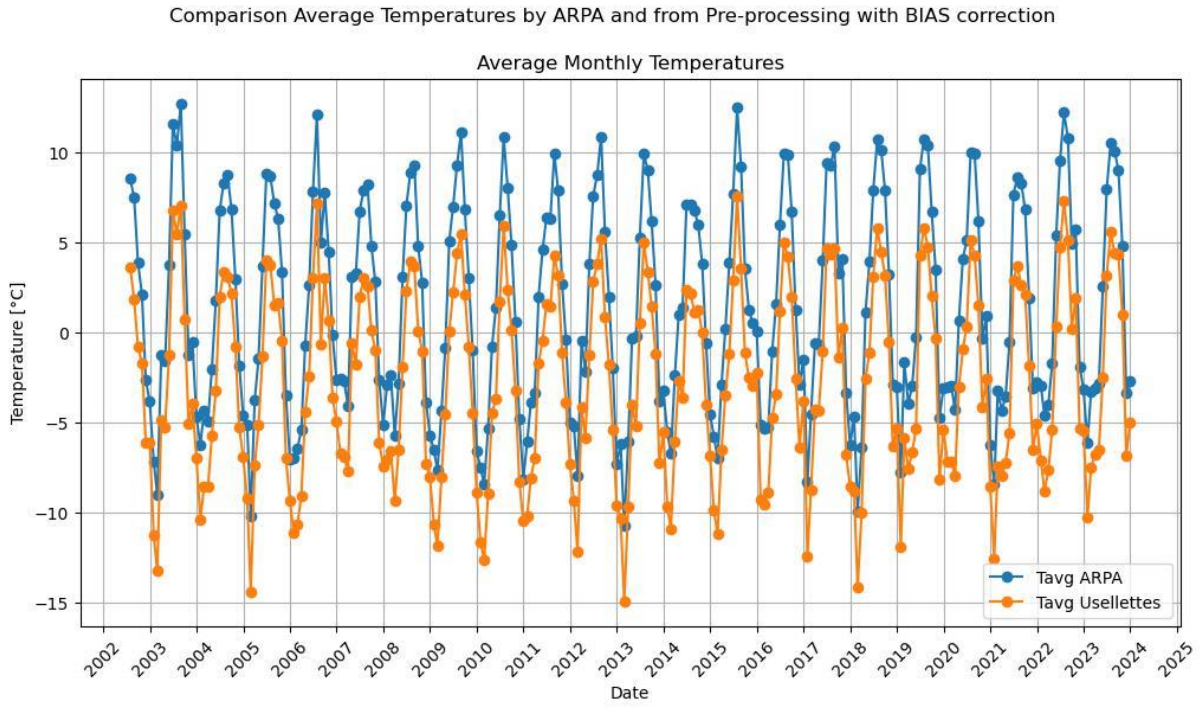

Figure 82 Temperatures, comparison of past data between recorded ARPA and preprocessed temperatures at Usellettes

Precipitation pre-processing

Concerning precipitations, the first assumption taken was that precipitations at the Glacier Lab station and at Usellettes were the same; BIAS detection was performed again through comparison but with a percentage BIAS. Historical precipitations at Usellettes were again computed with a monthly timescale, summing the amount of precipitation fallen in a month in

the year of available data for both the Glacier Lab and ARPA's data series. Then ratios between them were performed and their average was used to compute historical precipitation at Usellettes, multiplying the monthly sum of precipitation recorded by ARPA with the yearly Ratio obtained as the average of the monthly ratios obtained from the pre-processing procedure. A set of equations displaying the procedure is reported in equations 5 and 6 where "R" in the first equation is a vector containing all the monthly ratios, and "R_{year}" the average of the monthly ratios, resulted to be equal to 0.758. The monthly ratios are reported in table 4 and a comparison between historical precipitations at La Grande Tête and precipitations at Usellettes corrected with R_{year} is reported in figure 83.

Table 4 Precipitation in year 2023 in ARPA and GlacierLab stations with respectives ratios

Months 2023	ARPA [mm]	GlacierLab [mm]	Ratio GL/ARPA
Jan	108.15	63.45	0.587
Feb	70.15	10.86	0.155
Mar	153.06	82.36	0.538
Apr	100.28	81.55	0.813
May	143.74	91.97	0.640
Jun	98.8	86.97	0.880
Jul	61.8	55.69	0.901
Aug	123.76	86.71	0.701
Sep	72.46	70.05	0.967
Oct	183.06	109.03	0.596
Nov	298.05	210.16	0.705
Dec	112.29	181.34	1.615

Equation 5 Calculation of Ratios between measurements

$$\frac{Prec_{GlacierLab_{2023}}}{Prec_{ARPA_{2023}}} = R$$

Equation 6 Calculation of historical precipitation in the Usellettes glacier area

$$Prec_{Usellettes_{Historical}} = Prec_{ARPA_{Historical}} * R_{year}$$

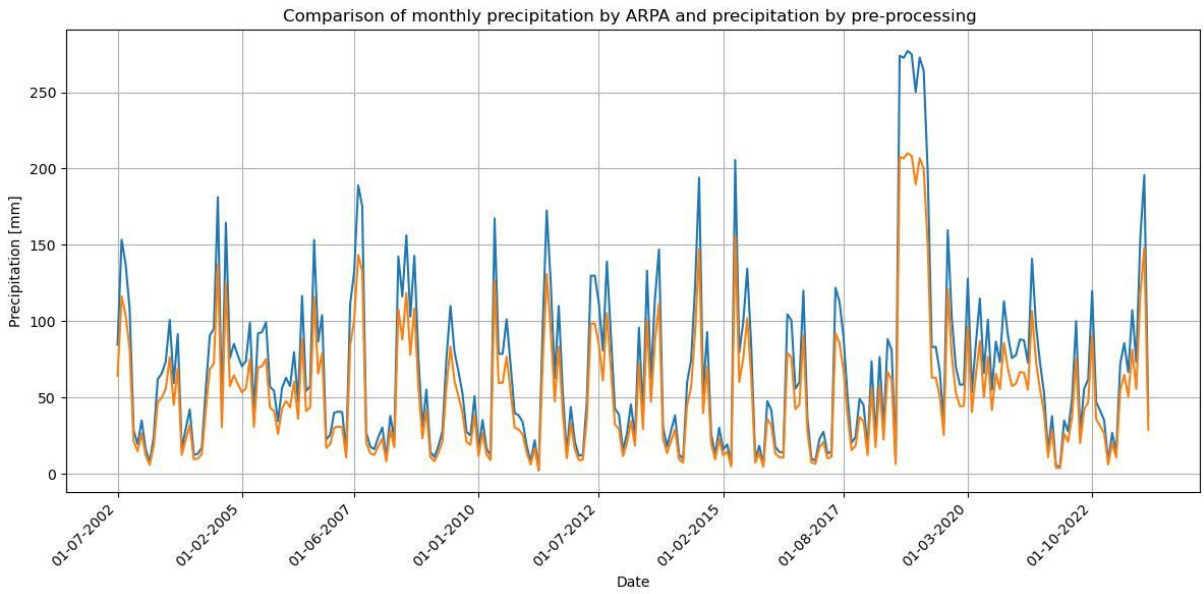

Figure 83 Precipitation, comparison of past data between recorded ARPA and preprocessed precipitation at Usellettes

6. Discussion

6.1 Evaluation of Radar Rain Gauge performances.

Radar Rain Gauges are gauges designed to work mainly with liquid precipitations, working well with an accuracy around 90%. They are not designed to work with solid precipitations since the reflection of the electromagnetic waves on their particles is different and makes them harder for the instrument to measure them. The attempt made in this thesis aimed at finding a cheaper, lighter and less labor needy instrument than weighting rain gauges to be used in high mountain environments to improve monitoring. The results, however, shows that radar rain gauges can't be entrusted with precipitation measurements during wintertime due to most of the precipitation being solid, while they perform well during hotter seasons with mostly liquid precipitation.

Considering the almost 29,000 total raining sample of 5 minutes:

- There are around 18,500 samples in which the radar rain gauge sense some precipitation, but the weighted rain gauge does not.

- There are around 1,100 samples in which the radar rain gauge does not sense precipitation, but the weighted rain gauge does.
- The 66% has an error of less than ±0.1 mm/5minutes.

These results are highly impacted by the time scale and the sensibility of the instruments. The radar rain gauge is subjected to snow deposition and to water condensation on the instrument, the snow deposited on the borders of the weighting rain gauge but actually fell into the bucket after some time can cause mismatching of the precipitation measurements. Both issues can be solved by activating the heated mode on the instruments but for safety reasons it was not activated during the sensing of the data used in this work. In this condition and environment, a radar rain gauge is not safe to use on a so accurate time scale.

On a daily time scale instead, out of the 325 days in which both instruments sense precipitations, only 27 days fit in the ±15%/day accuracy range reported by the designers; this is not a good result even considering the 59 days of recorded liquid precipitation, showing that there could be an error on the precipitation type recording, but also that the accuracy of the instrument in an unusual environment subjected to different phenomena might differ. There are also 71 days of radar rain gauge recording precipitation without anything sensed in the other instrument and 14 days in the opposite situation. These might again be due to mist in the first case (even small precipitation recording in a non-rainy day are recorded as rainy days in this analysis) and to time-lag recording of snow due to snow accumulation on the weighting rain gauge. It's important to note that it's easy in this type of analysis to produce a big relative error, especially with small amounts of precipitation and that a the quantitative analysis results should be preferred.

In figure 84 is reported a boxplot of the error in percentage, measured as the ratio of the measurements of the two instruments; as expected also by all the results shown in this thesis the solid precipitation measurements of the radar rain gauge usually differ of almost twice the actual measurement, which corresponds to the comparison of the two cumulative summations reported in figure 40. The other reported points, however, show how unreliable the instrument can be when solid precipitation is involved; it's important to underline that also these points are subjected to the time

lag of measurements due to snow deposition on the weighted rain gauge and to snow overestimation due to deposition on the radar rain gauge.

In liquid precipitation instead it's possible to note the modal value is around 1, meaning that usually the measurements in liquid precipitation are trustworthy; there are however some outliers, which might be due to other phenomena like mist, condensation and/or strong and average winds. It's also important to note that also in this type of analysis a big error is not hard to obtain, especially in days with small amount of precipitation (<1 mm/day).

Too few precipitation events were classified as Freezing Rain or Sleet, and no Hail was detected by the instrument; therefore, no consideration can be given on the instrument performances on this precipitation type.

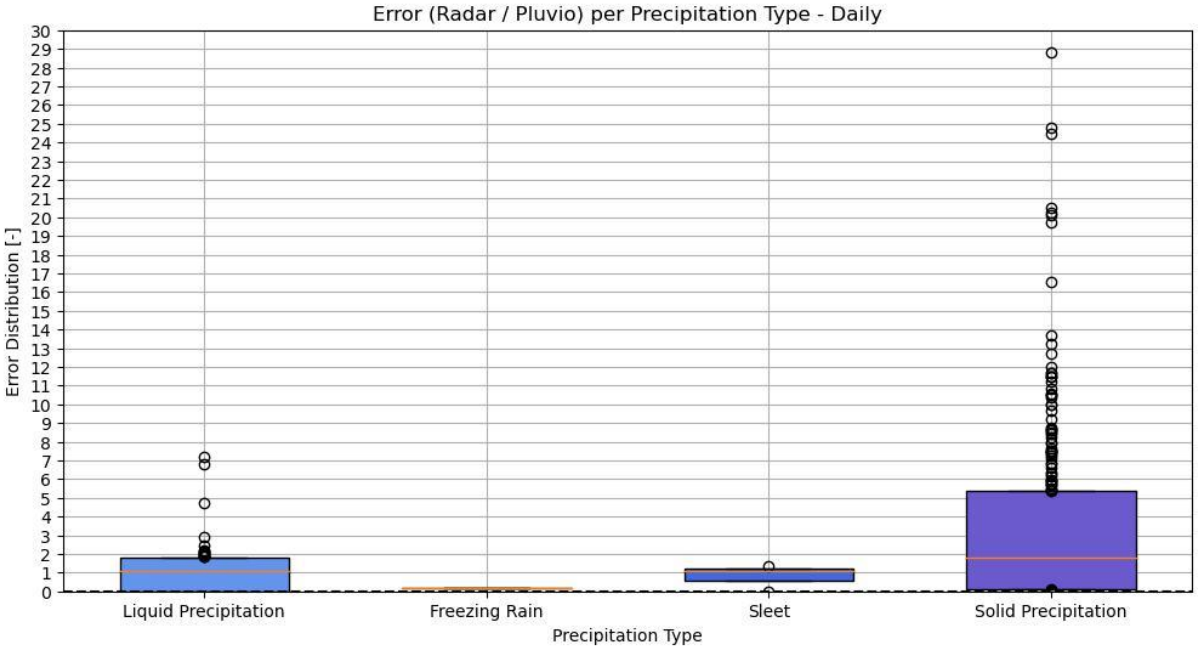

Figure 84 Error evaluation, daily boxplot of relative measurement error with precipitation type.

In light of this results, radar rain gauges are not suited for high mountain environments during wintertime due to solid precipitation presence, while they can perform fairly well during summertime measuring rainfalls. To better assess the performances of the instrument it would be important to perform again this analysis using the heating mode available in both the instruments, to avoid issues like time lags of the measurements, condensation, and snow deposition. This result is still of some usefulness, since it shows how rainfall measurements precision fall into the ranges guaranteed by the designers also in high mountain environments (±10%) for

most points and that this type of instrument might be used during high intensity rainfalls to try and predict other phenomena, like landslides.

6.2 Evaluation of model results through comparison between calibration data and pre-processed data

The outcome of the model showed in 5.2 is the result obtained from a pre-computed projection that uses the CMIP6 SSP126 scenario (DKRZ, s.d.); there are some considerations that can be taken on the calibration data that the model uses to compute the projection. In this section the results obtained are critically assessed comparing those data with data computed or gathered during the study

As already mentioned, the model uses the W5E5 dataset (Stefan Lange, 2021)for climate calibration, which contains spatial data regarding humidity, wind speed, temperatures, total irradiance, pressure, and precipitation. All these parameters are measured locally both by ARPA and the on-site station from PoliTO, but while precipitation and temperatures have a more direct impact on glaciers and are more directly impacted by climate change, the others are more difficult to relate to these phenomena. Precipitation and temperature were therefore pre-processed in 5.3 to allow comparison with the calibration dataset used by the model, the comparison is reported in figures 85 and 86. The pre-computed projection starts from year 2000 and can be ended in year 2100 or 2300; since it starts in an epoch in which area measurements are available and the calibration climatic data ends in year 2019, it's possible to assess the accuracy of the model in this starting phase comparing the series with the measured data (figure 87).

Observing temperatures reported in figure 85 it's clear that the model uses temperatures way higher than the one obtained by the pre-processing showed in this study. On Average temperatures used by the model are 5.71°C higher than the ones computed for Usellettes and 1.52 °C higher than those measured by the ARPA station. This discrepancy can be mainly attributed to the dimension of the mesh in the dataset, as already mentioned the dataset covers the entire globe at 0.5° horizontally, which corresponds to a grid of 3078.75 km^2, close to the surface of the whole Valle d'Aosta, several orders of magnitude bigger than the glacier's area or of the distance

between ARPA's and PoliTo's stations. This, however, damages the results sensibly, especially considering that the scenario taken was the most optimistic one.

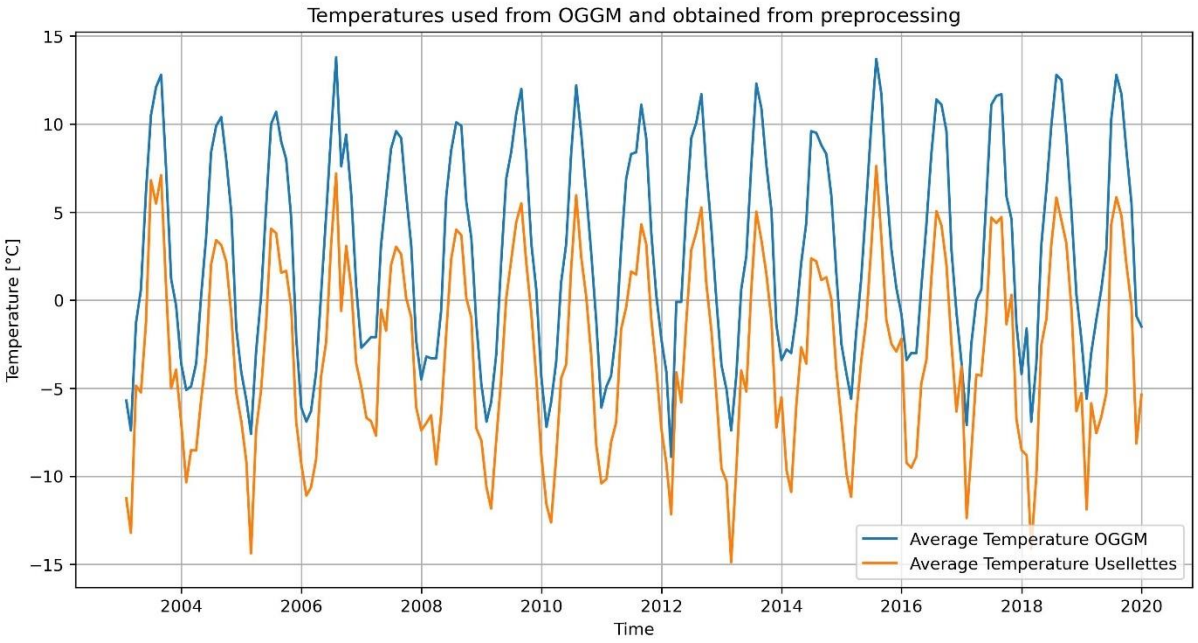

Figure 85 Temperatures, comparison of calibration data used by OGGM and preprocessed temperatures at Usellettes.

In figure 86 is reported the same comparison regarding precipitation. The comparison shows higher precipitation by OGGM, with an average discrepancy of around 380 mm per year which correspond to almost a quarter of the precipitation fell at the glacier station in year 2023. This difference impacts the outcome of the glacier's melting, but the entity and the direction of this impact is not easy to understand; if the precipitation is mostly liquid the melt-off of the glacier might be aggravated and therefore the mass balance will be affected negatively, while if the precipitation difference is mostly in solid precipitation there will be a higher melt-on of the glacier, and the mass balance will benefit. It's therefore difficult to assess the impact of precipitation but it must be kept in mind that the results might be subject to uncertainty.

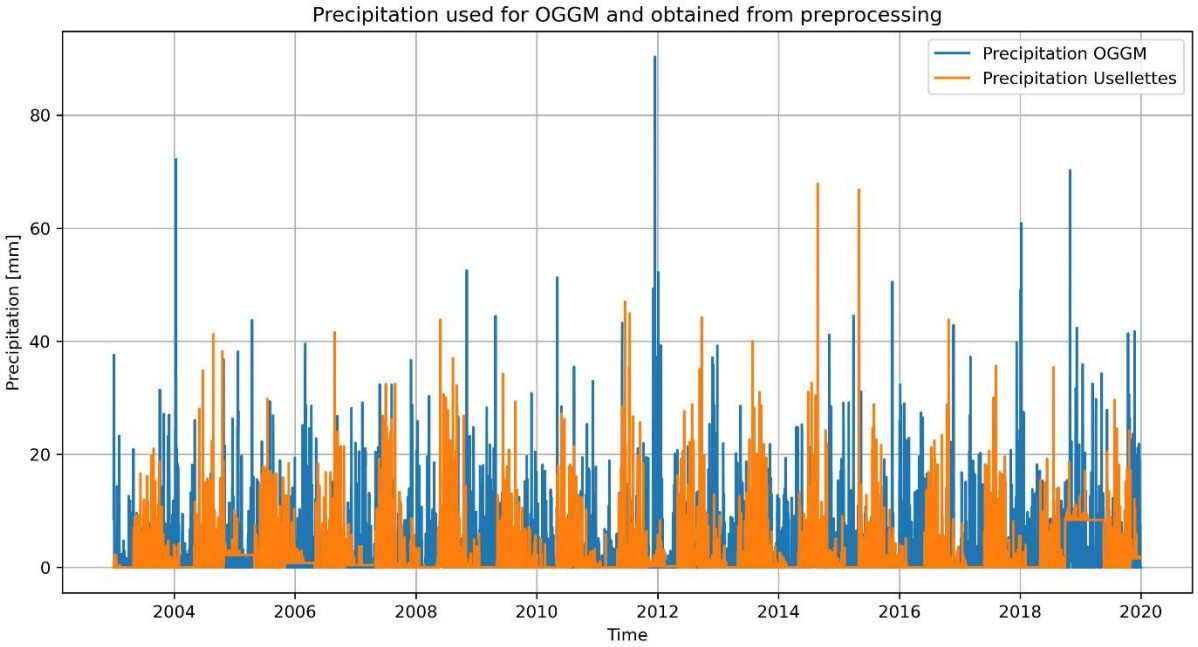

Figure 86 Precipitation, comparison of calibration data used by OGGM and preprocessed precipitation at Usellettes.

Lastly the evolution of the Area was compared with the measured borders available up to date, which were coupled with a minimum square's regression. Excluding the first one, recorded in 1999, the measured borders and the evolution from OGGM seems coherent, but in the more recent years the comparison shows a discrepancy equal to almost half of the surface; this discrepancy can be due to various factors. The areas used for calibration by OGGM and those measured in the study might be sensed in different time of the year and, even if it is less impacting unless it is very low, with different accuracy and resolution. Moreover, a peculiarity regarding this specific glacier is the definition of when the glacial appendix that was connected to the glacier stops being considered part of the Usellettes itself; this most likely causes the start of the drops in the curves, which looks similar but shifted in time.

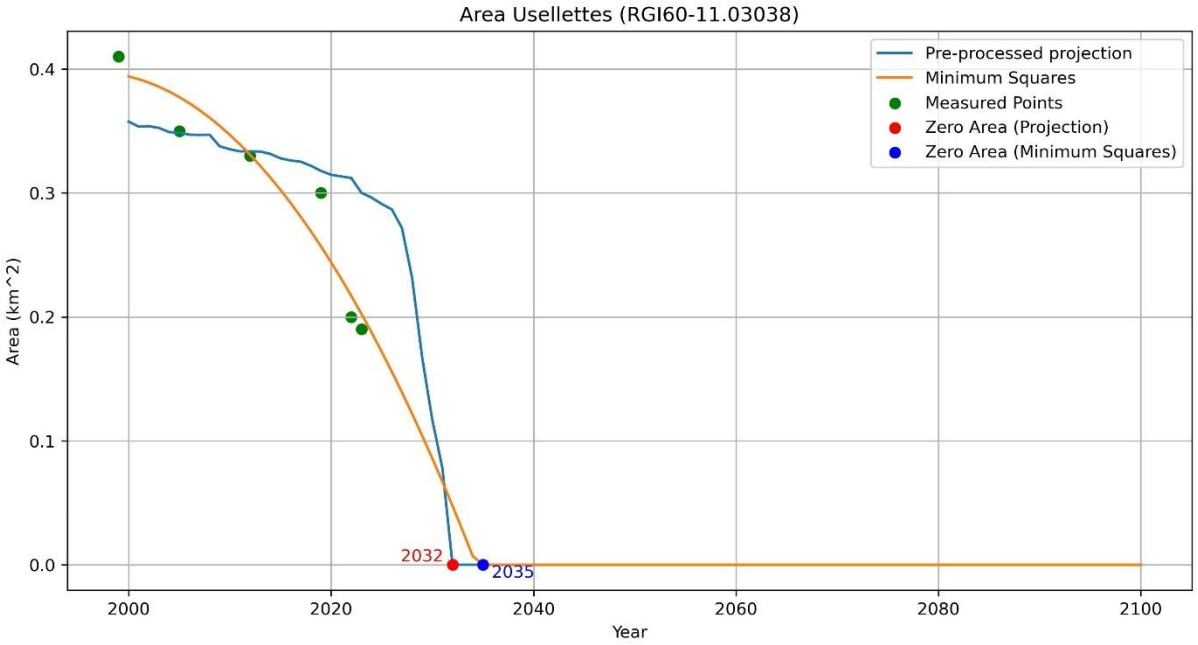

Figure 87 Pre-computed projection, evolution of Usellettes' Area compared with a minimum squares regression of the measured areas, 2000-2100. (Fabien Maussion, 2019)

However, overall, the model results seem reliable; the disappearance year seems comparable with the up-to-date rate of melting of the glacier, slightly anticipating it, but the surface area estimation doesn't seem to match with the reality. Keeping in mind that the temperatures used by the model are significantly higher than the measured ones in the sensed years, and that the prediction with the obtained by the measured points has small significance since it doesn't take into account any physical equation but strictly a mathematical regression, a more probable extinction date for the Usellettes glacier will be over year 2032, but no assurance can be granted on year 2035.

7. Conclusions

The main objectives of this thesis were two. The first one was to investigate the parameters measured by the Glacier Lab station installed in the whereabouts of the Rutor Glacier, and in doing so to assess the performances of the radar rain gauge comparing it with the measurements of the more traditional weighting rain gauge present in the same location. The second purpose of the thesis was to try to predict the extinction date of the Usellettes glacier, glacial body that contributes to the tourism of the area providing meltwater used by the close mountain refuge in a hydropower turbine; to model the evolution of the glacier many options were considered but the most effective solution in terms of model complexity and required results was the use of pre-computed projections by OGGM (Open Global Glacier Model).

The first part of the thesis found parameters complying with the values reported by the closest ARPA station “La Grande Tête”, showing expected differences in temperatures and a deficit in precipitation. The analysis of the radar rain gauges shows that this type of instrument is not ready yet to be totally entrusted with precipitation measurements in mountain environments due to the high frequency of solid precipitation events during winter, precipitation type that these instruments can’t yet measure precisely. They could however be used to measure liquid precipitation in the rest of the year since, even if impacted by the local conditions like winds and condensation, the accuracy of the instrument results to be high and complying with the results obtained by the weighting rain gauge. These results however might change if the two instruments used in this study are used on heated mode, since it might solve some issues related to snow deposition and condensation.

The second part of the thesis ran a pre-computed projection of the OGGM (Fabien Maussion, 2019) model on the Usellettes glacier, with the objective of predicting the extinction year of the glacier under investigation. The resulted extinction year is 2032 obtained with the default parameters of the model in the optimistic CMIP6 SSP126 scenario (DKRZ, s.d.). This result was then assessed through comparison of the calibration default data used by the model and by comparing the available area measurements of the glacier with the projection, finding that temperatures and precipitations used in calibration differ sensibly from the estimated data for the glacier

and that the projection predicts higher areas for the current years. It's important to note that the estimated temperatures are extracted with a bias computation obtained using a single year of data, which is usually not enough to obtain a high precision correction.

Considering the variability of the calibration data and the misalignment of the area measurements, the extinction year can't be safely predicted but can be assumed to be slightly beyond the result of the model.

References

C. Field, V. B.-K. (2012). *IPCC Glossary of terms. In: Managing the Risks of Extreme Events and Disasters to Advance Climate Change Adaptation.*

Centro Funzionale Regione Autonoma Valle d'Aosta. (2023). Retrieved from https://presidi2.regione.vda.it/str_dataview_station/1340

Christian Huggel, J. J. (2011). *Is climate change responsible for changing landslide activity in high mountains?* Retrieved December 2023, from https://onlinelibrary.wiley.com/doi/abs/10.1002/esp.2223?casa_token=LUkEWwMpTywAAAAA:0fMKu3W98kzIKH5cfoVqYrhqCXm_YLHHo-45UGmvPXbY56_LI_k-dL_Da3zGCiNcq2ZeOWzjN_ypIk0

Consortium, R. (2017). Randolph Glacier Inventory - A Dataset of Global Glacier Outlines, Version 6. Boulder, Colorado, USA. doi:https://doi.org/10.7265/4m1f-gd79

Daniel Viviroli, H. H. (2007). *Mountains of the world, water towers for humanity: Typology, mapping, and global significance.* Water Resource Research.

David R. Rounce, R. H. (2023). *Global glacier change in the 21st century:Every increase in temperature matters.* Science.

DKRZ, D. K. (n.d.). *The SSP Scenarios*. Retrieved December 2023, from https://www.dkrz.de/en/communication/climate-simulations/cmip6-en/the-ssp-scenarios

Elisabetta Corte, A. A. (2023). *Multitemporal characterisation of a proglacial system: a multidisciplinary approach.* Turin.

Fabien Maussion, A. B. (2019). *The Open Global Glacier Model (OGGM) v1.6.1.*

Google. (2024, January 12). *Google Earth*, 7.3.6.9750. Retrieved from Google Earth: https://earth.google.com/web/

H. Biemans, C. S. (2019). *Importance of snow and glacier meltwater for agriculture on the Indo-Gangetic Plain.*

HydroMet, O. (2023, December). *Lufft WS100 Radar Precipitation Sensor*. Retrieved from https://www.otthydromet.com/en/p-lufft-ws100-radar-precipitation-sensor/8367.U04

MeteoProject. (n.d.). *Osservatorio Meteorologico di Bivacco "Edoardo Camardella" (AO)*. Retrieved from meteoproject.it: https://www.meteoproject.it/ftp/stazioni/bivacco-camardella/dati.php

S. Ochoa-Rodriguez, L.-P. W. (2019). *A Review of Radar-Rain Gauge Data Merging Methods and.* Water Resources Research.

SCT. (2023). *Catasto Ghiacciai*. Retrieved from catastoghiacciai.partout.it: http://catastoghiacciai.partout.it/

Siya Cholakova, E. D. (2023). *Climate change adaptation in the ski industry: Stakeholders' perceptions regarding a mountain resort in Southeastern Europe.*

Stefan Lange, C. M. (2021). *WFDE5 over land merged with ERA5 over the ocean (W5E5 v2.0).* ISIMIP Repository. doi:https://doi.org/10.48364/ISIMIP.342217

UNFCCC. (2019). *The Paris Agreement - Publication.*

W. W. Immerzeel, A. F. (2019). *Importance and vulnerability of the world's.* Nature.com.

WGMS. (2024). *World Glacier Monitoring Service*. Retrieved from wgms.ch.

Xin Liu, Y. W. (2024). *Quantifying impacts of precipitation scenarios projected under climate change on annual probability of rainfall-induced landslides at a specific slope.*